

8-12-2022 1:45 PM

Application of passive acoustic emissions for inline monitoring of segregation prone mixtures in a V-blender

Katherine Wilson, *The University of Western Ontario*

Supervisor: Briens, Lauren A, *The University of Western Ontario*

A thesis submitted in partial fulfillment of the requirements for the Master of Engineering
Science degree in Chemical and Biochemical Engineering

© Katherine Wilson 2022

Follow this and additional works at: <https://ir.lib.uwo.ca/etd>

Recommended Citation

Wilson, Katherine, "Application of passive acoustic emissions for inline monitoring of segregation prone mixtures in a V-blender" (2022). *Electronic Thesis and Dissertation Repository*. 8801.
<https://ir.lib.uwo.ca/etd/8801>

This Dissertation/Thesis is brought to you for free and open access by Scholarship@Western. It has been accepted for inclusion in Electronic Thesis and Dissertation Repository by an authorized administrator of Scholarship@Western. For more information, please contact wlsadmin@uwo.ca.

Abstract

Powder mixing is a critical and complex step of pharmaceutical production. Process analytical technologies can enhance the quality of a product through mechanisms including improved monitoring during mixing processes. Passive acoustic emissions were examined during mixing in a V-blender. Vibrations from the emissions were measured through an accelerometer attached to the lid of the outer V-shell arm. Analysis to extract information from the emissions was refined to obtain information about particle flow versus individual particle behavior. The initially measured amplitude in segregation-prone mixtures was like that of the particle loaded on top. A stable mixture was reached when the measured amplitude plateaued to the approximate weighted average of the particles in the outer V-shell arm. Overall, the passive acoustic emissions method was refined and extended to segregation-prone mixtures, supporting the effectiveness of passive acoustic emissions for extracting information about mixing in pharmaceutical production to improve product quality and manufacturing efficiency.

Keywords

Pharmaceuticals, process analytical technologies, passive acoustic emissions, vibrations, mixing, powder processing, V-blender, segregation

Summary for Lay Audience

Tablets and capsules are the most common forms in which pharmaceuticals are produced. In order to manufacture tablets, combinations of various powders must be uniformly mixed. When powders are incorrectly mixed there is a risk that the tablet produced may have quality issues, such as containing too much or too little of the active ingredient. To ensure that high-quality standards are maintained powder mixtures must be monitored. Current monitoring methods are invasive, expensive, and inefficient. Passive acoustic emissions have the potential to provide a non-invasive, low capital cost, and effective method of monitoring mixing.

Passive acoustic emissions were measured using a sensor attached to the lid of a V-blender. Different tests were completed to see how the measured amplitudes of the emissions were affected by factors such as impact location. These tests helped to improve the understanding of the particle motion during mixing in relation to the measured vibrations. This understanding helped to identify that when analyzing the data, using the top 50 highest amplitudes would give reliable, accurate information about the mixture.

In mixtures with multiple ingredients, segregation becomes a risk. Segregation occurs when ingredients with different properties begin to separate out from each other. To evaluate segregation, one particle size was loaded into the V-shell with the second particle size being loaded on top. Initially, the amplitude measured was similar to the particle loaded on top. During mixing, the amplitude would begin to change, moving towards the amplitude of the particle loaded on the bottom, before reaching a stable mixture and plateauing. The plateaued amplitude was noted to be representative of the weighted average amplitude based on the relative fractions of the two particle sizes in the V-shell arm.

Overall, this research helps to support the potential for passive acoustic emissions to be used for monitoring powder mixtures. By refining the data analysis methods, the extracted information about the process is more accurate and reliable. As well, being able to identify undesired mixture properties such as segregation will help to improve final mixture quality.

Co-Authorship Statement

Chapters 3 and 4 have been or will be submitted to an international peer-reviewed journal. The individual contributions of the authors are indicated.

Chapter 3

Investigation of passive acoustic emissions during powder mixing in a V-blender

Authors: Katherine Wilson, Lauren Briens

Status: Published in Powder Technology

Katherine Wilson completed all experimental work and data analysis with guidance provided by Lauren Briens. The manuscript was written and revised by Katherine Wilson. Lauren Briens reviewed and provided comments for the manuscript

Chapter 4

Passive Acoustic Vibrations Application for Segregation Prone Mixture in a V-blender

Authors: Katherine Wilson, Lauren Briens

Status: To be submitted for publication in Powder Technology

Katherine Wilson completed all experimental work and data analysis with guidance provided by Lauren Briens. The manuscript was written and revised by Katherine Wilson. Lauren Briens reviewed and provided comments for the manuscript

Acknowledgments

I would first like to thank and acknowledge my supervisor Dr. Lauren Briens. Without Dr. Briens' continued support, mentorship, expertise, and friendship the completion of my thesis would not have been possible.

I would like to acknowledge the Ontario Graduate Scholarship (OGS) and the Western Graduate Research Scholarship (WGRS) and the Natural Sciences and Engineering Research Council (NSERC) of Canada for their financial contributions.

I would also like to thank Dr. Lars Rehmann and Dr. Paul Charpentier for serving on my advisory committee.

Lastly, I would like to thank my family: mom Belinda, dad Scott, and sisters Brittany and Therese for their love and encouragement throughout all aspects of my Masters work. I would also like to thank my partner Thomas for his continuous support and motivation during all the late nights and long days of research.

Table of Contents

Abstract	ii
Summary for Lay Audience	iv
Co-Authorship Statement	v
Acknowledgments	vi
Table of Contents	vii
List of Tables	xi
List of Figures	xii
Chapter 1	1
1 Introduction	1
1.1 Powder Mixing	2
1.1.1 Mechanisms of Mixing	3
1.1.2 Qualities of a good powder mixture	4
1.2 Batch versus Continuous processing	5
1.2.1 Batch processing	5
1.2.2 Continuous processing	6
1.3 Mixer Types and Geometries	7
1.3.1 V-blenders	7
1.4 Segregation	9
1.4.1 Pattern Formation	9
1.5 Coefficient of Restitution	13
1.6 Monitoring Mixing	15
1.6.1 Offline Monitoring	15
1.6.2 Process Analytical Technologies	16
1.7 Passive Acoustic Emissions Monitoring	17

1.8	References	19
Chapter 2	26
2	Review of Process Analytical Technologies.....	26
2.1	Near-Infrared Spectroscopy	27
2.1.1	Method of Monitoring.....	27
2.1.2	Advantages.....	35
2.1.3	Disadvantages	35
2.2	Raman Spectroscopy.....	35
2.2.1	Method of Monitoring.....	35
2.2.2	Advantages.....	38
2.2.3	Disadvantages	39
2.3	Optical Image Analysis.....	40
2.3.1	Method of Monitoring.....	40
2.3.2	Advantages.....	43
2.3.3	Disadvantages	44
2.4	Positron Emission Particle Tracking.....	44
2.4.1	Method of Monitoring.....	44
2.4.2	Advantages.....	47
2.4.3	Disadvantages	47
2.5	Magnetic Resonance Imaging.....	48
2.5.1	Method of Monitoring.....	48
2.5.2	Advantages.....	51
2.5.3	Disadvantages	51
2.6	X-ray Computed Tomography	51
2.6.1	Method of Monitoring.....	51
2.6.2	Advantages.....	53

2.6.3	Disadvantages	53
2.7	Passive Acoustic Emissions	53
2.7.1	Method of Monitoring.....	53
2.7.2	Advantages.....	59
2.7.3	Disadvantages	59
2.8	Conclusion	60
2.9	Thesis Objectives and Overview	64
2.10	References.....	65
Chapter 3	77
3	Investigation of Passive Acoustic Emissions during Powder Mixing in a V-blender .	77
3.1	Introduction.....	77
3.2	Materials and Methods.....	79
3.2.1	Materials	79
3.2.2	Equipment.....	81
3.2.3	Experimental Trials.....	82
3.3	Results.....	83
3.3.1	Visual Observations	83
3.3.2	Collision Tests	85
3.3.3	Detailed Rotation Trials.....	89
3.4	Discussion.....	91
3.5	Conclusions.....	99
3.6	References.....	101
Chapter 4	106
4	Passive Acoustic Emissions Application for Segregation Prone Mixture in a V-blender	106
4.1	Introduction.....	106

4.2 Materials and Methods.....	108
4.2.1 Materials	108
4.2.2 Equipment	110
4.2.3 Experimental Trials.....	110
4.3 Results.....	112
4.4 Discussion	120
4.5 Conclusion	126
4.6 References.....	128
Chapter 5.....	133
5 Conclusion	133
5.1 General Discussion and Conclusions.....	133
5.2 References	136
Curriculum Vitae	137

List of Tables

Table 1.1: Factors used for the identification of a successful mixture (adapted from Bridgewater, 2012 (6)).....	4
Table 2.1: Selection of available literature for NIR spectroscopy for mixing.....	30
Table 2.2: Summary of some literature available on the application of Raman spectroscopy to powder mixing operations.....	37
Table 2.3: A selection of previous studies of Image analysis for mixing.....	41
Table 2.4: Selection of available literature for PEPT	46
Table 2.5: A selection of previous studies of MRI analysis of mixing.....	49
Table 2.6: Summary of literature available for X-ray CT for mixing	52
Table 2.7: Summary table of available literature on applications of passive acoustic emission analysis.....	55
Table 2.8: Comparison of significant PATs currently under development (adapted from Crouter & Briens, 2019 (21) and Nadeem & Heindel, 2018 (126))	61
Table 3.1: Summary of particles used and their properties	80
Table 4.1: Summary of particles and their properties.....	109

List of Figures

Figure 1.1: Example steps for pharmaceutical tablet manufacturing processes (adapted from Aulton, 2002 (3))	1
Figure 1.2: Example design aid for selecting mixer type for a powder mixing process (adapted from Poux et al, 1991 (7))	3
Figure 1.3: Schematic of the 16-quart Patterson Kelly V-blender used throughout this research	8
Figure 1.4: Schematic of ‘Small-Out’ pattern in a V-shell (adapted from Alexander et al, 2003 (21)).....	11
Figure 1.5: Schematic of ‘Stripes’ pattern in a V-shell (adapted from Alexander et al, 2003 (21)).....	11
Figure 1.6: Schematic of ‘Inverse stripes’ pattern in a V-shell (adapted from Alexander et al, 2003 (21)).....	12
Figure 1.7: Schematic of ‘Left-Right’ pattern in a V-shell (adapted from Alexander et al, 2003 (21)).....	13
Figure 1.8: Schematic of ‘Big-Out’ pattern in a V-shell (adapted from Alexander et al, 2003 (21)).....	13
Figure 3.1: 16-quart V-shell schematic with dimensions labeled.....	81
Figure 3.2: Schematic of V-shell showing accelerometer location	82
Figure 3.3: Visualization of granule movement during rotation in the acrylic V-shell.....	84
Figure 3.4: Timeline of flow behavior during a rotation of the V-shell for 2 mm glass beads	85

Figure 3.5: Measured vibrations of a single 2 mm glass bead dropped onto the lid of the inverted empty 16-quart acrylic V-shell with the accelerometer affixed in the location shown in Figure 3.2	86
Figure 3.6: Measured vibrations of a single 2 mm glass bead dropped onto the inner wall arm of the inverted empty 16-quart acrylic V-shell	87
Figure 3.7: Measured vibrations of five 2 mm glass beads dropped onto the lid of the inverted empty 16-quart acrylic V-shell	88
Figure 3.8: Initial measured impact amplitudes of a single 2 mm glass bead dropped into an inverted empty 16-quart acrylic V-shell with various glass bead fill levels	89
Figure 3.9: One full rotation of 2 mm glass beads in the 16-quart steel V-shell showing Feature #1 (solid line, associated with the flow of particles when the V-shell is inverted), Feature #2 (dash line, associated with the flow of particles along the outer side of the V-shell arms), and Feature #3 (dotted line, associated with the flow of particles flowing towards the bottom of the V-shell)	90
Figure 3.10: Measured vibrations of 2 mm glass beads during half-rotation of the 16-quart steel V-shell showing Feature #1a (solid line, associated with collisions and the flow of particles along the inner walls of the V-shell arms towards the lid), Feature #1b (dash line, associated with the impact of particles with the lid), and Feature #1c (dotted line, associated with the particles flowing outwards across the lid)	91
Figure 3.11: Coefficient of Variation of Amplitude values for 2mm glass bead control samples in the 16-quart steel V-shell averaged over various peaks.....	96
Figure 3.12: Comparison of 2 mm Glass bead control sample in the 16-quart steel V-shell averaged over 3 peaks and 50 peaks	97
Figure 3.13(a): Coefficient of Variation of Amplitude values for Cut #3 (1.40-1.18mm) Starch Granules control samples in the 16-quart steel V-shell averaged over various peaks.	97

Figure 3.14: Mixture of 50% Starch Granules Cut#1 (2.36-2.00mm) and 50% Cut#3 (1.40-1.18mm) averaged over 50 peaks in a 16-quart steel V-shell with Cut#1 loaded horizontally on top	99
Figure 4.1: Schematic of V-shell showing accelerometer location	110
Figure 4.2: Schematic of the thief probe sampling location in the 16-qt V-shell.....	111
Figure 4.3: Comparison of 50-50 mixtures after 1200 avalanches in the Revolution Analyzer: Cut 1 and 4 (left), Cut 3 and 4 (right)	113
Figure 4.4: Visual observations of mixing of starch granules in the 16-qt acrylic V-shell. Dark dyed granules of Cut#1 were mixed with undyed light granules of Cut#4 in a 50-50% by volume ratio	114
Figure 4.5: Comparison of Thief Sample and Outer Arm composition of Starch Granules 50% Cut 1 (2.36-2.00mm), 50% Cut 4 (1.18mm-600 μ m) mixture in 16-qt Acrylic V-shell.....	115
Figure 4.6: Comparison of Outer Arm Cut 4 composition for various mixtures.....	116
Figure 4.7: Average vibration amplitude of starch granule control samples in 16-qt Steel V-shell; with horizontal error bars representing the size range of the cut and vertical error bars representing the maximum and minimum amplitude values recorded respectively	117
Figure 4.8: Glass beads 50% 1mm, 50% 2mm mixture in 16-qt Acrylic V-shell; with the percent difference from 50% composition of the 1mm glass beads of thief probe samples shown	118
Figure 4.9: Combined Loading Order Trials of Starch Granules 50% Cut 1 (2.36-2.00mm), 50% Cut 4 (1.18mm-600 μ m) mixture in 16-qt Acrylic V-shell	119
Figure 4.10: Combined Loading Order Trials of Starch Granules 50% Cut 2 (2.00-1.40mm), 50% Cut 3 (1.40-1.18mm) mixture in 16-qt Acrylic V-shell	120
Figure 4.11: Trajectory segregation flow path schematic showing the path of motion for larger and smaller particles	123

Figure 4.12: Trajectory segregation flow path schematic showing the path of motion for larger particles impacting with the V-shell joint and support.....	124
---	-----

Chapter 1

1 Introduction

Currently, approximately 80% of all pharmaceuticals are produced in the form of solid oral dosages, mainly in the form of tablets and capsules (1,2). Tablets provide a convenient and easy-to-transport dosage form with minimal potential for user error (1). Producing tablets is usually a multi-stage batch process (Figure 1.1). The mixing of various powder ingredients is a required step at many points during pharmaceutical tablet production.

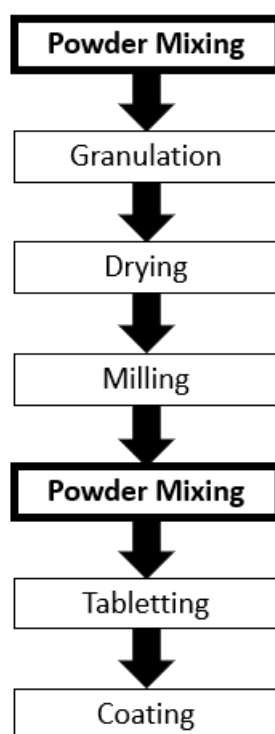


Figure 1.1: Example steps for pharmaceutical tablet manufacturing processes
(adapted from Aulton, 2002 (3))

Without proper monitoring and control of powder mixing, produced tablets may be inconsistent in quality and composition. This inconsistency could result in tablets having higher or lower concentrations of the active ingredients than intended, thus risking over

or underdosing the patient (2). Along with variations in the active ingredient concentration, poor powder mixtures can also result in tablets with incorrect properties such as variations in colour and tablet disintegration (4). Recently tablet formulas have been developed using higher potency active ingredients further increasing the importance of accurate process monitoring and control (5). It is critical that pharmaceutical powders are correctly mixed to ensure effective safe high-quality tablets.

1.1 Powder Mixing

Mixing is a highly complex process that still remains poorly understood. Due to a limited understanding of powder mixing, process design selections are often made based upon personal judgment and experience in lieu of any scientific principles. There are currently no generally accepted models or flow equations for powder mixtures (6). Experienced operators and designers have worked to produce guides to help with various sections of processes such as the guide shown in Figure 1.2 used to help in mixer selection (7).

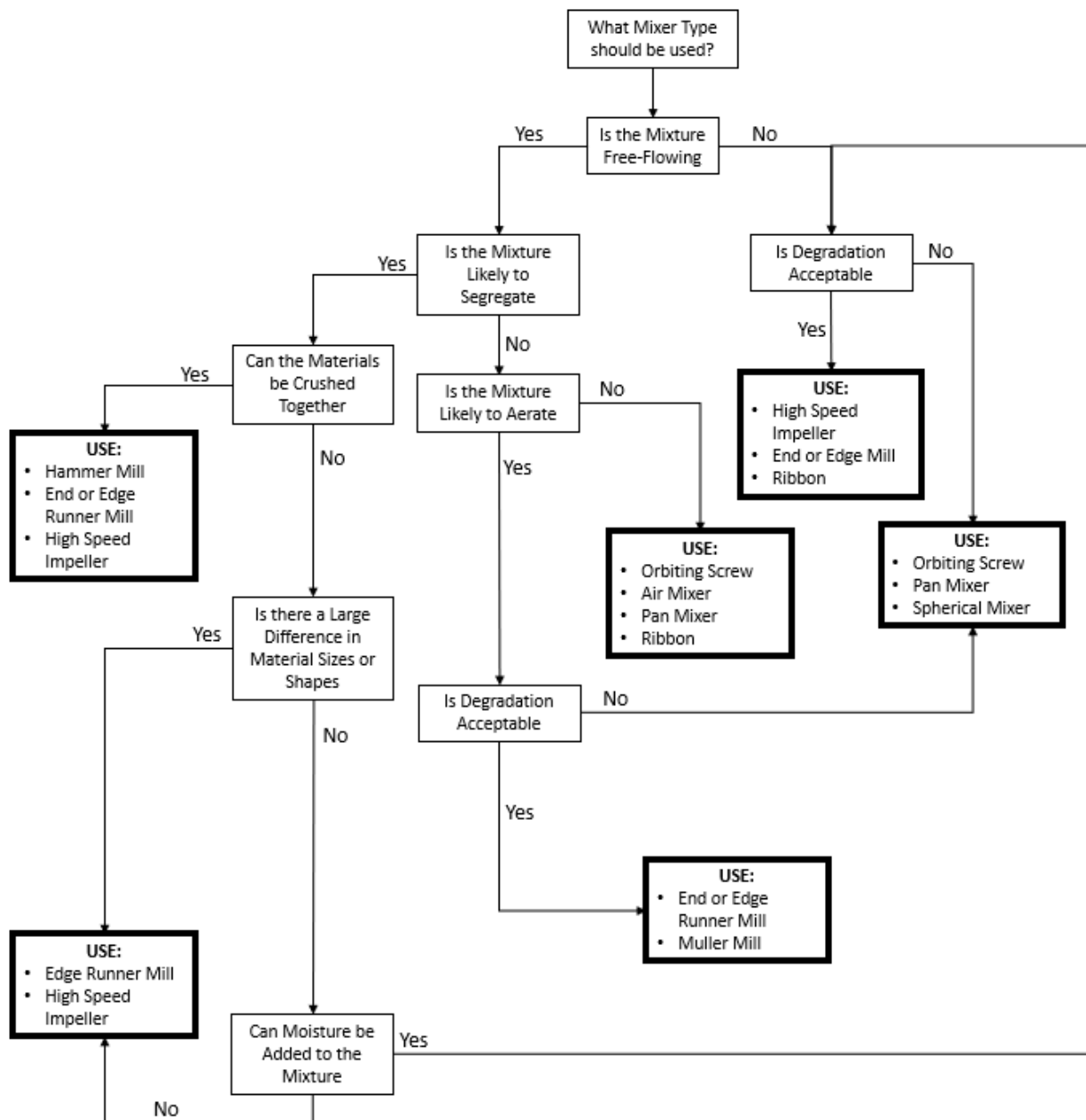


Figure 1.2: Example design aid for selecting mixer type for a powder mixing process
(adapted from Poux et al, 1991 (7))

1.1.1 Mechanisms of Mixing

Mixing occurs through three different mechanisms: diffusion, convection, and shear.

Depending upon the number of rotations and the mixer geometry, the dominant mechanism changes (8). Diffusion mixing is the blending of particles through the

movement of individual particles (6,9,10). Diffusion is a slow mechanism that promotes better length scale mixing (6,8). Convection mixing is the blending of particles through the movement of groups of particles. Convection promotes higher spatial homogeneity and interparticle surface area within the mixture (6). Shear mixing is the blending of particles through the development of slip planes throughout the mixture (9). Shear generally reduces agglomeration within the mixture (6).

1.1.2 Qualities of a good powder mixture

To identify the quality of a mixture, specific parameters have been identified. Bridgewater (2012) derived the six factors shown in Table 1.1 which provide a highly generalized basis on which to judge a mixture (6).

Table 1.1: Factors used for the identification of a successful mixture (adapted from Bridgewater, 2012 (6))

1. Is the mixture well mixed on a microscopic scale?
2. Is there no large concentration variation?
3. Is the final mixture structure random?
4. Is the mixture well mixed to a specific 'scale of scrutiny'?
5. Assuming the mixture is to be used in a chemical reaction, does the mixture structure allow for the desired rate of reaction?
6. Are the mixture characteristics what is desired?

To allow for a more accurate judgment of powder mixture quality, specific mixture characteristics can be examined. These characteristics vary depending upon the industry and the quality level required for the mixture (6). One such characteristic that may be critical for accurate mixture quality judgement is the acceptable level of segregation throughout the mixture. Without effective monitoring methods, the ability to evaluate characteristics of interest is limited.

1.2 Batch versus Continuous processing

Powder mixing processes can be classified as either batch or continuous processes. The process type has several effects on the design and operation of the mixing process. Most monitoring techniques developed for pharmaceutical powder mixtures have been limited to batch processes.

1.2.1 Batch processing

Batch mixing is a discontinuous process in which a specific amount of raw materials are added into a mixer subject to specific conditions and allowed to process for a specific amount of time. After the mixture has been blended under specified conditions, the entire mixture is discharged from the mixer and tested using offline techniques (10). The mixture is only allowed to continue to the next step if the test results are as desired. The use of batch processing in pharmaceutical production allows for tight quality control as the final powder mixture is intensely tested following each step (10,11).

The use of batch processing presents several disadvantages, limiting the possibility of process improvements:

1. The main disadvantage of batch processing is the lack of real-time information. This means that mixtures may be left to run for longer than required, potentially resulting in damage to the products through attrition (10).
2. Without real-time analysis, offline monitoring must be used, specifically thief probe monitoring. The use of thief probes has several drawbacks including the risk of sampling errors, disturbing the bed, and misrepresenting the overall

mixture (4,6,12). The samples from thief probes also require destructive testing to be analyzed thus resulting in the loss of some product (13).

3. Batch processing tends to require longer mixing times than continuous processing for the same amount of product (10). There is no widely agreed upon reasoning for this difference. However, it is theorized that it is due to a lack of real-time monitoring resulting in the mixture being mixed for longer than required or due to the large amount of ingredients added at the start of the process.
4. Due to the requirement for all materials for the mixture to be added at the beginning, batch mixers require large amounts of space limiting their cost-effectiveness and applications in high volume processes (11,14).
5. If testing results are found to be unacceptable, the entire batch must be discarded resulting in product waste (15).
6. Batch processes also lack optimization and process control options due to factors such as a low level of understanding of batch operations and a lack of widely accepted mathematical models (16). This low level of process control increases the risk of poor product yield and quality (16).

1.2.2 Continuous processing

Continuous mixing is a process in which materials are continuously fed into the mixer while also being continuously discharged (10). Continuous processes do not require the mixer to be stopped between batches (10). The use of continuous processing presents several advantages compared to batch processing:

1. The time required for continuous processing is typically lower than that of batch processing. There are several reasons for this lower time requirement including a lack of discrete loading and discharge times (10,16).
2. The continuous loading and discharge of the mixture allow for smaller equipment to be used while maintaining the same production rate, thus decreasing the mixer capital cost (14).
3. The continuous discharge of the feed allows for the implementation of continuous processing throughout all steps of production. This continuous production results

in a lower risk of segregation due to the ability to move batches directly from the mixer to the next stage of processing (10,14).

4. The presence of widely accepted mathematical models for continuous processes improves the overall understanding of the process (14,16). This understanding helps to improve the process design leading to further automation and higher product consistency (14).
5. Continuous mixers allow for process parameters to be more easily altered thus increasing the versatility of the process and limiting the amount of waste from unacceptably mixed products (14).

Despite the several advantages of continuous processing, without real-time, accurate and inline monitoring, continuous processing cannot be successfully implemented.

1.3 Mixer Types and Geometries

Mixers can be defined under two distinctive groups, stationary shell mixers and rotating shell mixers. Stationary shell mixers, also known as convective blenders, have a fixed shell with a rotating internal rotor (6). This type of mixer promotes mixing through convection and includes mixer geometries such as ribbon and centrifugal mixers (6,17). A major limitation of stationary shell mixers is their difficulty to clean, resulting in longer downtimes (6,17). Rotating shell mixers, also known as tumbling blenders, have a rotating shell (6). This type of mixer promotes mixing through diffusion and shear mixing and includes geometries such as the V-blender.

1.3.1 V-blenders

In this research, a V-blender was used for all experiments, see Figure 1.3. The V-blender is one of the most commonly used mixers in pharmaceutical processing (18-20). V-blenders are mixers that have a V-shaped shell, composed of two connected cylindrical shells, which is rotated about the horizontal axis at a set speed (6,17,18,20). V-shells come in various sizes and materials with the angle of the joint typically between 70° to 90° (18-20). As the V-shell rotates, gravity causes the particles to begin to tumble

allowing the mixture to combine while remaining relatively gentle to minimize any physical damage to the particles.

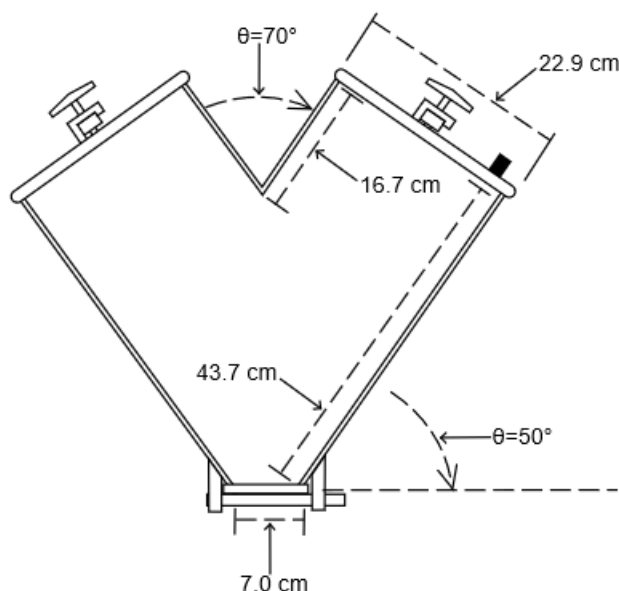


Figure 1.3: Schematic of the 16-quart Patterson Kelly V-blender used throughout this research

The V-blender allows for several operating conditions to be varied to ensure the desired outcome of the process is achieved. These parameters include the particle loading order, V-shell scale and fill level, and rotation rate (21-23). The required number of rotations to reach a uniformly combined mixture is affected by these conditions (23). The selected mixing time can also greatly affect the quality of the final mixture. If a mixture is not allowed to mix long enough, the mixture will not be fully combined, and if the mixture is allowed to mix too long, the mixture may de-mix or particles may be damaged through attrition (20).

V-blenders have several disadvantages due to their shell geometry. One disadvantage of note is the lack of mixing between V-shell arms (6,17,20). In a V-blender, most of the particle mixing is isolated within each arm. Particles from both arms only interact when the V-shell is rotated between 180° to 360° , while particles are tumbling from the V-shell lids towards the bottom plate (6,17). The mixing in this phase is limited as only a small percentage of the particles tumble across to the other arm. This limited interaction can

increase the amount of time required for a mixture to combine fully. Another significant disadvantage of V-blenders is that they promote segregation of mixtures (6,17,21). As pharmaceutical mixtures require a high degree of uniformity, it is critical to limit and identify mixture segregation.

1.4 Segregation

Segregation or de-mixing is the process through which particles separate (24). This separation leads to low-quality non-uniform mixtures with variations in composition throughout the powder bed. Segregation propagation is dependent upon several factors such as particle and process properties. The particle properties that have been found to have the largest impact on segregation risk are particle size, density, and cohesivity (6,21,24). Segregation occurs when particles begin to follow separate paths throughout the powder bed. Mixtures with larger variations in particle size and density have a higher risk of segregation. The mixer geometry is a highly impactful process property. Mixer geometries such as V-blenders and tote mixers have been shown to promote segregation due to unique particle motion during the rotation of the shells (6,17).

1.4.1 Pattern Formation

Pattern formation has been explored for several mixer geometries including rotation drum, tetrapodal, and V-blenders. Previous research has primarily been conducted by Alexander et al (2003) and Alexander et al (2004), and they have identified four distinct segregation patterns that can develop during powder mixing in a V-blender: ‘Small-out’, ‘Stripes’, ‘Inverse stripes’, and ‘Left-right’ (21,25). The formation of these patterns was primarily dependent upon the rotation rate and the fill level of the V-shell. The velocities of the particles can vary throughout the V-shell and these differences at the wall and joint of the V-shell are thought to be responsible for the pattern formation. For both the wall and V-shell joint, trajectory segregation controls the development of the mixture. Trajectory segregation is segregation during mixing due to particles with higher inertia having a higher tendency to follow a straight path of motion. The rotation rate of the V-shell can impact the inertia as, at faster rates, the inertia of all particles will be higher. At

the wall, in the first half of the rotation, mixtures with slower rotation rates will promote the smaller particles staying close to the walls due to friction and the larger particles following a curved path towards the V-shell center due to having higher inertia. In the second half of the rotation, the locations of the large and small particles are inverted. The effect of friction lessens as the force of inertia increases. Thus, at higher rotation rates, the trajectory segregation decreases at the wall. At the joint, mixtures with lower rotation rates will promote smaller particles turning to follow the flow of the V-shell thus staying closer to the middle of the V-shell and the larger particles continue to follow their previous straight path of motion for longer before turning. At higher rotation rates, both smaller and larger particles will impact the joint at a high speed thus disrupting their original path of motion; the smaller particles will then migrate through the mixture resulting in the particle locations being the inverse of what is observed at slower rates. The combinations of the wall and joint speeds contribute to the formation of the four currently identified patterns (21,25).

‘Small-out’ describes a pattern in which the smaller particles migrate horizontally to the outer sides of the mixer leaving the larger particles in the center of the V-shell (figure 1.4). This pattern results in the particles being nearly completely segregated with minimal mixing of the particles. The ‘Small-out’ pattern develops in mixtures with lower rotation rates and fill levels, with previous research showing the fill volume and rotation rate range in which this pattern develops is approximately 30-60% and 4 to 12 rpm respectively. ‘Small-out’ patterns occur when the particle velocity is slow at both the wall and the V-shell joint (21,25).

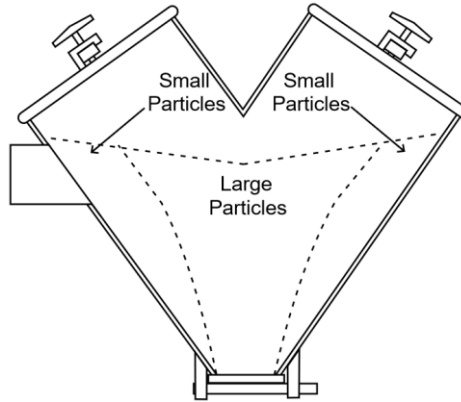


Figure 1.4: Schematic of ‘Small-Out’ pattern in a V-shell (adapted from Alexander et al, 2003 (21))

‘Stripes’ describes a pattern in which the smaller particles migrate into the center of each arm of the V-shell leaving the larger particles on either side of the smaller particles (figure 1.5). The ‘Stripes’ pattern develops at high fill levels for all rotation rates up to 30 rpm. Previous research indicates that the ‘Stripes’ pattern develops during processes with a fill volume and rotation rate of approximately 62-80% and 4 to 30 rpm respectively. ‘Stripes’ patterns occur when the particle velocity is fast at the wall and slow at the V-shell joint (21,25).

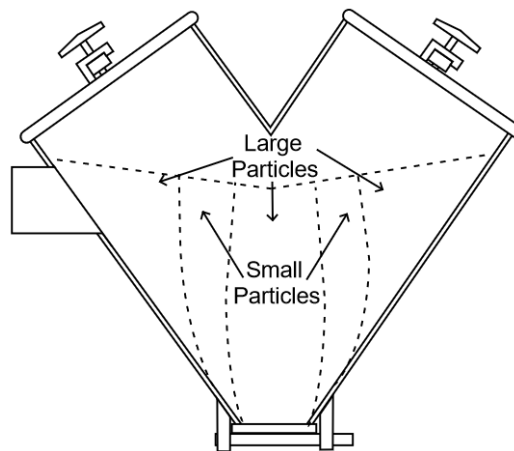


Figure 1.5: Schematic of ‘Stripes’ pattern in a V-shell (adapted from Alexander et al, 2003 (21))

‘Inverse stripes’ describes a pattern in which the larger particles migrate into the center of each arm of the V-shell leaving the smaller particles on either side of the larger particles (figure 1.6). The ‘Inverse stripes’ pattern only occurs over a small range of conditions between a fill rate of approximately 30-45% and a rotation rate of approximately 6 to 12 rpm. ‘Inverse stripes’ patterns occur when the particle velocity is slow at the wall and fast at the V-shell joint (21,25).

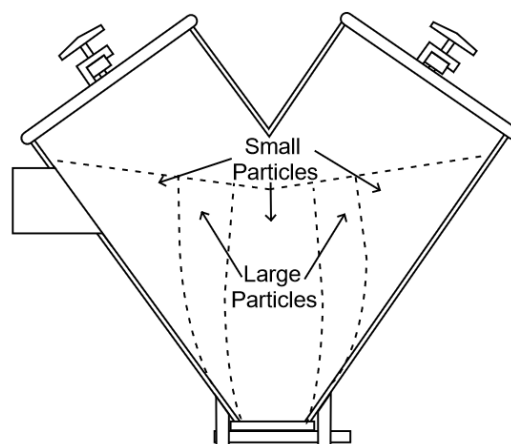


Figure 1.6: Schematic of ‘Inverse stripes’ pattern in a V-shell (adapted from Alexander et al, 2003 (21))

The ‘Left-right’ pattern is currently not well understood. This pattern is characterized by the segregation of the smaller particles into the outer arm of the V-shell and the larger particles into the inner arm of the V-shell (Figure 1.7). This pattern does not fully segregate the particles, rather it affects the concentration of each particle type in each arm and these concentration levels can change depending on the process conditions and particle characteristics. While developing the ‘Left-right’ pattern, an unstable transitionary pattern will be temporarily developed. This pattern is called the ‘Big-out’ pattern. The ‘Big-out’ pattern is a pattern in which the larger particles migrate horizontally to the outer sides of the mixer leaving the smaller particles in the center of the V-shell (figure 1.8). Previous research has seen the ‘Big-out’ pattern develop under ‘Left-right’ conditions around 50 revolutions and devolve around 250 revolutions. Previous research indicates that the ‘Left-right’ pattern develops in processes with a fill volume and rotation rate of approximately 30-80% and 6 to 30 rpm respectively. ‘Left-

right' patterns occur when the particle velocity is fast at both the wall and V-shell joint (21,25).

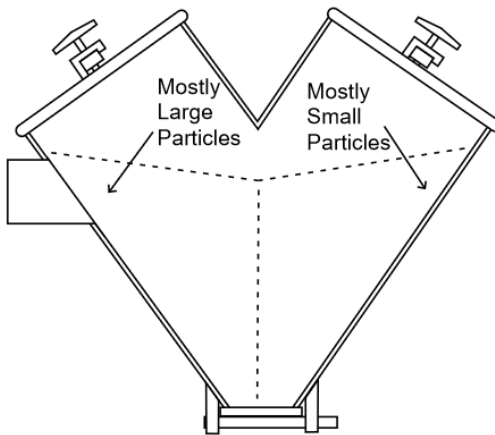


Figure 1.7: Schematic of 'Left-Right' pattern in a V-shell (adapted from Alexander et al, 2003 (21))

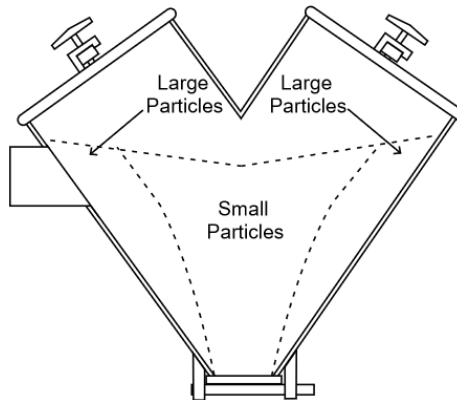


Figure 1.8: Schematic of 'Big-Out' pattern in a V-shell (adapted from Alexander et al, 2003 (21))

1.5 Coefficient of Restitution

The coefficient of restitution (COR) is the ratio of a particle's energy before a collision to the particle's energy after a collision (26-29). The COR can be described as the ratio of the particle's velocity before and after a collision or the particle's drop height compared

to its rebound height (30). This ratio provides a measure of the energy lost in a collision, with perfectly elastic collisions where there is no energy loss having a COR value of one (26-29). Conversely, in perfectly plastic collisions where all energy is dissipated, the COR value is zero. In a V-blender, the gentle tumbling of the mixer allows energy to mostly be dissipated through vibrational waves caused by changes in the local stress (31).

During mixing, a particle begins to move with a specific kinetic energy. When the particle collides with the V-shell wall or another particle, the kinetic energy is then transformed in one of many ways. This energy may be transformed through factors such as plastic deformation, air drag, particle rotation, and stress waves (32). With the particles and conditions selected for this research, it was assumed that minimal kinetic energy is transformed into factors other than stress waves. Upon impact, the localized stress changes causing the propagation of stress waves. These stress waves then travel through the V-shell until reaching the sensor affixed on to the V-shell lid. The distance of the collision location from the sensor will impact the measurements due to the attenuation of the stress waves.

COR is greatly impacted by the physical characteristics of the particles and the V-shell. If ductile particles are used, more energy will be lost through plastic deformation thus lowering the COR (29). The COR will be affected by the density and mass of the particles, as with higher density or mass, the kinetic energy of the particle increases (29).

Dependent upon the conditions, location, and angle of impact, the resultant COR value will differ. Previous research has shown that the COR of a particle colliding with an angled surface will decrease as the surface angle is increased, up to an angle of approximately 50-60° after which point the value levels out (33). It is also found that the velocity at which the particle collides has a large impact on the COR. As the velocity of a particle increases, more energy will be transferred into the V-shell, and thus the COR value will be lower (33). This is true up to a critical velocity after which increases in the velocity will not impact the COR (33).

Passive acoustic emission analysis measures the energy transferred into the V-shell as stress waves from particle collisions. The stress waves, in the form of vibrations, are

measured using an accelerometer affixed to the lid of the V-shell. The COR measures the energy retained by the particle after a collision and can be used to model the energy transfer of a collision. During mixing, differences in the particle parameters such as mass or velocity will affect the amplitude of the measured vibrations. Depending on the kinetic energy of the particle at the time of impact the COR value will increase or decrease. If the particle has high kinetic energy upon impact the energy transferred will be higher, thus resulting in higher measured vibration amplitude and a lower COR value. Therefore, the COR provides a critical parameter for modeling powder mixing, allowing for models to be developed based on mixture and particle parameters.

1.6 Monitoring Mixing

1.6.1 Offline Monitoring

Thief probe sampling is the most commonly used method for analyzing the quality of powder mixtures within the pharmaceutical industry (4,6). In thief probing, samples of the powder mixture are removed from multiple locations across the powder bed using a thief probe and analyzed through various destructive tests (4,13,34). Thief probes are comprised of two separate rods, one inner and one outer, which have cavities to allow for sample collection. To procure a sample, the rods are inserted into the powder bed; the inner rod is then rotated to allow for the sample to flow into the cavities. There are several types of thief probes that can be used such as the globe-pharma, groove, and plug thief probes, with the groove thief probe minimizing error (4,35).

Despite their widespread adoption, thief probes are error-prone even when implementing specific sampling procedures. One of the main error risks of thief probe sampling is that the collected samples may not be representative of the mixture. This error can occur due to channeling caused by the insertion of the probe. Channeling disrupts the internal structure of the powder bed causing potential segregation (4,36). Samples may also be incorrect or unattainable if the powders being mixed are cohesive in nature (6,37).

Cohesive powders are not able to flow easily thus potentially impacting the sample as the powders must flow in the probe cavities. Another disadvantage of thief probes is the loss

of product due to destructive testing methods. Samples removed via thief probing must be tested using destructive methods such as UV spectroscopy (13). This method of destructive testing is high in cost due to product loss. In addition, any batch that is found to be unacceptable must be disposed of thus leading to further costs. The offline nature of thief probes prevents real-time information from being available, contributing to the risk of having to dispose of batches. For powder mixing processes to be improved new methods of monitoring must be developed.

1.6.2 Process Analytical Technologies

Quality by design (QbD) is a concept first developed by Joseph M. Juran (38). QbD is a philosophy in which products and processes are designed with quality as a conscious focus, making use of factors such as solid scientific principles and systematic risk management approaches to achieve specific quality goals (39). In QbD, quality is not an afterthought or metric only thought of during testing, rather the entire product or process itself is designed to maintain and achieve high levels of quality. One factor that can be used to ensure the QbD philosophy is being followed in pharmaceutical processes is the use of Process Analytical Technology (PAT). PAT is defined as “A system for designing, analyzing, and controlling manufacturing through timely measurements (i.e., during processing) of critical quality and performance attributes of raw and in-process materials and processes with the goal of ensuring final product quality” (40). PATs are currently in development to further improve the monitoring of powder mixtures along with various other manufacturing processes across several industries. The utilization of PATs for monitoring powder mixtures helps to address the disadvantages of thief probe sampling such as powder bed disturbance and the need for destructive testing. Implementation of PATs would also allow pharmaceutical processes to move toward continuous processing helping to lower costs and improve the quality and efficiency of tablet manufacturing.

In chapter 2, a detailed review of PATs currently in development for monitoring powder mixing is presented. The PATs that will be covered vary widely in their monitoring methods and each has challenges currently limiting their application in industry. PATs include near infrared spectroscopy (41-47), Raman spectroscopy (12,13,51-54), magnetic

resonance imaging (51-54), X-ray computed tomography (55-57), image analysis (58-65), and passive acoustic emissions (31,32,66-70).

1.7 Passive Acoustic Emissions Monitoring

Acoustics is the study of energy in the form of waves that is produced by a source, transmitted through a medium, and accepted by a receiver (69,70). The first recorded studies of acoustics were completed in the 6th Century B.C.E. in which Pythagoras identified that pitch produced is dependent upon the length of a string (70). Galileo (1564-1642 C.E.) later expanded upon the understanding of acoustics, identifying the importance of frequency and the impact of string properties such as tension and density (70). Acoustics is based upon the principal of transmission and the fundamental mechanics of wave transmission (69). The principal of transmission considers the change in position from equilibrium of a particle. The fundamental mechanics of wave transmission expand upon the principal of transmission to define the concept of propagation. When a source acts upon a particle causing a change in position from equilibrium, this particle will act as a source for its adjacent particles. These adjacent particles will then change in position, acting as a source for their adjacent particles, this pattern will continue allowing the waves to be transmitted throughout the medium. In this research acoustic waves transmitted through a solid were measured. When transmitted through a solid the acoustic waves are composed of a combination of the transverse and longitudinal waves produced by the source. The magnitude of the wave can be defined using several particle parameters including displacement and velocity.

Passive acoustic emissions in the context of mixing in a V-blender are defined as the kinetic energy of a particle that is transformed into acoustic or vibrational waves upon a particle collision. Passive acoustic emissions are due to particle-particle and particle-shell collisions. Passive acoustic emissions monitoring is a PAT based upon acoustic or vibrational waves propagated during particle collisions during mixing due to sudden changes in the localized stress. The analysis of the vibrational wave amplitudes can be used to monitor changes in the powder bed including in the powder bed structure (5). Passive acoustic emissions or vibration measurements provide several advantages over

other PATs currently in development. This method of monitoring provides a non-invasive low-cost option that can be implemented without permanent mixer modifications. A more detailed discussion and literature review of passive acoustic emissions monitoring is presented in chapter 2.

Previous research showed that passive acoustic emissions monitoring can indicate when the endpoint of a mixture between a particle and a lubricant has been achieved through changes in the measured amplitude of the vibrations (5,30,31,71,72). This research has also provided a greater understanding of particle motion during mixing in a V-shell. The results of these studies showed the potential for passive acoustic emissions applications. However, due to the segregation-prone nature of V-blenders, further analysis is required to determine if passive vibrations can be used to monitor more than just the endpoint of a mixture of particles and lubricant. As well further signal analysis is required to confirm connections between the motion and the measured vibrations.

1.8 References

1. Debotton N, Dahan A. Applications of polymers as pharmaceutical excipients in solid oral dosage forms. *Med Res Rev* 2016; 37: 52-97
2. Léonard G, Bertrand F, Chaouki J, Gosselin PM. An experimental investigation of effusivity as an indicator of powder blend uniformity. *Powder Technol* 2008; 181: 149-159.
3. Aulton, M. *Pharmaceutics: The Science of Dosage Form Design*. Edinburgh; New York: Churchill Livingstone 2002; 379 – 396.
4. Muzzio F, Goodridge C, Alexander A, Arratia P, Yang H, Sudah O, Mergen G. Sampling and characterization of pharmaceutical powders and granular blends. *Int. J. Pharm* 2003; 250: 51-64.
5. Crouter A, Briens L. Methods to assess mixing of pharmaceutical powders. *AAPS PharmSciTech* 2019; 20: 84.
6. Bridgewater, J. Mixing of powders and granular materials by mechanical means—a perspective. *Particuology* 2012; 10: 397-427.
7. Poux M, Fayolle P, Bertrand J, Bridoux D, Bousquet J. Powder mixing: Some practical rules applied to agitated systems. *Powder Technol*; 68: 213-234.
8. Domike RD, Cooney CL. Particles and Blending. In Cullen PJ, Románach RJ, Abatzoglou N, Rielly CD eds. *Pharmaceutical Blending and Mixing*: John Wiley & Sons 2015; 81-100.
9. Ortega-Rivas E. *Unit Operations of Particulate Solids: Theory and Practice*. Boca Raton: CRC Press 2016.
10. Weinekötter R, Gericke H. *Mixing of Solids*: Springer 2006.
11. Weinekötter R. Mixing of Solid Materials. In Merkus H, Meesters G, eds. *Production, Handling and Characterization of Particulate Materials*: Springer 2016; 291-326
12. Hausman D, Cambron R, Sakr A. Application of Raman spectroscopy for on-line monitoring of low dose blend uniformity. *Int. J. Pharm* 2005; 298: 80-90.
13. Vergote G, De Beer T, Vervaet C, Remon J, Baeyens W, Diericx N, Verpoort F. In-line monitoring of a pharmaceutical blending process using FT-Raman spectroscopy. *Eur J Pharm Sci*; 21: 479-485.

14. Engisch W, Muzzio F. Using Residence Time Distributions (RTDs) to Address the Traceability of Raw Materials in Continuous Pharmaceutical Manufacturing. *J Pharm Innov* 2016; 11: 64-81.
15. Asachi M, Nourafkan E, Hassanpour A. A review of current techniques for the evaluation of Powder Mixing. *Adv Powder Technol* 2018; 29: 1525–1549.
16. Plumb K. Continuous Processing in the Pharmaceutical Industry: Changing the Mind Set. *Chem Eng Res Des* 2005; 83: 730-738.
17. Van der Wel P. Powder Mixing. *Powder Handl Process* 1999; 11: 83-86.
18. Kuo HP, Hsu RC, Hsiao YC. Investigation of axial segregation in a rotating drum. *Powder Technol* 2005; 153: 196-203.
19. Pereira GG, Cleary PW. De-mixing of binary particle mixtures during unloading of a V-blender. *Chem Eng Sci* 2013; 94: 93-107.
20. Brone D, Wightman C, Connor K, Alexander A, Muzzio F, Robinson P. Using flow perturbations to enhance mixing of dry powders in V-blenders. *Powder Technol* 1997; 91: 165-172.
21. Alexander A, Muzzio F, Shinbrot T. Segregation patterns in V-blenders. *Chem Eng Sci* 2003; 58: 487-496.
22. Lemieux M, Bertrand F, Chaouki J, Gosselin P. Comparative study of the mixing of free-flowing particles in a V-blender and a bin-blender. *Chem Eng Sci* 2007; 62: 1783-1802.
23. Brone D, Alexander A, Muzzio F. Quantitative characterization of mixing of dry powders in V-blenders. *AIChE J* 1998; 44: 271-278.
24. Oka S, Sahay A, Meng W, Muzzio F. Diminished segregation in continuous powder mixing. *Powder Technol* 2017; 309: 79-88.
25. Alexander A, Shinbrot T, Johnson B, Muzzio F. V-blender segregation patterns for free-flowing materials: Effects of blender capacity and fill level. *Int J Pharm* 2004; 269: 19-28.
26. Sandeep CS, Senetakis K, Cheung D, Choi CE, Coop MR, Ng CWW. Experimental study on the coefficient of restitution of grain against block interfaces for natural and engineered materials. *Can Geotech J* 2021; 58: 35-48.

27. Lun CKK, Savage SB. The Effects of an Impact Velocity Dependent Coefficient of Restitution on Stresses Developed by Sheared Granular Materials. *Acta Mech* 1986; 63: 15-44.
28. Goldsmith W. *Impact; the theory and physical behaviour of colliding solids*. London, England: E Arnold; 1960.
29. Marinack Jr MC, Musgrave RE, Higgs III CF. Experimental Investigations on the Coefficient of Restitution of Single Particles. *Tribol Trans* 2013; 56: 572-580.
30. Aguiar CE, Laudares F. Listening to the coefficient of restitution and the gravitational acceleration of a bouncing ball. *Am J Phys* 2003; 71: 499-501
31. Crouter A, Briens L. The effect of granule moisture on passive acoustic emissions in a V-blender. *Powder Technology* 2016; 299: 226-234.
32. Cameron A, Briens L. Monitoring lubricant addition in pharmaceutical tablet manufacturing through passive vibration measurements in a V-blender. *Powder Technol* 2020; 364: 708-718.
33. Salman AD, Verba A, Lukenics Zs, Szabó M. Effects of impact velocity and angle on collision. *Period Polytech Chem Eng* 1991; 35: 43-51.
34. Deveswaran R, Bharath S, Basavaraj B, Abraham S, Furtado S, Madhavan V. Concepts and Techniques of Pharmaceutical Powder Mixing Process: A Current Update. *Res J Pharm Technol* 2009; 2: 245-249.
35. Garcia TP, Wilkinson SJ, Scott JF. The Development of a Blend-Sampling Technique to Assess the Uniformity of a Powder Mixture. *Drug Dev Ind Pharm* 2001; 27: 297-307.
36. Hausman D, Cambron R, Sakr A. Application of Raman spectroscopy for on-line monitoring of low dose blend uniformity. *Int J Pharm* 2005; 298: 80-90.
37. Susana L, Canu P, Santomaso A. Development and characterization of a new thief sampling device for cohesive powders. *Int J Pharm* 2011; 416: 260-267.
38. Yu LX, Amidon G, Khan MA, Hoag SW, Polli J, Raju GK, Woodcock J. Understanding Pharmaceutical Quality by Design. *APPS J* 2014; 16: 771-783.
39. Beg S, Hasnain MdS, Rahman M, Swain S. Chapter 1 - Introduction to Quality by Design (QbD): Fundamentals, Principles, and Applications. In: Beg S, Hasnain MdS eds. *Pharmaceutical Quality by Design*: Academic Press 2019; 1-17.

40. U.S. Department of Health and Human Services, Food and Drug Administration, Center for Drug Evaluation and Research (CDER), Center for Biologics Evaluation and Research (CBER). Guidance for Industry – Q8(R2) Pharmaceutical Development; 2009. Available from: <https://www.fda.gov/regulatory-information/search-fda-guidance-documents/q8r2-pharmaceutical-development>
41. Sulub Y, Konigsberger M, Cheney J. Blend uniformity end-point determination using near-infrared spectroscopy and multivariate calibration. *J Pharm Biomed Anal* 2011; 55: 429-434.
42. Jaumot J, Igne B, Anderson C, Drennen C, de Jaun A. Blending process modeling and control by multivariate curve resolution. *Talanta* 2013; 117: 492-504.
43. Besseling R, Damen M, Tran T, Nguyen T, van den Dries K, Oostra W, Gerich A. An efficient, maintenance free and approved method for spectroscopic control and monitoring of blend uniformity: the moving F-test. *J Pharm Biomed Anal* 2015; 114: 471-481.
44. Lee WB, Widjaja E, Heng PWS, Chan LW. Near infrared spectroscopy for rapid and inline detection of particle size distribution variability in lactose during mixing. *Int J Pharm* 2019; 566: 454-462.
45. Rinnan A, van den Berg F, Engelsen SB. Review of the most common preprocessing techniques for near infrared spectra. *TrAC* 2009; 28: 1201-1222.
46. Tewari J, Strong R, Boulas P. At-line determination of pharmaceuticals small molecules' blending end point using chemometric modeling combined with Fourier transform near infrared spectroscopy. *Spectrochim Acta A Mol Biomol Spectrosc* 2017; 173: 886-891.
47. El-Hargrasy A, Drennen J. A Process Analytical Technology approach to near-infrared process control of pharmaceutical powder blending. Part III: Quantitative near-infrared calibration for prediction of blend homogeneity and characterization of powder mixing kinetics. *J Pharm Sci* 2006; 95: 422-434.
48. De Beer T, Bodson C, Dejaegher B, Walczak B, Vercruysse P, Burggraeve A, Lemos A, Delattre L, Heyden Y, Remon J, Vervaet C, Baeyens W. Raman spectroscopy as a process analytical technology (PAT) tool for the in-line monitoring and understanding of a powder blending process. *J Pharm Biomed Anal* 2008; 48: 772-779.

49. Allen P, Bellamy LJ, Nordon A, Littlejohn D, Andrews J, Dallin P. In situ monitoring of powder blending by non-invasive Raman spectrometry with wide area illumination. *J Pharm Biomed Anal* 2013; 76: 28-35.
50. Riolo D, Piazza A, Cottini C, Serafini M, Lutero E, Cuoghi E, Gasparini L, Botturi D, Marino IG, Aliatis I, Bersani D, Lottici PP. Raman spectroscopy as a PAT for pharmaceutical blending: Advantages and disadvantages. *J Pharm Biomed Anal* 2018; 149: 329-334.
51. Nakagawa M, Altobelli Sam Caprihan A, Fukushima E, Jeong EK. Non-invasive measurements of granular flows by magnetic resonance imaging. *Exp Fluids* 1993; 16: 54-60.
52. Hill KM, Caprihan A, Kakalios J. Bulk Segregation in Rotated Granular Material Measured by Magnetic Resonance Imaging. *PLR* 1997; 78: 50-53.
53. Kawaguchi T, Tsutsumi K, Tsuji Y. MRI Measurement of Granular Motion in a Rotating Drum. *Part Part Syst Charact* 2006; 23: 266-271.
54. Porion P, Sommier N, Faugère AM, Evesque P. Dynamics of size segregation and mixing of granular materials in a 3D-blender by NMR imaging investigation. *Powder Technol* 2004; 141: 55-68.
55. Yang C, Fu X. Development and validation of a material-labeling method for powder process characterization using X-ray computed tomography. *Powder Technol* 2004; 146: 10-19.
56. Chester A, Kowalski J, Coles M, Muegge E, Muzzio F, Brone D. Mixing dynamics in catalyst impregnation in double-cone blenders. *Powder Technol* 1999; 102: 85-94.
57. Liu R, Yin X, Li H, Shao Q, York P, He Y, Xiao T, Zhang J. Visualization and quantitative profiling of mixing and segregation of granules using synchrotron radiation X-ray microtomography and three dimensional reconstruction. *Int J Pharma* 2013; 445: 125-133.
58. Bulent Koc A, Silleli H, Koc C, Dayioğlu M. Monitoring of Dry Powder Mixing with Real-Time Image Processing. *J Appl Sci* 2007; 7: 1218-1223.
59. Le Coënt A, Rivoire A, Briançon S, Lieto J. An original image-processing technique for obtaining the mixing time: The box-counting with erosions method. *Powder Technol* 2005; 152: 62-71.

60. Chen C, Yu C. Two-dimensional image characterization of powder mixing and its effects on the solid-state reactions. *Mater Chem Phys* 2004; 85: 227-237.
61. Realpe A, Velázquez C. Image processing and analysis for determination of concentrations of powder mixtures. *Powder Technol* 2003; 134: 193-200.
62. Liu X, Zhang C, Zhan J. Quantitative comparison of image analysis methods for particle mixing in rotary drums. *Powder Technol* 2015; 282: 32-36.
63. Ammarcha C, Gatumel C, Dirion J, Cabassud M, Berthiaux H. Continuous powder mixing of segregating mixtures under steady and unsteady state regimes: Homogeneity assessment by real-time on-line image analysis. *Powder Technol* 2017; 315: 39-52.
64. Daumann B, Fath A, Anlauf H, Nirschl H. Determination of the mixing time in a discontinuous powder mixer by using image analysis. *Chem Eng Sci* 2009; 64: 2320-2331.
65. Berthiaux H, Mosorov V, Tomczak L, Gatumel C, Demeyre JF. Principal component analysis for characterising homogeneity in powder mixing using image processing techniques. *Chem Eng Process* 2006; 45: 397-403.
66. Tily P, Porada S, Scruby C, Lidington S. Monitoring of mixing processes using acoustic emission. In: Harnby N, Benkreira H, Carpenter K, Mann R, eds. *Fluid Mixing III*. Rugby: The Institute of Chemical Engineers 1988; 75-94.
67. Bellamy L, Nordon A, Littlejohn D. Non-invasive monitoring of powder mixing with near infrared spectrometry and acoustics. *Spectrosc Eur* 2004; 16: 30-32.
68. Allen P, Bellamy L, Nordon A, Littlejohn D. Non-invasive monitoring of the mixing of pharmaceutical powders by broadband acoustic emission. *Analyst* 2010; 135: 518-524.
69. Bruneau M. *Fundamentals of Acoustics*. London, England: ISTE Ltd; 2006.
70. Anselmet F, Mattei PO. *Acoustics, aeroacoustics and vibrations*. Hoboken, New Jersey: John Wiley & Sons Inc; 2016.
71. Cameron A, Briens L. An Investigation of Magnesium Stearate Mixing Performance in a V-Blender Through Passive Vibration Measurements. *AAPS PharmSciTech* 2019; 20: 199.

72. Cameron A, Briens L. Monitoring Magnesium Stearate Blending in a V-Blender Through Passive Vibration Measurements. AAPS PharmSciTech 2019; 20: 269.

Chapter 2

2 Review of Process Analytical Technologies

Pharmaceutical production of tablets requires the mixing of several powder components. Powder mixing is a highly complicated process that needs methods to ensure that the final product will meet the high-quality requirements for pharmaceutical production. Currently, pharmaceutical powder mixing is mainly monitored using thief probe analysis. Thief probe analysis is an offline monitoring method that utilizes a probe to remove samples of powder from the powder bed and analyze the samples using destructive testing methods (1-3). The use of thief probe analysis has several disadvantages including powder bed disruption, sampling errors, and mixture misrepresentation (1,4-6). While these disadvantages can be somewhat mitigated by strict adherence to procedures, previous examples such as the 1993 case of *The United States versus Barr Laboratories* show that, even with careful actions, thief probe analysis still presents various error risks (7-9).

A lack of real-time, inline monitoring techniques limits the transition of pharmaceutical processing from batch towards continuous processing. Continuous processing provides several advantages for pharmaceutical processing including minimizing factors such as mixing times, equipment size, segregation risk, and cost (10-12). Continuous processing also allows for the creation of mathematical models to further improve the quality and optimization of mixing processes through an improved understanding of the motion of particles during mixing (11,12). However, without accurate inline monitoring methods, continuous processing remains very challenging.

Process analytical technologies (PATs) are methods used to monitor, analyze, design, and control processes (13,14). The use of these technologies can provide real-time, inline critical information on powder behaviours and mixture quality (13,14). One of the most critical parameters of mixture quality that can be identified using PATs is mixture homogeneity. Homogeneity is defined by Merriam Webster's dictionary as "the quality or state of being of a similar kind or of having a uniform structure or composition throughout" and can provide insight into a mixture's endpoint or segregation levels (15).

The information collected by PATs can be used to improve and optimize process designs and operation parameters to further improve the safety, quality, and efficiency of mixing processes (14). Using PATs supports the QbD philosophy, ensuring high quality standards can be achieved through the process itself. Despite the support of PATs by many regulatory groups, industry has been hesitant to embrace PATs (14,16). Providing accurate literature supporting the applications and benefits of PATs may help to encourage industry stakeholders to adopt PATs more readily.

PATs can be sorted into four different categories: Spectroscopic, Velocimetric, Tomographic, and Passive Acoustic Emissions. Spectroscopic PATs are based upon electromagnetic radiation. When a particle is exposed to electromagnetic radiation the specific resonance wavelengths measured will be unique based upon the particle's molecular structure (17). Spectroscopic PATs include near-infrared spectroscopy and Raman spectroscopy. Velocimetric PATs are based upon the tracing of specific particles throughout the particle bed during mixing. These particles may be radioactive, sensitive to electromagnetic radiation, or have distinct visual differences from the bulk powder. Velocimetric PATs include optical image analysis and positron emission particle tracking. Tomographic PATs are based upon the transmission and reflectance of an energy wave applied to a bulk powder (18-20). The information collected is used to produce images of the bulk powder and the bulk powder cross-section. Tomographic PATs include magnetic resonance imaging and X-ray computed tomography. Passive acoustic emission monitoring is based upon acoustic emissions released during impacts between particles and the mixer wall, and between different particles (21).

2.1 Near-Infrared Spectroscopy

2.1.1 Method of Monitoring

NIR spectroscopy relies on analyzing how particles react when exposed to NIR light. When exposed to NIR light, molecule bonds within the particle absorb the light causing the molecules to vibrate (17,22). Vibrations vary relative to the bond compositions present. The wavelength range for NIR light is generally from 780 nm to 2500 nm (23-26). The main bonds observed during NIR spectroscopy use are C-H, O-H, S-H, and N-H

bonds (24-26). Variations in the vibrations measured allow for the composition of a mixture to be determined.

Data collected via NIR spectroscopy requires intensive pre-processing. Five of the most common pre-processing methods are normalization, standard normal variate (SNV), Savitzky–Golay algorithm, multiplicative scatter correction (MSC), and detrending (DT). The normalization method divides the spectra data by the mean value of the individual spectrums (27). Unlike other methods, normalization does not shift the spectra. The SNV method subtracts the mean value of the full spectrum from the spectra data (28). This value is then divided by the standard deviation of the spectra. The SNV method is used to remove baseline contributions and interference related to particle scatter and size. The Savitzky–Golay algorithm method fits the spectra data to a polynomial (29). This method is used to provide a simple derivative calculation and a smoothed fit. The Savitzky–Golay algorithm method has also been noted to be more sensitive to noise than other pre-processing techniques (30). The MSC method uses linear regression on a reference spectrum (31). This linear regression allows coefficients to be determined for use in the scattering effects mitigation calculation. The MSC method helps to reduce noise in the data caused by scattering (32). The DT method fits spectra data points to a low degree polynomial (27). The newly fit data points are then subtracted from the spectrum data. The DT method mitigates baseline shift and curvilinearity variances by providing an adjusted spectrum (28).

Post-processing of NIR data is performed using various techniques. Two of the most common techniques are principal component analysis (PCA) and partial least squares (PLS). The PCA method uses a singular matrix of spectra data to reconstruct the NIR spectra (33,34). The singular matrix is decomposed into several lower dimension matrixes which are then analyzed. This analysis provides spectral data that is used for several applications such as determining spectra uniformity. The PLS method uses data regression to reconstruct collinear variables into orthogonal variables. These orthogonal variables can be used for various applications such as predicting analytical values. Other post-processing methods include principal component regression, relative standard deviation, and moving block standard deviation.

Based on available literature, NIR spectroscopy is the PAT most heavily under development (Table 2.1). NIR spectroscopy has been applied to various processes with several studies showing its effectiveness for monitoring powder mixing. In multi-component powder mixing applications, NIR spectroscopy has been found to be effective at identifying composition, homogeneity, and endpoint. Specific setups and processing techniques have been studied for NIR spectroscopy, allowing for optimization of the process design (35).

Table 2.1: Selection of available literature for NIR spectroscopy for mixing

Reference	Components	Mixer	Pre-processing	Post-processing	Purpose	Results
(36)	Micro-crystalline cellulose, Acetaminophen, Colloidal silicon dioxide, Magnesium stearate	Continuous horizontal stationary drum mixer	SNV, SG	PLS	Identify mixture concentration	Results support the potential for continuous mixing as a real time monitoring method to determine component concentrations
(37)	Milled acetaminophen, Lactose 100M, Lactose 125M	Continuous horizontal stationary angled drum mixer	Unspecified	Relative Standard Deviation	Identify the effect of varying process parameters	Results show the effects. These results support the potential of NIR monitoring to monitor process parameters
(38)	Calcium carbonate, maize starch	Continuous horizontal stationary drum mixer	Unspecified	Unspecified	Determine effectiveness of monitoring method for process	Results show that NIR monitoring is highly effective at monitoring continuous and batch processes on and offline

Reference	Components	Mixer	Pre-processing	Post-processing	Purpose	Results
(39)	Active, Magnesium stearate, granules	Continuous blender	SNV, SG	PLS	Identify mixture concentration and effect of varying process parameters	Results show varying parameters such as mass flow and rotation speed effects the PLS model.
(40)	Naproxen sodium, Lactose monohydrate, Magnesium stearate	Continuous low shear tumble mixer	Roots mean standard error of prediction, and relative standard deviation	PCA, MCS, PLS	Determine effectiveness of newly proposed model-based strategy for inline modeling	Results show proposed calibration model for NIR is effective in providing more control of the mixing process
(41)	Salicylic acid, Fast-Flo lactose, Methanol	Batch V-shell mixer	Second derivative	Principal component regression, PLS, multiterm linear regression	Identify blend homogeneity	Results show the proposed calibration model was successful in predicting the blend homogeneity measured by the NIR monitor
(42)	Actives, Microcrystalline Cellulose, Dibasic calcium phosphate, Polyplasdone	Batch tumbling mixer	SG, SNV, relative standard deviation	PLS	Identify mixture end point	Results showed that NIR monitoring is effective at determining the end point of a mixture, even in small scale commercial applications

Reference	Components	Mixer	Pre-processing	Post-processing	Purpose	Results
	XL, Sodium bicarbonate, Lactose, Silica, Crosspovidone, Talc					
(43)	Actives, Microcrystalline Cellulose, Silicon dioxide, Magnesium stearate, Croscarmellose sodium, Mannitol	Batch V-shell mixer	Unspecified	PLS, principal component regression	Identify mixture uniformity and end point	<p>Results showed that NIR monitoring is effective.</p> <p>The performance of NIR models depend on factors such as the materials and analytical techniques selected</p>
(44)	Active, Lactose, Talc, unspecified minor excipients	Bin mixer	SNV, second derivative, SG	Moving block standard deviation	Identify mixture end point	Results showed that NIR can determine mixture end point, and that the proposed mechanistic approach provides a potential solution for using NIR monitoring without calibration

Reference	Components	Mixer	Pre-processing	Post-processing	Purpose	Results
(45)	Unspecified 3 component powder blend	Y-cone mixer	SNV, DT	Moving block standard deviation	Identify mixture uniformity	Results showed that NIR can be used for online monitoring through the use within a fully automated system
(46)	Granulated acetaminophen, Micro Crystalline Cellulose, Magnesium stearate	Vortex shaker	Baseline correction, MSC, SNV, first derivative, second derivative	PLS	Monitor API concentration at the mixer discharge	Results showed that NIR can be used for real-time-release of mixtures based on the mixture uniformity
(34)	Active, Micro Crystalline Cellulose, Dibasic calcium phosphate anhydrous, Sodium starch glycolate, Magnesium stearate	Flobin blender	Raw spectral data, Detrending, SNV, Savitzky-Golay variation (second derivatives), SNV + Detrending	Mean standard deviation versus blend time, Dissimilarity versus blend time, PCA, Guided PCA, Soft independent modelling of class analogy	To investigate the effectiveness of various pre- and post-treatments for monitoring mixture homogeneity	Results showed that there was minimal differences in results between the various pre- and post-treatments tests, it was noted that Savitzky-Golay variation was more sensitive to noise than other pre-treatments

Reference	Components	Mixer	Pre-processing	Post-processing	Purpose	Results
(25)	2 unspecified powders, one fine and one coarse	Nauta mixer	MSC, mean spectrum	PLS	Propose and present a new method for in-line monitoring of powder mixtures through NIR	Results showed that the proposed NIR method can be used for in-line real time monitoring of mixture homogeneity
(35)	Acetylsalicylic acid, α -lactose monohydrate	Blending vessel with a four-bladed stirrer	Wave-number averaging, cutting of the spectral band, SNV	PLSR	Present a multi-probe NIR setup to monitor blend behaviour throughout the powder bed	Results showed that the multi-probe NIR setup is effective in monitoring the initial state, segregation, blending dynamics, and particle motion
(47)	Starch, Carboxymethyl starch, Microcrystalline cellulose, Otilonium bromide	Unspecified	SNV	Moving block standard deviation, dissimilarity, mean square of differences	Identify mixture uniformity and end time	Results showed that the NIR monitoring method proposed is as accurate as current industry standards. Without the correct data analysis mixtures with similar spectra may not be distinguishable

2.1.2 Advantages

NIR spectroscopy provides an effective method for inline monitoring of mixing. Previous studies have shown success in identifying a multi-component composition, homogeneity, and endpoint. Extensive previous literature has provided a strong understanding of the strengths of NIR spectroscopy and strategies for optimization. NIR spectroscopy can be applied to systems as an inline or offline monitoring system thus increasing applications. As NIR spectroscopy is able to accurately identify the chemical composition of particles, it can also complement or be integrated into other methods.

2.1.3 Disadvantages

NIR spectroscopy is a very expensive monitoring method. NIR signals have extensive pre-processing and post-processing requirements leading to increased equipment and labour costs (48). Along with high costs due to data analysis requirements, NIR spectroscopy also requires permanent equipment modification. Window ports and probes must be added in various locations around the equipment (49). NIR spectroscopy probes can only take measurements in the area immediately local to the probe. Without the costly addition of multiple probes, accurate monitoring is challenging. To ensure the strategic probe location, prior knowledge of the mixing process is required. The added windows and probes also have complications due to the window fouling. The measurements collected by the NIR probes may also be negatively impacted by process factors including moisture content, particle size, polymorphism, and packing density.

2.2 Raman Spectroscopy

2.2.1 Method of Monitoring

Raman spectroscopy is a monitoring method based on differences in light scattering (50,51). When a powder mixture is exposed to monochromatic light, the particles in the mixture will absorb a portion of the light while scattering the rest. Depending on the molecular composition and the polarizability of the particles present, light is absorbed

and scattered differently (50). Typically, the light will be elastically scattered, with the scattered light maintaining the same frequency as the monochromatic light. However, a small section of the light will interact with an excited electron and the light will be scattered with a frequency lower or higher than the frequency of the monochromatic light. If the scattered light has a lower frequency, Anti-Stokes lines will occur, and if the light has a higher frequency, Stokes lines will occur (52,53). Anti-stokes and Stokes lines refer to the spectral lines that occur when light is scattered. The spectrum produced from the scattered light is referred to as the Raman spectrum (52,54). The Raman spectrum provides an overview of the composition of the mixture. After scattering, the difference in energy between the scattered light and the original monochromatic light is referred to as the Raman shift. Probes are used to detect the scattered photons. Measurements collected from the probes are used to provide insight into factors including the composition of a mixture and its homogeneity. When interpreting the measurements to identify homogeneity, data can be compared to previously obtained control spectra of the desired homogeneous mixture.

Raman spectroscopy has been studied for several pharmaceutical processing applications including tablet analysis (55), mixing (2,4,56-58), fluidization (59,60), granulation (61,62), and extrusion (63,64). In applications, the most common wavelength used was 785 nm. Monitoring of powder mixing using Raman spectroscopy has limited published literature available (Table 2.2). Most research on monitoring powder mixing using Raman spectroscopy has focused on proving the effectiveness of this method and comparing it to other significant monitoring methods such as NIR spectroscopy, high-performance liquid chromatography (HPLC), and acoustic emission analysis (2,4,57,58). While these studies have identified potential limitations of Raman spectroscopy, overall, it was determined that Raman spectroscopy can provide accurate inline monitoring of powder mixture homogeneity.

Table 2.2: Summary of some literature available on the application of Raman spectroscopy to powder mixing operations

Reference	Components	Mixer	Wavelength	Purpose	Results
(2)	Paraffinic wax, Drum dried corn starch, Sodium starch glycolate, drug pellets	Planetary mixer	1064nm	To determine the effectiveness of FT-Raman spectroscopy for inline monitoring of powder mixing	FT-Raman spectroscopy effectively monitored powder mixing
(4)	Azimidide dihydrochloride, spray-dried lactose, crospovidone, Magnesium stearate	V-blender	785nm	To determine the effectiveness of Raman spectroscopy for low dose mixtures using univariate and multivariate methods	Raman spectroscopy is effective for monitoring low dose mixtures in V-blenders
(56)	Diltiazem hydrochloride, Avicel PH 102, lactose DCL 21, silicon dioxide	GraI™ 10 high shear mixing system	785nm	To determine a new strategy for implementing Raman spectroscopy for monitoring powder mixing to identify the endpoint and provide insight into the process	Raman spectroscopy is effective for monitoring the endpoint and homogeneity of a mixture, it also provided important insight into the mixing process
(57)	Microcrystalline cellulose (Avicel PH-101), aspirin, aspartame	Convective mixer with impeller	785nm	To describe the first application of a PhAT probe to monitor powder mixing and determine the effects of particle size on Raman spectroscopy	Mixing profiles were produced and results were compared with those of NIR spectrometry and acoustic emissions, Raman

Reference	Components	Mixer	Wavelength	Purpose	Results
					spectroscopy was found to be less sensitive than NIR spectroscopy but was able to identify the endpoint of the mixture and the concentration of the mixture in real time
(58)	Unspecified API, lactose, Magnesium stearate	Dyna-MIX® blender with two simultaneous rotating axes	473.1nm	To determine the effectiveness of Raman spectroscopy for mixtures with low API concentrations and the effects of low API concentration on blend time, results of Raman spectroscopy monitoring to HPLC were compared	Detailed mixing profiles were produced at a high speed rate, however, Raman spectroscopy cannot fully replace HPLC

2.2.2 Advantages

Raman spectroscopy allows for real-time inline monitoring. There are minimal sample preparation and pre-processing requirements. Raman spectroscopy shows potential for the use of automation to control batch processes. Implementation of automation helps to improve the efficiency and quality of processes.

Raman spectroscopy has several advantages over other forms of spectroscopy including NIR spectroscopy. When comparing the data analysis requirements for both methods, Raman spectroscopy is noted to use much simpler methods. Raman spectroscopy can also be applied to more diverse situations including mixtures with moist powders, crystalline compounds, and multiple components. The water present in moist powders can mask the results obtained from NIR spectroscopy thus Raman spectroscopy is preferred for mixtures with moist powders. Most spectroscopy methods are not highly sensitive to crystalline compounds. However, Raman spectroscopy is sensitive to polymorphism and is therefore preferred for mixtures including crystalline compounds. Raman spectroscopy is preferred over other spectroscopy methods for multicomponent mixtures as the measured peaks obtained through Raman spectroscopy are more intense than other spectroscopy methods, thus allowing for higher chemical specificity. High chemical specificity allows for more simplistic univariate analysis.

2.2.3 Disadvantages

Raman spectroscopy shares several disadvantages with NIR spectroscopy. One such disadvantage is the requirement for a line of sight into the mixture to be monitored. This requirement means that equipment must be designed with transparent areas or windows. If Raman spectroscopy is applied to pre-existing systems, costly equipment alterations may be required. As well, to allow for accurate monitoring, several probes must be installed, thus leading to further equipment alterations and costs. The system requirements to use Raman spectroscopy create potential further complications in the form of windows or probes becoming obscured or fouled.

A significant disadvantage for Raman spectroscopy is the risk of fluorescence. Fluorescence occurs when a molecule fully absorbs a photon and then releases a lower energy photon (52,65). If fluorescence occurs, the measurements obtained may be masked thus decreasing the accuracy of this measurement. Depending on the components under analysis and the wavelength used, fluorescence may occur. This risk decreases the acceptable application for Raman spectroscopy. Other disadvantages of Raman spectroscopy include size requirements for sample zones and inaccuracies when monitoring mixtures with large variations in particle sizes.

2.3 Optical Image Analysis

2.3.1 Method of Monitoring

Optical image analysis is one of the earliest non-invasive, inline monitoring methods. Optical image analysis utilizes cameras to take images and/or videos during the mixing process and identify any visual changes that occur. The changes observed in optical image analysis rely on tracer particles or colour changes throughout the powder bed (66,67). Tracer particles are used for studies where optical image analysis is used to monitor specific elements of particle motion during powder mixing, such as trajectory. Colour changes in the powder bed are used to monitor the homogeneity of multi-colour powder mixtures. A critical component of optical imaging is selecting the camera location(s). Mixtures can be monitored during the mixing process or during the ejection of material from the mixer. To monitor the mixture during the mixing process, mixers usually must either be transparent or have windows to allow for cameras to see within the mixer shell. The use of optical image analysis with tracer particles requires the use of particle image velocimetry to correlate consecutive images taken at a specific time difference. This method is used to determine the velocity and displacement vectors of particles within a selected region.

Due its age, optical image analysis has a large amount of literature available (Table 2.3). Studies have been completed with various mixer geometries, components, and camera locations. Mixer geometries have included both vessels with impellers and without impellers. The literature has indicated that the use of several cameras in locations around the mixer improves the accuracy of the monitoring results. Most often cameras are located either above the mixer or above the outlet. Optical image analysis has been found to be effective in identifying the mixing profile, homogeneity, and segregation of a powder mixture.

Table 2.3: A selection of previous studies of Image analysis for mixing

Reference	Components	Mixer	Camera Location	Purpose	Results
(68)	Glass beads	Acrylic cylindrical vessel with impeller	At the wall	Gain insight into the fundamentals of powder mixing	Results provided insight into particle motion when being mixed in vessels with impellers
(69)	Lactose anhydrous, microcrystalline cellulose, pregelatinized starch, blue color additive, chocolate	Unspecified	Outside of mixer, above a sample cell	Identify mixture uniformity and localized component concentrations	Results showed that the image analysis could identify powder concentrations to an appropriate degree
(70)	Titanium, silica, carbon black	Hand shaking bottle, vibrating bottle, mechanical stirrer, and stirring with ultrasonic shaking	Outside of mixer, above flat plate where samples were placed	Determine important process characteristics, such as mixing profile	These findings improved understanding of powder mixing, such as what mixture properties are important for the quality of the mixture
(67)	Unspecified powders	Glass shell with anchor and helical ribbons	Placed outside 75 cm away from the shell facing horizontally into the center of the shell	Determine mixing time	Method successfully indicated point of uniformity, allowing for the determination of mixing time

Reference	Components	Mixer	Camera Location	Purpose	Results
(71)	Rigid glass beads, non-rigid rubber particles	Acrylic rotating drum mixer	N/A	Monitor axial segregation during powder mixing in a rotating drum mixer	Method successfully monitored segregation propagation during mixing and identified the parameters that effect segregation
(72)	Semolina, undyed and dyed with iodine	N/A	Above conveyor belt	Monitoring mixture homogeneity, determine homogeneity ratio	Image analysis of the powder was able to produce a sense of the segregation present in the sample
(66)	White plaster, black and red powder dyes	Batch style vessel mixer	Above the mixing chamber, observing one side of the vessel	Monitor overall mixture	Results showed image processing was able to monitor mixture in real time to determine the degree of uniformity
(73)	Cement, ultramarine blue	Discontinuous horizontal twin-shaft paddle mixer	Above the mixing chamber, observes full length of the mixer	Identify mixing time for a process	Optical image analysis can effectively determine the required mixing time of a batch. Requirements of the method include the camera having access to the mixing chamber and three-dimensional mixing transport must occur

Reference	Components	Mixer	Camera Location	Purpose	Results
(74)	Lactose monohydrate, microcrystalline cellulose, HPMC, croscarmellose sodium	Vessel with three bladed impellers	Above the vessel, angled perpendicular to the powder surface	Identify the effects of scaling vessels and processes on flow patterns during mixing	Effects on the flow pattern was identified and a model was created to describe the flow behaviour
(75)	Red oak chips, glass beads	Double screw mixer	Four cameras were used showing the top, bottom, right, and left sides of the shell	Evaluate the effects of operating parameters on powder mixing	Optimal operating parameters were identified to encourage optimal mixing performance
(76)	Red and white plastic balls	Drum mixer with glass plate on the front end	In front of mixer glass plate	Comparison of difference image analysis methods	Concluded that overall image analysis should be standardized due to potential deviances in calculated mixing time dependent on methods
(77)	Couscous, undyed and dyed with iodine	hemi-cylindrical continuous mixer with screw blade	Outside of mixer, above outlet conveyor belt	Monitoring mixture homogeneity	Image analysis can provide information regarding segregation present in the process

2.3.2 Advantages

Optical image analysis is a valuable tool for preliminary studies into powder mixing. This method allows for observations of factors such as segregation patterns and mixture

homogeneity. The vast amount of literature available for optical image analysis and the maturity of the method allows for a well understood method that requires low-cost equipment.

2.3.3 Disadvantages

Optical image analysis requires components to be different colours. Pharmaceutical powders are most often white, thus for image analysis to be used powders must be dyed without impacting their properties. As well, to view the multi-coloured components, equipment would need to be modified with multiple windows. These modifications are costly and may present challenges when trying to meet strict manufacturing regulations. Window locations must be selected carefully as the only areas of the powder bed that will be analyzed is the powder adjacent to the windows. This limitation may result in image analysis results that are not representative of the full mixture. The window locations may not be clear to select as image analysis methods are not standardized (67). This lack of standardization results in a limited understanding of image analysis as literature is difficult to compare. For some equipment it may not always be possible to have windows or to access the window locations. Damage to the windows also risks impacting the image quality thus impacting the measured results.

2.4 Positron Emission Particle Tracking

2.4.1 Method of Monitoring

Positron emission particle tracking (PEPT) is a monitoring method that uses radioactive particle tracking (RPT). Sensors detect the disintegration of radioactive particles within a powder bed to non-invasively provide information regarding the velocity or location of these particles (78,79). PEPT is one of the most common RPT methods. Positrons released produce photons when interacting with electrons in the surrounding bulk powder. The photons are released linearly in opposite directions, sensors are then able to detect the photons. The line between the detectors that coincides with the photons is referred to as the line of response (LoR), the location of the particle lies within the LoR

(80). This information is then used to determine the trajectory and the velocity of the tracer particle.

PEPT has been investigated for mixer geometries including V-blenders, drum mixers, and bladed mixers (Table 2.4). Literature has described different components and tracers. One tracer identified for PEPT monitoring is radioactive Magnesium stearate (81). Magnesium stearate is a common powder lubricant used for pharmaceutical manufacturing, highlighting how PEPT can be applied to monitoring powder mixing for pharmaceutical production. The use of PEPT has helped to provide detailed information on particle motion during mixing, see table 3.4 (79). The level of detail in this information cannot be attained using most other monitoring methods. This information helps to improve understanding of the motion of particles allowing for more accurate mixing models to be developed and verified. Current research shows potential for PEPT to be applied for monitoring particle circulation, particle dispersion, particle behaviour, and the effects of process parameters on mixing processes.

Table 2.4: Selection of available literature for PEPT

Reference	Components	Tracer	Mixer	Purpose	Results
Kuo et al., 2005	Glass beads	Glass beads irradiated with ^{18}F	Acrylic V-blender	Monitoring particle motion during powder mixing	PEPT successfully monitored the mixture, providing insight into particle circulation, flow patterns, and axial dispersion
Perrault et al., 2010	MCC PH101, spray-dried lactose	Radioactive Magnesium stearate monohydrate	Acrylic V-blender	Monitoring Magnesium stearate powder mixing	PEPT successfully monitored the mixture, determined the effects of process conditions on powder formulas including Magnesium stearate, and validated the use of Magnesium stearate as a tracer
Portillo et al., 2010	Edible lactose, fast flo lactose	Ion-exchange resin tracer with absorbed ^{18}F	Continuous cylindrical mixer with impeller	Identify the effects of the process parameters, impeller rotation rate, powder cohesion, and powder flow rate, on the powder flow during mixing	PEPT successfully monitored the mixture and provided information otherwise unattainable to improve the understanding of process parameter effects and particle motion during

Reference	Components	Tracer	Mixer	Purpose	Results
					mixing. The results help to validate the results of existing literature on particle motion during mixing.
Marigo et al., 2013	Glass beads	Glass beads irradiated with a 33 MeV ^3He beam	Turbula Mixer	To validate a DEM model of the motion and granular flow of particles during mixing	The DEM model was verified for mono-sized particle bed transition behaviours in relation to operating speed, and in general the measured and predicted behaviours were found to be similar with a systematic offset

2.4.2 Advantages

PEPT monitoring is a highly effective method for providing detailed information for process characterization during powder mixing. This monitoring method provides the ability to accurately monitor a small number of tracer particles throughout the powder bed, allowing for detailed monitoring of the motion of the tracer particles during the mixing process including particle location and velocity. Unlike some other methods, PEPT is a non-invasive inline method for powder mixtures within opaque mixers without requiring windows to be installed.

2.4.3 Disadvantages

Tracer particles are required for PEPT monitoring. Tracer particles must be selected carefully to ensure they will be effective with no negative effects on the powder mixture.

Detector locations must be placed around the mixer in specific locations. These locations must be selected using calibration and optimization procedures based on factors such as mixer geometry and tracer particle characteristics of each system. The detailed detector installation and tracer particles required leads to higher costs and research time thus limiting the potential for PEPT systems outside of lab or pilot scale applications. PEPT is also not easily applicable to monitoring powder homogeneity or segregation as PEPT can only monitor the tracer particles (81). Therefore, industrial applications for PEPT are limited. In addition, PEPT monitoring also may require very long experiments to be completed if there is a small number of tracer particles, thus elongating processing times.

2.5 Magnetic Resonance Imaging

2.5.1 Method of Monitoring

Magnetic Resonance Imaging (MRI) analysis, also known as Nuclear Magnetic Resonance (NMR) imaging, is a monitoring technique based upon the NMR of a particle. Utilizing magnetic fields and the Larmor frequencies of atomic nuclei, MRI analysis is able to monitor the spatial distribution of different nuclei throughout the mixture (84-86). Larmor frequencies are a measure of an atomic nucleus' rotational frequency. When the magnetic field surrounding an atomic nucleus is changed, the nucleus becomes agitated. Within the nucleus agitated protons precess around the magnetic field. The proton precess frequency is defined as the Larmor frequency. Larmor frequencies are dependent upon the composition of the particle and proportional to the strength of the magnetic field (84). MRI equipment measure Larmor frequencies by detecting fluctuations in an electrical signal referred to as the NMR signal (84). The NMR signals can be used to identify components and monitor the mixture.

Several previous studies have been completed using MRI analysis in a variety of applications (Table 2.5). Most studies of MRI applications to mixing processes have focused on applications utilizing rotating horizontal drum mixers. In these studies, the cylindrical mixing shell was placed inside an MRI/RF coil, allowing for horizontal slice images to be taken from the center of the drum. Mixing studies were completed using

various components. MRI analysis of mixing has been used to monitor segregation, concentration, and uniformity. These studies show how MRI analysis can provide insight into particle motion and how operational parameters such as mixer geometry impact mixing processes.

Table 2.5: A selection of previous studies of MRI analysis of mixing

Reference	Components	Mixer	Purpose	Results
(85)	Mustard Seeds	Cylindrical Drum Mixer	Identify if MRI can be applied to monitor a solid mixture	MRI can identify velocities, concentrations, and components throughout a mixture, supporting the potential for MRI applications in mixture monitoring
(87)	Mustard Seeds, Glass Beads, Sugar Balls	Rotating Tube	Monitoring pattern formation, segregation, and mixing progress under various conditions	MRI can monitor Axial and Radial Transport. Patterns that developed were able to be identified
(88)	50-50 binary mixture of plastic spheres and pharmaceutical pills	Cylindrical Drum Mixer	Study Bulk Segregation	MRI identified complex segregation structure within the bulk
(89)	2mm diameter spherical particles containing oil cores	Cylindrical Drum Mixer	Develop a new method using MRI to study correlations of random processes and measure velocity	A general parametric method was successfully developed

Reference	Components	Mixer	Purpose	Results
			autocorrelation functions.	
(90)	Sugar Beads, Sugar Beads with Silicon Oil	Turbula Shaker Mixer	Monitoring particle segregation, and mixing	MRI effectively monitored the segregation and mixing of the mixture
(91)	Poppy Seeds, Sugar Beads	Turbula Shaker Mixer	Monitoring particle motion, segregation, and mixing progress under various conditions	MRI can effectively monitor mixing in a Turbula shaker mixer
(92)	3mm diameter spherical particles containing liquid cores	Cylindrical Drum Mixer	Monitoring effects of end wall property on particle flow	MRI effectively identified how wall friction effects mixture flow
(93)	Polystyrene spheres, Gelatin spheres filled with liquid vitamin E	Tapered Drum Mixer	To study radial and axial segregation	MRI effectively monitored the segregation and mixing of the mixture

2.5.2 Advantages

MRI analysis provides a completely non-invasive monitoring technique. There is no requirement for tracers to be added to the mixture. This method also requires no modifications or specific measurement orientation.

2.5.3 Disadvantages

MRI analysis requires the components of the mixture to be sensitive to magnetic induction. If the components do not have free protons, they will not be detected. To mitigate this issue, non-sensitive particles can be coated in an appropriate oil. However, this coating must have no significant impact on the mixtures. The infrastructure required for MRI analysis is also very expensive and difficult to operate, limiting MRI analysis mostly to academia.

2.6 X-ray Computed Tomography

2.6.1 Method of Monitoring

X-ray Computed Tomography (X-ray CT) is an advanced type of X-ray imaging utilized for inline monitoring. In X-ray CT monitoring, a powder mixture is exposed to X-rays, producing cross-sectional images of the powder bed (19). This method works by analyzing differences in the amount of energy absorbed by each particle to produce images. X-ray CT is able to produce individual cross-sections of the powder bed along with images of the 3D structure of the powder bed. Unlike some other 3D imaging techniques, X-ray CT produces a 3D image through multiple projections of the powder bed (20,94).

Several studies have been completed on the application of X-ray CT for monitoring powder mixing (Table 3.6). Available literature shows the potential for X-ray CT applications for various mixer geometries including V-blenders, double cone mixers, and rotating cylinder mixers. X-ray CT monitoring was utilized for applications including monitoring the dynamics of mixing, mixture homogeneity, and segregation. The findings

of these studies indicate that X-ray CT monitoring can identify how process parameters, including particle size, fill level, and rotation rate, can affect the quality of a powder mixture.

Table 2.6: Summary of literature available for X-ray CT for mixing

Reference	Components	Mixer	Purpose	Results
(19)	Oblong pellets	Double-cone mixer	To study the dynamics of powder mixing	X-ray CT monitoring is able to identify radial mixing, axial mixing, dead zones, density gradients in the bed, and other mixture attributes
(94)	Size 0 HPMC capsules filled with Celphere particles impregnated with lead (II)m acetate trihydrate	V-blender	To develop and validate a method for material-labeling	<p>A method was developed using X-ray CT and the impregnated particles for monitoring powder processes including mixing</p> <p>The effects of particle size and loading configuration on mixing was identified</p>
(20)	Non-spherical starch granules, spherical Celphere	Cylindrical drum mixer	To monitor mixture homogeneity and segregation. Also, to gain insight into mixing to allow for the development of profiling	X-ray CT successfully provided 3D information regarding the mixing and segregation of a powder mixture

2.6.2 Advantages

X-ray CT provides an efficient, non-invasive, non-destructive monitoring method. X-ray CT is able to provide imaging of particles at micron resolution (95). The detailed information provided by X-ray CT allows for more in-depth understanding of particle motion within the mixer. This detail analysis makes X-ray CT a very valuable monitoring method for laboratory and research settings.

2.6.3 Disadvantages

X-ray CT is not considered viable for industry applications. The high cost and complicated process cause this PAT to be only useful in laboratory applications. Additionally X-ray CT can be a complex monitoring technique as multiple projections of different areas of the powder sample must be taken to create one image.

2.7 Passive Acoustic Emissions

2.7.1 Method of Monitoring

Passive acoustic emission or vibration analysis is a monitoring method based upon measuring stress waves. During mixing, when a particle collides with another particle or the wall of the mixer, energy is released in the form of waves (21,96,97). Stress waves from the collisions are measured using sensors placed around the mixer. Microphones or accelerometers can be used to measure the vibrations propagated by the stress waves. Particle properties and powder flow will affect the energy released from collisions. Unlike other methods, passive acoustic emission analysis does not require a mixture to be exposed to any outside stimulus, such as X-rays.

When a particle collides with either the mixer wall or another particle there is a sudden change to the local stress and energy is released in the form of transient elastic waves (96,97). Waves produced can be categorized as longitudinal, transverse, and Rayleigh. Longitudinal waves are waves that can exist in any phase and propagate parallel to the energy source. Transverse waves are waves that can only exist in the solid phase and

propagate perpendicular to the energy source. Rayleigh waves form ellipse in semi-infinite medium and are a combination of longitudinal and transverse waves.

All waves can be characterized by wavelength, frequency, speed, and amplitude.

Wavelength (λ) is the distance from one point on the wave to the next instance of that point, for example from one peak to the next. Frequency (f) can be categorized in three magnitude regions as infrasonic (<20 Hz), audible (20-20,000 Hz), and ultrasonic (>20,000 Hz) and is the reciprocal of the period of the wave (98). The period is the length of time required to complete one full wave cycle. The speed (c) of a wave is determined based on its wavelength and frequency:

$$c = \lambda f \quad (eq. 1)$$

In passive acoustic emission analysis, the amplitude is a critical wave characteristic. The amplitude is the distance from the equilibrium line of the wave to a peak or a trough. The energy released during a collision is proportional to the amplitude squared. To monitor a mixture, changes in the amplitude of the wave must be measured and analyzed. A portion of the energy transmitted after the collision is attenuated. Attenuation occurs mainly through heat, particle rotation, sound, and scattering (99). When the collision occurs far from the sensor, more attenuation will occur as the wave must travel further.

Previous research has examined the application of passive acoustic emission analysis to several processes including mixing, absorption, compaction, direct energy deposition, drying, fluidization, granulation, powder bed fusion, and hydro and pneumatic transport. These studies have shown the robustness and high potential of passive acoustic emissions as a process monitoring method. The passive vibrations can identify dispersion in a mixture when the amplitude moves from a state of changing amplitude to a stable new amplitude. This change in amplitude has been used to study several mixtures including mixtures of granules and Magnesium stearate. Adding a boundary layer lubricant of Magnesium stearate formed a barrier around other particles that attenuated the collision energy resulting in a lowered amplitude (99-102). The dispersion of the lubricant could

therefore be tracked through the amplitude profile and the endpoint identified through a low and stable amplitude value.

Table 2.7: Summary table of available literature on applications of passive acoustic emission analysis

Reference	Application	Mixer	Components	Purpose
(97)	Mixing	Kenwood mixer	Various	Monitor powder mixing
(103)	Mixing	High shear blender	Cellulose, Asprin	Compared NIR to passive vibrations and determine the benefits of using both for monitoring mixing.
(104)	Mixing	Convective mixer three blades	Microcrystalline cellulose, Aspirin, Citric Acid	Monitor powder mixing, study the ability of passive vibrations to monitor the effects of mixtures with secondary compounds
(100)	Mixing	V-blender	Sugar Spheres, Pharmaceutical Granules, Magnesium stearate	Determine if passive vibrations can monitor mixtures of particles with a powder lubricant
(101)	Mixing	V-blender	Glass Beads, Pharmaceutical Granules, Magnesium stearate	Determine the effect of loading configuration and fill level on mixing performance of a

				mixture of particles and Magnesium stearate
(102)	Mixing	V-blender	Glass Beads, Pharmaceutical Granules, Magnesium stearate	Determine the effectiveness and accuracy of passive vibrations for monitoring mixing of particles with a powder lubricant
(99)	Mixing	V-blender	Glass Beads, Pharmaceutical Granules, Magnesium stearate	To further evaluate passive vibrations for monitoring mixing of particles with a powder lubricant
(105)	Absorption	N/A	Water, ceramic Raschig Rings, ceramic Intalox saddles, glass marbles	Monitor operations related to absorption
(106)	Compaction	N/A	Aspirin AC 360, saccharose, and cornstarch	Identify defects and abnormalities
(107)	Direct Energy Deposition	N/A	Stainless steel gas atomized powder	Monitor mass flow rate
(108)	Drying	N/A	Stainless steel gas atomized powder	Monitor mass flow rate

(109)	Fluidization	N/A	Crystalline cellulose	Monitor overall fluidization during granulation
(110)	Fluidization	N/A	Lactose monohydrate, microcrystalline cellulose, HPMC, croscarmellose, USP distilled water	Monitor process condition changes
(111)	Granulation	N/A	Lactose monohydrate, microcrystalline cellulose, and aqueous polyvinylpyrrolidone solution	Monitor physical property changes
(112)	Granulation	N/A	Lactose monohydrate, and polyvinylpyrrolidone	Monitor overall granulation process
(113)	Granulation	N/A	Lactose monohydrate, corn-starch, polyvinylpyrrolidone, and water	Monitor changes in granule properties, identify process end point
(114)	Granulation	N/A	Microcrystalline cellulose, lactose monohydrate, hydroxypropyl, and deionized water	Monitor physical property changes
(115)	Granulation	N/A	Lactose monohydrate, microcrystalline cellulose, Povidone, cross-linked Povidone, and deionized water	Identify process end point

(116)	Granulation	N/A	Mannitol, microcrystalline cellulose, hypromellose 2910, Magnesium stearate, maize starch, dextrose anhydrous, and croscarmellose sodium	Identify process end point
(117)	Granulation	N/A	Cornstarch, mannitol, microcrystalline cellulose, hypromellose 2910, and croscarmellose sodium	Monitor size and density
(118)	Granulation	N/A	MCC spheres, sugar spheres, dextrose anhydrous, mannitol, microcrystalline cellulose, hypromellose 2910, and croscarmellose sodium	Monitor to determine particle size correlations
(119)	Granulation	N/A	Cornstarch, mannitol, microcrystalline cellulose, hypromellose 2910, and croscarmellose sodium	Monitor process condition changes
(120)	Powder Bed Fusion	N/A	Pre-alloyed gas atomized powder Ti6Al4V ELI	Monitor of balling effect, real time defect detection

(121)	Transport (hydro)	N/A	Rocks, and silica sand slurry	Identify defects (oversized components)
(122)	Transport (pneumatic)	N/A	Silica flour	Monitor process condition changes
(123)	Transport (pneumatic)	N/A	Oblong tablets	Identify tablet breakage
(124)	Transport (pneumatic)	N/A	Glass beads, and polyvinylchloride	Identify flow regime
(125)	Transport (pneumatic)	N/A	Polyethylene pellets, glass beads, and polyvinylchloride	Identify flow regime

2.7.2 Advantages

Passive vibration analysis is a non-invasive method of extracting information about powder mixing. Sensors are attached to the outer shell of the mixer, allowing measurements to be taken without impacting the powder bed avoiding the common issue of channeling. The sensor can also be attached to the mixer without permanent alterations, thus minimizing cost and easily extending applications to pre-existing equipment. As well, analysis does not require destructive testing methods thus minimizing cost as product is not lost through testing.

2.7.3 Disadvantages

Passive acoustic emissions or vibrations are commonly acquired at high frequencies to ensure that emissions at least within the audible range are captured. This results in large

volumes of measured data with corresponding challenges for storage and processing. These challenges have declined with time as digital systems continuously improved. As the application to pharmaceutical processes such as powder mixing is relatively new, there is a lack of research for guidance. However, this disadvantage is also an opportunity for discovery and the motivation behind the research presented in this thesis.

2.8 Conclusion

Monitoring powder mixtures is critical to ensure that quality and safety standards are met. Powder mixing is one of the most complicated processes in pharmaceutical production. Currently, thief probes are used for monitoring. However, this method is inefficient, inaccurate, and offline. To improve powder mixing processes, several PATs have been developed. These PATs provide further insight into particle motion during mixing and can identify factors such as mixture homogeneity and segregation. Table 2.8 was adapted from Crouter and Briens (21), and Nadeem and Heindel (126) to provide a summary of the significant PATs currently under development.

Table 2.8: Comparison of significant PATs currently under development (adapted from Crouter & Briens, 2019 (21) and Nadeem & Heindel, 2018 (126))

	NIR Spectroscopy	Raman Spectroscopy	Optical image	PEPT	MRI	X-ray CT	Passive Vibration Analysis
Measured parameter	Absorption energy	Scattered light	Colour	Positron detection	Magnetic field	X-ray attenuation	Vibrations
Applications of PAT							
Mixture homogeneity	YES	YES	YES		YES	YES	YES
Endpoint	YES	YES					YES
Composition	YES	YES					
Velocity profile			YES	YES	YES		
Flow regime					YES		
Particle pathway				YES	YES		
Advantages of PAT							
No vessel modification required				YES			YES

Potential for online Monitoring	YES	YES					
Able to monitor multicomponent mixtures	YES	YES					
Non-invasive				YES	YES	YES	YES
3D image				YES	YES	YES	
Low cost			YES				YES
Easy operation			YES				
Disadvantages of PAT							
Vessel modification required	YES	YES	YES				
Window fouling	YES	YES	YES				
Data can be difficult to interpret	YES						
Localized Measurements	YES						
High Cost				YES	YES	YES	

Specific requirements for components (i.e., colour, sensitivity to magnetic fields, etc.)			YES		YES		
Addition of tracers required				YES		YES	
Cannot assess multicomponent mixtures				YES	YES	YES	
Cannot be applied to industry				YES	YES	YES	
Safety risk						YES	
Instantaneous monitoring not possible						YES	
Poor method development							YES
Large data analysis required							YES

2.9 Thesis Objectives and Overview

The objective of this thesis research was to further advance the application of passive acoustic emissions for potential monitoring of powder mixing. This included an extended study into the connection between the emissions and particle behaviour in the V-shell and led to an improvement in the information extracted from the emissions about the process. With improvements in the measurement analysis, the mixing process can be studied in more detail and monitoring for disruptions such as segregation could be implemented. The following chapters address the stated objectives as follows:

Chapter 3 discusses the features of the measured passive acoustic emissions. Glass beads and starch particles were used to connect the measurements to the motion of the particles. The effects of fill level and collision location were examined.

Chapter 4 uses starch granules to extend the application of passive acoustic emissions to pharmaceutically relevant powders and common challenges such as segregation.

Chapter 5 reflects on the work completed to date as well as discusses potential future work.

2.10 References

1. Muzzio F, Goodridge C, Alexander A, Arratia P, Yang H, Sudah O, Mergen G. Sampling and characterization of pharmaceutical powders and granular blends. *Int. J Pharm* 2003; 250: 51-64.
2. Vergote G, De Beer T, Vervaet C, Remon J, Baeyens W, Diericx N, Verpoort F. In-line monitoring of a pharmaceutical blending process using FT-Raman spectroscopy. *Eur J Pharm Sci* 2004; 21: 479-485.
3. Deveswaran R, Bharath S, Basavaraj B, Abraham S, Furtado S, Madhavan V. Concepts and Techniques of Pharmaceutical Powder Mixing Process: A Current Update. *Res J Pharm Technol* 2009; 2: 245-249.
4. Bridgewater, J. Mixing of powders and granular materials by mechanical means—a perspective. *Particuology* 2012; 10: 397-427.
5. Hausman D, Cambron R, Sakr A. Application of Raman spectroscopy for on-line monitoring of low dose blend uniformity. *Int J Pharm* 2005; 298: 80-90.
6. Susana L, Canu P, Santomaso A. Development and characterization of a new thief sampling device for cohesive powders. *Int J Pharm* 2011; 416: 260-267.
7. Muzzio F, Goodridge C, Alexander A, Arratia P, Yang H, Sudah O, Mergen G. Sampling and characterization of pharmaceutical powders and granular blends. *Int. J Pharm* 2003; 250: 51-64.
8. Berman J, Schoeneman A, Shelton JT. Unit Dose Sampling: A Tale of two Thieves. *Drug Dev Ind Pharm* 1996; 11: 1121-1132.
9. Burgess CL. Chapter 4 Issues related to the United States v. Barr Laboratories, Inc. In: Riley CM, Rosanske TW, eds. *Progress in Pharmaceutical and Biomedical Analysis* 1996; 3: 101-117.
10. Weinekötter R, Gericke H. *Mixing of Solids*: Springer 2006.
11. Plumb K. Continuous Processing in the Pharmaceutical Industry: Changing the Mind Set. *Chem Eng Res Des* 2005; 83: 730-738.
12. Engisch W, Muzzio F. Using Residence Time Distributions (RTDs) to Address the Traceability of Raw Materials in Continuous Pharmaceutical Manufacturing. *J Pharm Innov* 2016; 11: 64-81.

13. U.S. Department of Health and Human Services, Food and Drug Administration, Center for Drug Evaluation and Research (CDER), Center for Biologics Evaluation and Research (CBER). Guidance for Industry – Q8(R2) Pharmaceutical Development; 2009. Available from: <https://www.fda.gov/regulatory-information/search-fda-guidance-documents/q8r2-pharmaceutical-development>
14. U.S. Department of Health and Human Services, Food and Drug Administration, Center for Drug Evaluation and Research (CDER), Center for Veterinary Medicine (CVM), Office of Regulatory Affairs (ORA). Guidance for Industry PAT — A Framework for Innovative Pharmaceutical Development, Manufacturing, and Quality Assurance; 2004. Available from: <https://www.fda.gov/media/71012/download>
15. Merriam-Webster. Homogeneity. Available from: <https://www.merriam-webster.com/dictionary/homogeneity>.
16. U.S. Department of Health and Human Services, Food and Drug Administration, Center for Drug Evaluation and Research (CDER). Quality Considerations for Continuous Manufacturing Guidance for Industry; 2019. Available from: <https://www.fda.gov/media/121314/download>
17. Koller DM, Posch A, Hörl G, Voura C, Radl S, Urbanetz N, Fraser SD, Tritthart W, Reiter F, Schlingmann M, Khinast JG. Continuous quantitative monitoring of powder mixing dynamics by near-infrared spectroscopy. *Powder Technol* 2011; 205: 87-96.
18. Kak A, Slaney M. Principles of Computerized Tomographic Imaging. New York, USA: SIAM 2001.
19. Chester A, Kowalski J, Coles M, Muegge E, Muzzio F, Brone D. Mixing dynamics in catalyst impregnation in double-cone blenders. *Powder Technol* 1999; 102: 85 – 94.
20. Liu R, Yin X, Li H, Shao Q, York P, He Y, Xiao T, Zhang J. Visualization and quantitative profiling of mixing and segregation of granules using synchrotron radiation X-ray microtomography and three dimensional reconstruction. *Int J Pharma* 2013; 445: 125-133.
21. Crouter A, Briens L. Methods to assess mixing of pharmaceutical powders. *AAPS PharmSciTech* 2019; 20: 84.
22. Asachi M, Nourafkan E, Hassanpour A. A review of current techniques for the evaluation of Powder Mixing. *Adv Powder Technol* 2018; 29: 1525–1549.

23. Burgess C, Hammond J. Wavelength standards for the near-infrared spectral region. *Spectroscopy* 2007; 22:
24. Roggo Y, Chalus P, Maurer L, Lema-Martinez C, Edmond A, Jent N. A review of near infrared spectroscopy and chemometrics in pharmaceutical technologies. *J Pharm Biomed Anal* 2007; 44: 683-700.
25. Berntsson O, Danielsson LG, Lagerholm B, Folestad S. Quantitative in-line monitoring of powder blending by near-infrared reflection spectroscopy. *Powder Technol* 2002; 123: 185-193.
26. Huang AN, Kuo HP. Developments in the tools for the investigation of mixing in particulate systems – A review. *Adv Powder Technol* 2014; 25: 163-173.
27. Blanco M, Coello J, Iturriaga H, MasPOCH S, de la Pezuela C. Effect of Data Preprocessing Methods in Near-Infrared Diffuse Reflectance Spectroscopy for the Determination of the Active Compound in a Pharmaceutical Preparation. *Appl Spectrosc* 1997; 51: 240-246.
28. Barnes RJ, Dhanoa MS, Lister SJ. Standard Normal Variate Transformation and De-Trending of Near-Infrared Diffuse Reflectance Spectra. *Appl Spectrosc* 1989; 43: 772-777.
29. Savitzky A, Golay M. Smoothing and Differentiation of Data by Simplified Least Squares Procedures. *Anal Chem* 1964; 36: 1627-1639.
30. Sekulic SS, Wakeman J, Doherty P, Hailey PA. Automated system for the on-line monitoring of powder blending processes using near-infrared spectroscopy: Part II. Qualitative approaches to blend evaluation. *J Pharm Biomed Anal* 1998; 17: 1285-1309.
31. Geladi P, MacDougall D, Martens H. Linearization and scatter-correction for near-infrared reflectance spectra of meat. *Appl Spectrosc* 1985; 39: 491-500.
32. Lu Y, Qu Y, Song M. [Research on the correlation chart of near infrared spectra by using multiple scatter correction technique]. *Guang Pu Xue Yu Guang Pu Fen Xi Spectrosc Spect Anal* 2007; 27: 877-880.
33. Jolliffe IT, Cadima J. Principal component analysis: a review and recent developments. *Pil Trans R Soc A* 2016; 374.

34. Sekulic SS, Wakeman J, Doherty P, Hailey PA. Automated system for the on-line monitoring of powder blending processes using near-infrared spectroscopy Part II. Qualitative approaches to blend evaluation. *J Pharm Biomed Anal* 1998; 17: 1285-1309.
35. Scheibelhofer O, Balak N, Koller DM, Khinast JG. Spatially resolved monitoring of powder mixing processes via multiple NIR-probes. *Powder Technol* 2013; 243: 161-170.
36. Vanarase A, Alcalà M, Jerez Rozo JI, Muzzio F, & Romañach R. Real-time monitoring of drug concentration in a continuous powder mixing process using NIR spectroscopy. *Chem Eng Sci* 2010; 65: 57288-5733.
37. Portillo PM, Ierapetritou MG, Muzzio F. Effects of rotation rate, mixing angle, and cohesion in two continuous powder mixers—A statistical approach. *Powder Technol* 2009; 194: 21
38. Kehlenbeck V. Use of Near Infrared Spectroscopy for in- and Off-Line Performance Determination of Continuous and Batch Powder Mixers: Opportunities & Challenges. *Procedia Food Sci* 2011; 1: 2015-2022.
39. Martínez L, Peinado A, Liesum L, Betz G. Use of near-infrared spectroscopy to quantify drug content on a continuous blending process: Influence of mass flow and rotation speed variations. *Eur J Pharm Biopharm* 2013; 84: 606-615.
40. Quiñones L, Velazquez C, Obregon L. A novel multiple linear multivariate NIR calibration model-based strategy for in-line monitoring of continuous mixing. *AIChE J* 2014; 60: 3123-3132.
41. El-Hagrasy AS, Drennen III JK. A Process Analytical Technology approach to near-infrared process control of pharmaceutical powder blending. Part III: Quantitative near-infrared calibration for prediction of blend homogeneity and characterization of powder mixing kinetics. *J Pharm Sci* 2006; 95: 422-434.
42. Besseling R, Damen M, Tran T, Nguyen T, van den Dries K, Oostra W, Gerich A. An efficient, maintenance free and approved method for spectroscopic control and monitoring of blend uniformity: the moving F-test. *J Pharm Biomed Anal* 2015; 114: 471-481.

43. Tewari J, Strong R, Boulas P. At-line determination of pharmaceuticals small molecules' blending end point using chemometric modeling combined with Fourier transform near infrared spectroscopy. *Spectrochim Acta A Mol Biomol Spectrosc* 2017; 173: 886-891.
44. Sibik J, Chalus P, Maurer L, Murthy A, Krimmer S. Mechanistic approach in powder blending PAT: Bi-layer mixing and asymptotic end point prediction. *Powder Technol* 2017; 308: 306-317.
45. Hailey PA, Doherty P, Tapsell P, Oliver T, Aldridge PK. Automated system for the on-line monitoring of powder blending processes using near-infrared spectroscopy part I. System development and control. *J Pharm Biomed Anal* 1996; 14: 551-559.
46. Vanarase AU, Järvinen M, Paaso J, Muzzio F. Development of a methodology to estimate error in the on-line measurements of blend uniformity in a continuous powder mixing process. *Powder Technol* 2013; 241: 263-271.
47. Blanco M, Gozález Bañó R, Bertran E. Monitoring powder blending in pharmaceutical processes by use of near infrared spectroscopy. *Talanta* 2002; 56: 203-212.
48. Rinnan A, van den Berg F, Engelsen SB. Review of the most common preprocessing techniques for near infrared spectra. *TrAC* 2009; 28: 1201-1222.
49. Sulub Y, Konigsberger M, Cheney J. Blend uniformity end-point determination using near-infrared spectroscopy and multivariate calibration. *J Pharm Biomed Anal* 2011; 55: 429-434.
50. Smith E, Dent G. Chapter 1 Introduction, Basic Theory and Principles. In *Modern Raman Spectroscopy: A Practical Approach*, Second Edition. John Wiley & Sons Ltd 2019; 1-20.
51. Rantanen J. Process analytical applications of Raman spectroscopy. *J Pharm Pharmacol* 2007; 59: 171-177.
52. Hollas, J. Rotational Raman Spectroscopy. In *Modern Spectroscopy*. Wiley 2004; 122 - 137.
53. Britannica. Stokes lines. Available from: <https://www.britannica.com/science/Stokes-lines>

54. Smith E, Dent G. Chapter 3 The Theory of Raman Spectroscopy. In *Modern Raman Spectroscopy: A Practical Approach*, Second Edition. John Wiley & Sons Ltd 2019; 77-99.
55. Wikström H, Romero-Torres S, Wongweragiat S, Williams JAS, Grant ER, Taylor LS. On-Line Content Uniformity Determination of Tablets Using Low-Resolution Raman Spectroscopy. *Appl Spectrosc* 2006; 60: 672-681.
56. De Beer T, Bodson C, Dejaegher B, Walczak B, Vercruysse P, Burggraeve A, Lemos A, Delattre L, Heyden Y, Remon J, Vervaet C, Baeyens W. Raman spectroscopy as a process analytical technology (PAT) tool for the in-line monitoring and understanding of a powder blending process. *J Pharm Biomed Anal* 2008; 48: 772-779.
57. Allen P, Bellamy LJ, Nordon A, Littlejohn D, Andrews J, Dallin P. In situ monitoring of powder blending by non-invasive Raman spectrometry with wide area illumination. *J Pharm Biomed Anal* 2013; 76: 28-35.
58. Riolo D, Piazza A, Cottini C, Serafini M, Lutero E, Cuoghi E, Gasparini L, Botturi D, Marino IG, Aliatis I, Bersani D, Lottici PP. Raman spectroscopy as a PAT for pharmaceutical blending: Advantages and disadvantages. *J Pharm Biomed Anal* 2018; 149: 329-334.
59. Aaltonen J, Kogermann K, Strachan CJ, Rantanen J. In-line monitoring of solid-state transitions during fluidisation. *Chem Eng Sci*
60. Aghbashlo M, Sotudeh-Gharebagh R, Zarghami R, Mujumdar AS, Mostoufi N. Measurement Techniques to Monitor and Control Fluidization Quality in Fluidized Bed Dryers: A Review. *Dry Technol* 2014; 32: 1005-1051.
61. Walker G, Bell SEJ, Greene K, Jones DS, Andrew G. Characterisation of fluidised bed granulation processes using in-situ Raman spectroscopy. *Chem Eng Sci* 2009; 64: 91-98.
62. Walker G, Bell SEJ, Vann M, Jones DS, Andrew G. Fluidised bed characterisation using Raman spectroscopy: Applications to pharmaceutical processing. *Chem Eng Sci* 2007; 62: 3832-3838.
63. Grymonpré W, Bostijn N, Van Herck S, Verstraete G, Vanhoorne V, Nuhn L, Rombouts P, De Beer T, Remon JP, Vervaet C. Downstream processing from hot-

- melt extrusion towards tablets: A quality by design approach. *Int J Pharm* 2017; 531: 235-245.
64. Saerens L, Dierickx L, Lenain B, Vervaet C, Remon JP, De Beer T. Raman spectroscopy for the in-line polymer–drug quantification and solid state characterization during a pharmaceutical hot-melt extrusion process. *Eur J Pharm Biopharm* 2011; 77: 158-163.
65. Breitenbach J, Schrof W, Neumann J. Confocal Raman-Spectroscopy: Analytical Approach to Solid Dispersions and Mapping of Drugs. *Pharm Res* 1999; 16: 1109-1113.
66. The changes observed in optical image analysis rely on tracer particles or colour changes throughout the powder bed (Bulent Koc A, Silleli H, Koc C, Dayioğlu M. Monitoring of Dry Powder Mixing with Real-Time Image Processing. *J Appl Sci* 2007; 7: 1218-1223.
67. Le Coënt A, Rivoire A, Briançon S, Lieto J. An original image-processing technique for obtaining the mixing time: The box-counting with erosions method. *Powder Technol* 2005; 152: 62-71.
68. Malhotra K, Mujumdar AS, Imakoma H, Okazaki M. Fundamental particle mixing studies in an agitated bed of granular materials in a cylindrical vessel. *Powder Technol* 1988; 55: 107-114.
69. Realpe A, Velázquez C. Image processing and analysis for determination of concentrations of powder mixtures. *Powder Technol* 2003; 134: 193-200.
70. Chen C, Yu C. Two-dimensional image characterization of powder mixing and its effects on the solid-state reactions. *Mater Chem Phys* 2004; 85: 227-237.
71. Kuo HP, Hsu RC, Hsiao YC. Investigation of axial segregation in a rotating drum. *Powder Technol* 2005; 153: 196-203.
72. Berthiaux H, Mosorov V, Tomczak L, Gatumel C, Demeyre JF. Principal component analysis for characterising homogeneity in powder mixing using image processing techniques. *Chem Eng Process* 2006; 45: 397-403.
73. Daumann B, Fath A, Anlauf H, Nirschl H. Determination of the mixing time in a discontinuous powder mixer by using image analysis. *Chem Eng Sci* 2009; 64: 2320-2331.

74. Cavinato M, Artoni R, Bresciani M, Canu P, Santomaso AC. Scale-up effects on flow patterns in the high shear mixing of cohesive powders. *Chem Eng Sci* 2013; 102: 1-9.
75. Kingston TA, Heindel TJ. Granular mixing optimization and the influence of operating conditions in a double screw mixer. *Powder Technol* 2014; 266: 144-155.
76. Liu X, Zhang C, Zhan J. Quantitative comparison of image analysis methods for particle mixing in rotary drums. *Powder Technol* 2015; 282: 32-36.
77. Ammarcha C, Gatumel C, Dirion J, Cabassud M, Berthiaux H. Continuous powder mixing of segregating mixtures under steady and unsteady state regimes: Homogeneity assessment by real-time on-line image analysis. *Powder Technol* 2017; 315: 39-52.
78. Parker DJ, Dijkstra AE, Martin TW, Seville JPK. Positron emission particle tracking studies of spherical particle motion in rotating drums. *Chem Eng Sci* 1997; 52: 2011-2022.
79. Portillo PM, Vanarase AU, Ingram A, Seville JK, Ierapetritou MG, Muzzio F. Investigation of the effect of impeller rotation rate, powder flow rate, and cohesion on powder flow behavior in a continuous blender using PEPT. *Chem Eng Sci* 2010; 65: 5658-5668.
80. Parker DJ, Leadbeater TW, Fan X, Hausard MN, Ingram A, Yang Z. Positron imaging techniques for process engineering: recent developments at Birmingham. *Meas Sci Technol* 2008; 19: 1-10.
81. Perrault M, Bertrand F, Chaouki J. An investigation of magnesium stearate mixing in a V-blender through gamma-ray detection. *Powder Technol* 2010; 200: 234-245.
82. Kuo HP, Knight PC, Parker DJ, Seville JPK. Solids circulation and axial dispersion of cohesionless particles in a V-mixer. *Powder Technol* 2005; 152: 133-140.
83. Marigo M, Davies M, Leadbeater T, Cairns DL, Ingram A, Stitt EH. Application of Positron Emission Particle Tracking (PEPT) to validate a Discrete Element Method (DEM) model of granular flow and mixing in the Turbula mixer. *Int J Pharm* 2013; 446: 46-58.
84. Kawaguchi, T. MRI measurement of granular flows and fluid-particle flows. *Adv Powder Technol* 2010; 21: 235-241

85. Nakagawa M, Altobelli Sam Caprihan A, Fukushima E, Jeong EK. Non-invasive measurements of granular flows by magnetic resonance imaging. *Exp Fluids* 1993; 16: 54-60.
86. Dyakowski T, Jaworski AJ. Non-Invasive Process Imaging – Principles and Applications of Industrial Process Tomography. *Chem Eng Technol* 2003; 26: 697-706.
87. Metcalfe G, Shattuck M. Pattern formation during mixing and segregation of flowing granular materials. *Applications* 1996; 233: 709-717.
88. Hill KM, Caprihan A, Kakalios J. Bulk Segregation in Rotated Granular Material Measured by Magnetic Resonance Imaging. *PLR* 1997; 78: 50-53.
89. Caprihan A, Seymour JD. Correlation Time and Diffusion Coefficient Imaging: Application to a Granular Flow System. *J Magn Reason* 2000; 144: 96-107.
90. Sommier N, Porion P, Evesque P, Leclerc B, Tchoreloff P, Couarraze G. Magnetic resonance imaging investigation of the mixing-segregation process in a pharmaceutical blender. *Int J Pharm* 2001; 222: 243-258.
91. Porion P, Sommier N, Faugère AM, Evesque P. Dynamics of size segregation and mixing of granular materials in a 3D-blender by NMR imaging investigation. *Powder Technol* 2004; 141: 55-68.
92. Maneval JE, Hill KM, Smith BE, Caprihan A, Fukushima E. Effects of end wall friction in rotating cylinder granular flow experiments. *Granul Matter* 2005; 7: 199-292.
93. Kawaguchi T, Tsutsumi K, Tsujii Y. MRI Measurement of Granular Motion in a Rotating Drum. *Part Part Syst Charact* 2006; 23: 266-271.
94. Yang C, Fu X. Development and validation of a material-labeling method for powder process characterization using X-ray computed tomography. *Powder Technol* 2004; 146: 10-19.
95. Stock RS. X-ray microtomography of materials. *Int Mater Rev* 1999; 44: 141-164.
96. Kinsler LE, Frey AR, Coppens AB, Sanders JV. Fundamentals of acoustics. USA: John Wiley & Sons Inc. 2000.

97. Tily P, Porada S, Scruby C, Lidington S. Monitoring of mixing processes using acoustic emission. In: Harnby N, Benkreira H, Carpenter K, Mann R, eds. *Fluid Mixing III*. Rugby: The Institute of Chemical Engineers 1988; 75-94.
98. Boyd J, Varley J. The uses of passive measurement of acoustic emissions from chemical engineering processes. *Chem Eng Sci* 2001; 56: 1749-1767.
99. Cameron A, Briens L. Monitoring lubricant addition in pharmaceutical tablet manufacturing through passive vibration measurements in a V-blender. *Powder Technol* 2020; 364: 708-718.
100. Crouter A, Briens L. The effect of granule moisture on passive acoustic emissions in a V-blender. *Powder Technology* 2016; 299: 226-234.
101. Cameron A, Briens L. An Investigation of Magnesium Stearate Mixing Performance in a V-Blender Through Passive Vibration Measurements. *AAPS PharmSciTech* 2019; 20: 199.
102. Cameron A, Briens L. Monitoring Magnesium Stearate Blending in a V-Blender Through Passive Vibration Measurements. *AAPS PharmSciTech* 2019; 20: 269.
103. Bellamy L, Nordon A, Littlejohn D. Non-invasive monitoring of powder mixing with near infrared spectrometry and acoustics. *Spectrosc Eur* 2004; 16: 30-32.
104. Bellamy L, Nordon A, Littlejohn D. Non-invasive monitoring of powder mixing with near infrared spectrometry and acoustics. *Spectrosc Eur* 2004; 16: 30-32.
105. Allen P, Bellamy L, Nordon A, Littlejohn D. Non-invasive monitoring of the mixing of pharmaceutical powders by broadband acoustic emission. *Analyst* 2010; 135: 518-524.
106. Hansuld E, Briens L, Briens C. Acoustic detection of flooding in absorption columns and trickle beds. *Chem Eng Process* 2008; 47: 871-878.
107. Serris E, Perier-Camby L, Thomas G, Desfontaines M, Fantozzi G. Acoustic emission of pharmaceutical powders during compaction. *Powder Technol* 2002; 128: 296-299.
108. Whiting J, Springer A, Sciammarella F. Real-time acoustic emission monitoring of powder mass flow rate for directed energy deposition. *Addit Manuf* 2018; 23: 312-318.

108. Briens L, Smith R, Briens C. Monitoring of a rotary dryer using acoustic emissions. *Powder Technol* 2008; 181: 115-120.
109. Tsujimoto H, Yokoyama T, Huang C, Sekiguchi I. Monitoring particle fluidization in a fluidized bed granulator with an acoustic emission sensor. *Powder Technol* 2000; 113: 88-96.
110. Vervloet D, Nijenhuis J, Ommen J. Monitoring a lab-scale fluidized bed dryer: A comparison between pressure transducers, passive acoustic emissions and vibration measurements. *Powder Technol* 2010; 197: 36-48.
111. Whitaker M, Baker GR, Westrup J, Goulding PA, Rudd DR, Belchamber RM. Application of acoustic emission to the monitoring and end point determination of a high shear granulation process. *Int J Pharm* 2000; 205: 79-91.
112. Briens L, Daniher D, Tallevi A. Monitoring high-shear granulation using sound and vibration measurements. *Int J Pharm* 2007; 331: 54-60.
113. Daniher D, Briens L, Tallevi A. End-point detection in high-shear granulation using sound and vibration signal analysis. *Powder Tech* 2008; 181: 130-136.
114. Papp MK, Pujara CP, Pinal R. Monitoring of high-shear granulation using acoustic emission: Predicting granule properties. *J Pharm Innov* 2008; 3: 113-122.
115. Gamble J, Dennis AB, Tobyn M. Monitoring and end-point prediction of a small scale wet granulation process using acoustic emission. *Pharm Dev Technol* 2009; 14: 299-304.
116. Hansuld EM, Briens L, McCann JAB, Sayani A. Audible acoustics in high-shear wet granulation: Application of frequency filtering. *Int J Pharm* 2009; 378: 37-44.
117. Hansuld E, Briens L, Sayani A, McCann J. Monitoring quality attributes for high-shear wet granulation with audible acoustic emissions. *Powder Technol* 2012; 216: 117-123.
118. Hansuld E, Briens L, Sayani A, McCann J. An investigation of the relationship between acoustic emissions and particle size. *Powder Technol* 2012; 219: 111-117.
119. Hansuld E, Briens L, Sayani A, McCann J. The effect of process parameters on audible acoustic emissions from high-shear granulation. *Drug Dev Ind Pharm* 2013; 39: 331-341.

120. Kouprianoff D, Yadroitsava I, du Plessis A, Luwes N, Yadroitsev I. Monitoring of Laser Powder Bed Fusion by Acoustic Emission: Investigation of Single Tracks and Layers. *Front Mech Eng* 2021; 7: 1-17.
121. Albion K, Briens L, Briens C, Berruti F. Modelling of oversized material flow through a horizontal hydrotransport slurry pipe to optimize its acoustic detection. *Powder Technol* 2009; 194: 18-32.
122. Hou R, Hunt A, Williams R. Acoustic monitoring of pipeline flows: particulate slurries. *Powder Technol* 1999; 106: 30-36.
123. Albion K, Briens L, Briens C, Berruti F. Detection of the breakage of pharmaceutical tablets in pneumatic transport. *Int J Pharm* 2006; 322: 119-129.
124. Albion K, Briens L, Briens C, Berruti F. Flow regime determination in horizontal pneumatic transport of fine powders using non-intrusive acoustic probes. *Powder Technol* 2007; 172: 157-166.
125. Albion K, Briens L, Briens C, Berruti F, Book G. Flow regime determination in upward inclined pneumatic transport of particulates using non-intrusive acoustic probes. *Chem Eng Process* 2007; 46: 520-531.
126. Nadeem H, Heindel TJ. Review of noninvasive methods to characterize granular mixing. *Powder Technol* 2018; 332:331-350.

Chapter 3

3 Investigation of Passive Acoustic Emissions during Powder Mixing in a V-blender

3.1 Introduction

Approximately 80% of all pharmaceuticals are in oral solid dosage form, such as tablets, due to convenience for consumers and ease of manufacturing (1,2). Powders must be mixed during solid dosage manufacturing. Mixing is critical to ensure production of tablets with correct amounts of active drug and excipients, uniform weight, and consistent, reproducible properties (1). Mixing, however, is a complex process that is dependent on many factors ranging from powder properties to blender geometry and operation (3). Further research is still needed to better understand the process and to develop methods for monitoring and control.

Pharmaceutical solid dosage manufacturing is still commonly conducted batch-wise. After every batch mixing step, samples are withdrawn and tested off-line to ensure that the blend is uniform, consistent, and will result in a final product with desired properties (4). Process analytical technologies (PATs) are mechanisms to design, analyze and control processes in pharmaceutical manufacturing through the measurement of critical process parameters that affect quality attributes of the active pharmaceutical ingredient (API) of the specified dosage form (5). The tools being developed to measure the process parameters for mixing include near infrared spectroscopy (NIR) (6-12), image analysis (13-16), magnetic nuclear resonance imaging (MRI) (17-20), radioactive tracers (21-23), and passive acoustic emissions or vibration measurements (24-26).

Acoustics is the production by a source, transmission through a medium, and reception by a receiver of energy in the form of waves (27,28). Passive acoustic emissions are being explored in various industries to provide insight into physicochemical changes that occur during a process. In the pharmaceutical industry, passive acoustic emissions have been investigated for monitoring high-shear and fluidized bed granulation (29-37), fluidized bed drying (38), and mixing (24,25,39-43). Few studies have been completed to investigate the application of passive acoustic emissions for monitoring powder mixing.

Initially, the focus was on developing mixing profiles and determining the mixing endpoint for convective or high-shear mixers (39-41). A fixed shell easily allowed external attachment of sensors to measure the passive acoustic emissions. The research has extended to tumbling mixers. Crouter and Briens showed that passive acoustic emissions could indicate the dispersion of lubricant magnesium stearate into a powder in a V-blender; an accelerometer attached to the lid of the V-blender measured the emissions from the particle-particle and particle-equipment collisions and changes in the amplitude of the emissions indicated the progress of the lubricant dispersion (25). Cameron and Briens extended the research to other particles and the effect of process parameters such as loading configuration and fill level (24,42,43). The major advantage of passive acoustic emissions over other technologies is the non-invasive and real-time means of collecting process information. The challenges include efficient extraction of relevant information from large volumes of data.

As particles flow within a V-blender, there are many particle-particle and particle-equipment collisions. The kinetic energy of a particle is both retained by the particle and dissipated during a collision. The amount of energy retained versus dissipated depends on particle properties, particle flow, and the equipment. For conditions within a V-blender, dissipation as particle or equipment deformation is not significant; most dissipated energy is released as stress waves that are transmitted as passive acoustic emissions that are audible and whose vibrations can be measured by a microphone or accelerometer attached externally to the V-blender (25).

Passive acoustic emissions from particle collisions during flow in a V-blender that are measured by an external sensor have been shown to be affected by particle mass/density, blender scale and fill level, and lubricant dispersion throughout the powder. Increasing the particle mass through size or density increases the measured vibration amplitudes as the particle kinetic energy at collision is high resulting in increased energy dissipation and transmission to the sensor. The blender scale and fill level affect particle velocities (44-47). During tumbling, particles can fall freely over longer distances in larger blenders and blenders with lower fill levels and thus reach higher velocities with higher kinetic energies before collisions. Lubricant addition and its dispersion affect the energy

dissipation upon collision; boundary layer lubricants such as magnesium stearate form a layer around particles which further dissipates energy during a collision resulting in lower energy transmission to the sensor (25).

Mixing powders in a V-blender is a complex process. As the V-blender is inverted, the particles fall and separate into each arm of the V-shell (3,42,48). As the V-shell rotates from inverted to an upright position, the particles converge at the bottom. This flow pattern affects the rate and extent of mixing (3,48). Large physical property differences between particles, such as size and density differences, increase the likelihood of segregation (49-51). Segregation is also influenced by process parameters, such as the geometry of the mixer, with V-blenders being shown to not be ideal for segregation-prone mixtures (50). The process parameters also impact the segregation pattern formed, with the most significant being the fill volume and rotational speed (50). Although some conditions under which segregation and specific segregation patterns have been described, the mechanisms are not fully understood and therefore remain challenging to accurately predict when they might occur and to initiate any adjustments to minimize their development.

Preliminary research has shown promise for extracting important information about mixing in a V-blender using passive acoustic emissions. The objective of this research is to further investigate and understand the connection between the emissions and particle flow within the specific geometry of a V-blender. More information about mixing can help predict segregation and other challenges thereby mitigating manufacturing disruptions. Development of a passive acoustic emissions monitoring method to monitor mixing inline and in real-time would improve manufacturing efficiency while ensuring a consistent and high-quality product.

3.2 Materials and Methods

3.2.1 Materials

Experimental trials were completed using glass beads and starch granules. The glass beads were selected as a model system: monosize spheres, uniform composition, and size ranges close to those of pharmaceutical granules. The starch granules were irregular in

shape and exhibited a range of sizes. The starch granules were sieved into four size cuts: 2.00 – 2.36 mm, 1.40 – 2.00 mm, 1.18 – 1.40 mm, and 0.006 – 1.18 mm. Flowability of the particles was examined using a Mercury Scientific Revolution Powder Analyzer. A sample size of 118 cm³ was placed in a drum with a diameter of 11 cm and a width of 3.5 cm and rotated at 0.3 rpm until 128 avalanches had occurred with an avalanche defined as a rearrangement of 0.65 mole% of the particles in the drum. Optical measurements provided dynamic density and avalanche time measurements. Samples were measured in triplicate with average values reported. The apparent density of the particles was estimated by volume displacement measurements using 4°C distilled water. Samples were measured in triplicate with average values reported. Photos of the starch granules were taken and examined with Image Pro software to estimate the circularity of the granules. Image Pro defines circularity as $\frac{Perimeter^2}{4\pi * Area}$, with a perfectly circular particle having a value of 1 (45). Table 3.1 summarizes the particles and their properties.

Table 3.1: Summary of particles used and their properties

Particle	Size (mm)	Apparent Density (g/cm ³)	Dynamic Density (g/cm ³)	Sphericity (-)	Avalanche Time (s)
Glass	2.00	2.5	1.49	1.0	3.4
Glass	1.00	2.5	1.49	1.0	2.2
Starch	2.00 – 2.36	1.3	0.45	0.7	3.6
Starch	1.40 – 2.00	1.3	0.43	0.7	4.8
Starch	1.18 – 1.40	1.3	0.46	0.7	4.1
Starch	0.006 – 1.18	1.3	0.50	0.7	3.1

3.2.2 Equipment

A Patterson-Kelly V-blender was used for the experimental trials, rotating at a fixed speed of 25 rpm. Two V-shells were used: a 16-quart (15.1 L) steel V-shell and a 16-quart (15.1 L) transparent acrylic V-shell. The geometry of the V-shells is detailed in Figure 3.1. The lids and bottom plate were the same for both V-shells; only the material of the V-shell was varied between steel or acrylic. The V-shells were filled to 25% volume with the specified particles.

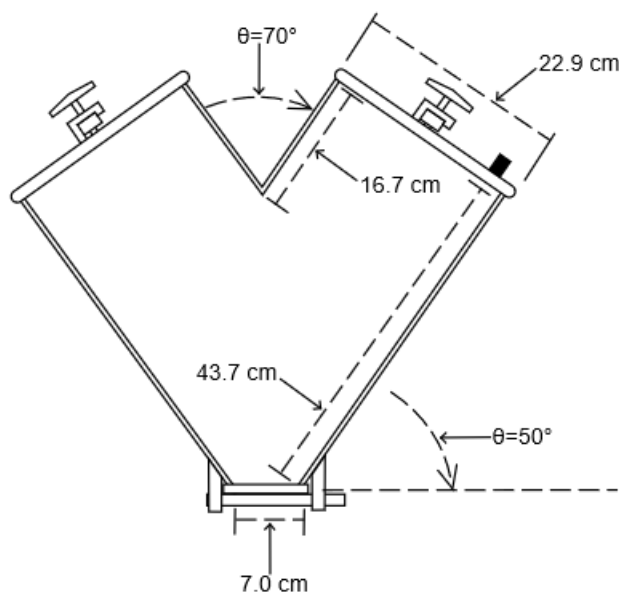


Figure 3.1: 16-quart V-shell schematic with dimensions labeled

Vibrations from passive acoustic emissions were measured using a PCB Piezotronics Accelerometer (model 353B34) combined with an ICP signal conditioner (model 480E09) securely attached to the lower front center of the outer arm of the V-shell at a radial position of $r/R = 0.74$ (Figure 3.2). The vibrations were recorded at an acquisition frequency of 40,000 Hz using Labview with a National Instruments DAQ-6036E card. The measurements were filtered using a Daubechies wavelet filter to remove the large oscillations due to the V-shell motion, allowing the focus to be on the vibrations from the particles inside the V-shell (46).

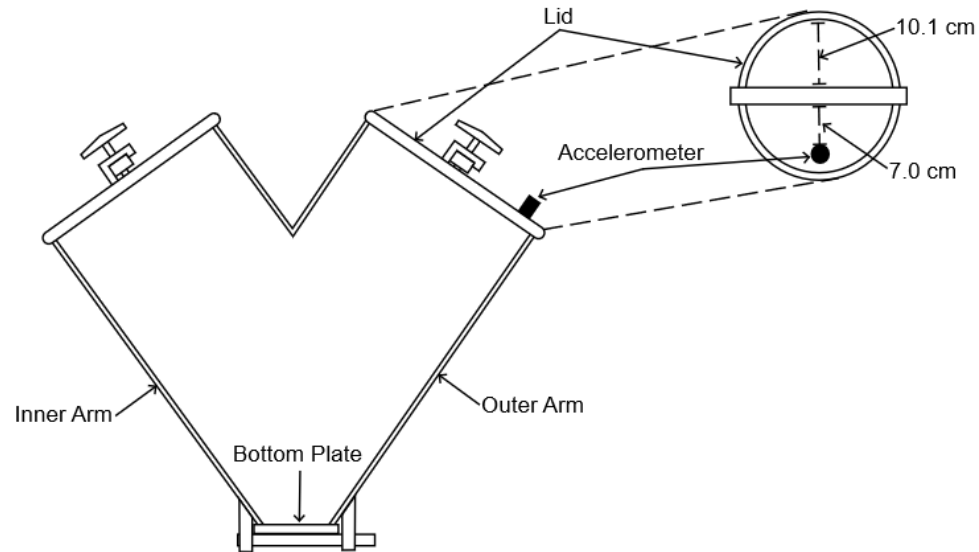


Figure 3.2: Schematic of V-shell showing accelerometer location

3.2.3 Experimental Trials

Four different types of trials were conducted.

3.2.3.1 Rotation Tests

Tests were conducted with the 16-quart steel V-shell using both glass beads and granules filled to 25% volume in which the V-shell rotation was stopped after quarter, half, and full rotations. Comparisons of the recorded vibrations were used to confirm relationships between the vibration features and the behavior of the particles within the V-shell.

3.2.3.2 Visualization

Tests were conducted with the 16-quart transparent acrylic V-shell to allow visual observations and photos and videos to be taken. Visualization of particle motion within the V-shell was critical to identifying particle flow patterns and contributions to the features of the vibration measurements.

3.2.3.3 Collision Tests

Collision tests with particles were conducted using the 16-quart V-shells with the accelerometer attached to the lid as indicated in Figure 3.2. The V-shell was inverted; individual particles and groups of five particles were dropped from a consistent height into the V-shell from the open base and vibration measurements were recorded. The particles were dropped to impact the inner arms of the V-shell and the lid of the V-shell. The accelerometer was moved onto different areas of the lid to allow for analysis of impacts at different distances from the accelerometer. Tests were conducted with an empty V-shell and in a V-shell with beds of particles in the upper arms resting on top of the lids. The various tests were designed to simulate the possible impact situations of a particle when the V-shell is inverted to allow further examination of the features of the vibration measurements.

3.2.3.4 Feature Information

Tests were conducted using the 16-quart metal and acrylic V-shells using both glass beads and granules filled to 25% volume. The shells were rotated for 50 to 200 revolutions and the vibrations recorded. These vibration measurements were used to examine methods for extracting information.

3.3 Results

3.3.1 Visual Observations

Visual observations of the 16-quart acrylic V-shell filled to 25% volume with starch granules allowed identification of particle movement as the V-shell rotated (Figure 3.3). When the V-shell is first inverted, many of the particles collide with the inner wall arms before flowing along the arms to impact the lids. Upon inversion, only a few particles fall unimpeded almost the full height of the V-shell to collide directly with the lids. The particles begin to accumulate along the inner arms and on the top of the lids such that many particles collide with other particles instead of directly with the V-shell walls or lids. As the V-shell continues to rotate, particles flow across the lids to the outer walls and slide

towards the bottom of the V-shell. The particles continue to slide, colliding mostly with the lower walls and accumulating on the bottom plate.

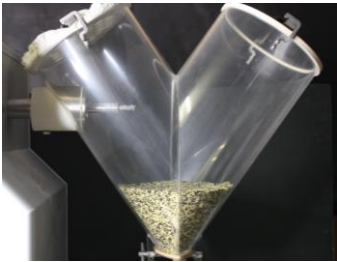
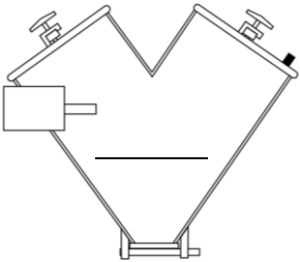

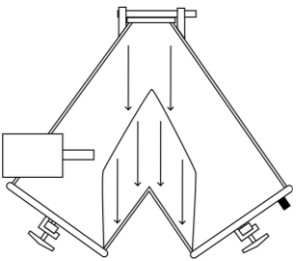
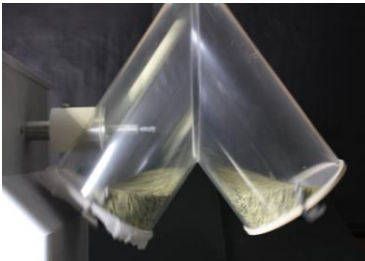
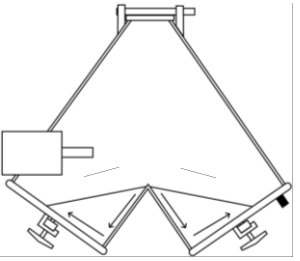

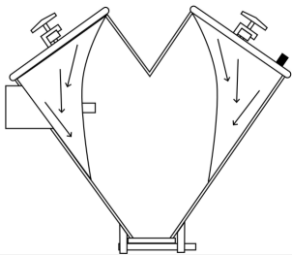
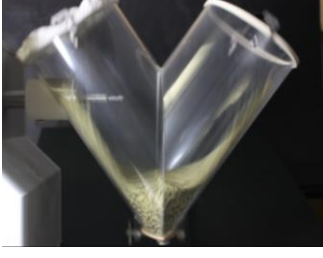
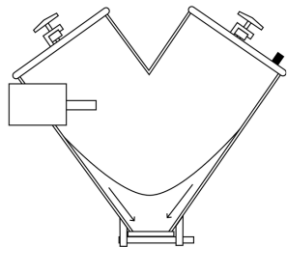
		Prior to rotation
		Granules impact the inner arms of the V-shell
		Granules impact the lids and then accumulate in the upper arms
		Granules impact and flow along the outer arms of the V-shell
		Granules flow along the outer arms and impact the V-shell near its base and impact the bottom plate

Figure 3.3: Visualization of granule movement during rotation in the acrylic V-shell

Recordings of the particle motion in the acrylic V-shell allowed estimates of the time intervals for each phase of motion described. The V-shell was rotated at a fixed rate of 25 rpm; each rotation was about 2.4 seconds and there was significant overlap of some of the phases. Figure 3.4 shows the estimated time intervals for the phases with 2 mm glass beads. The estimated time intervals for the other sizes of glass beads and for starch granules were very similar; variability was attributed to flowability differences. As shown in Table 1, the avalanche time for glass beads was 2.2 to 3.4 seconds and, for the starch granules, it was overall higher with a range of 3.1 to 4.8 seconds. These low values indicate free-flowing powders with the spherical glass beads exhibiting slightly better flowability than the more irregular-shaped starch granules (52).

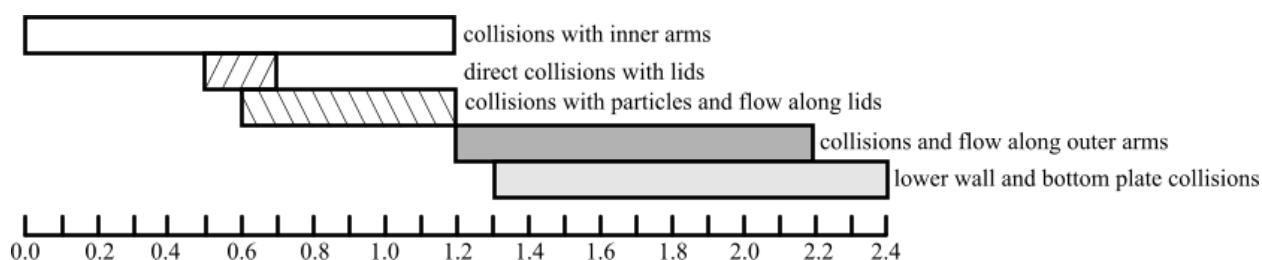


Figure 3.4: Timeline of flow behavior during a rotation of the V-shell for 2 mm glass beads

3.3.2 Collision Tests

Collision tests were conducted to better understand the relationship between the observed particle flow patterns and collisions and the vibrations measured by the accelerometer. These tests used 16-quart steel and 16-quart acrylic V-shells. Particles were dropped into the inverted V-shell under specific conditions. Vibrations created from a collision between a particle and the V-shell were measured and examined.

Figure 3.5 shows the measured signal of a single 2 mm glass bead dropped onto the lid with the attached accelerometer of an inverted empty 16-quart acrylic V-shell. The measured amplitude for the initial impact with the V-shell lid was approximately 100 mV, with subsequent peaks from rebound collisions lower in amplitude. Extended

experiments showed that the measured amplitude increased as the initial impact approached the accelerometer location, reaching approximately 115 mV with direct impact at the accelerometer location.

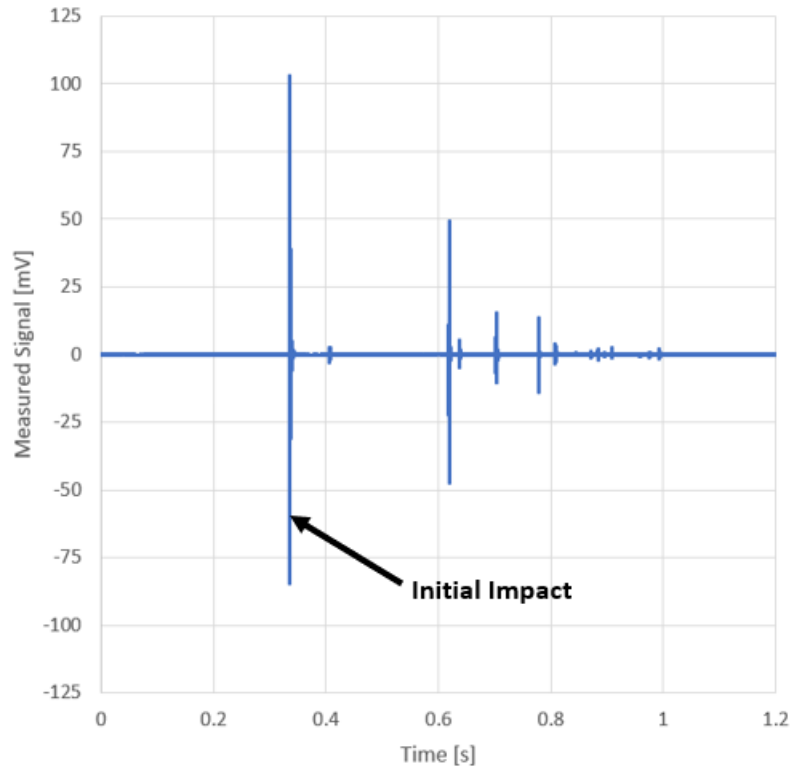


Figure 3.5: Measured vibrations of a single 2 mm glass bead dropped onto the lid of the inverted empty 16-quart acrylic V-shell with the accelerometer affixed in the location shown in Figure 3.2

When a 2 mm glass bead is dropped such that, the initial collision was with the inner arms, the measured amplitude was just over 50 mV. The second peak was larger due to rebound and collision with the lid; further peak amplitudes were low due to small bounces and collisions with the lid (Figure 3.6).

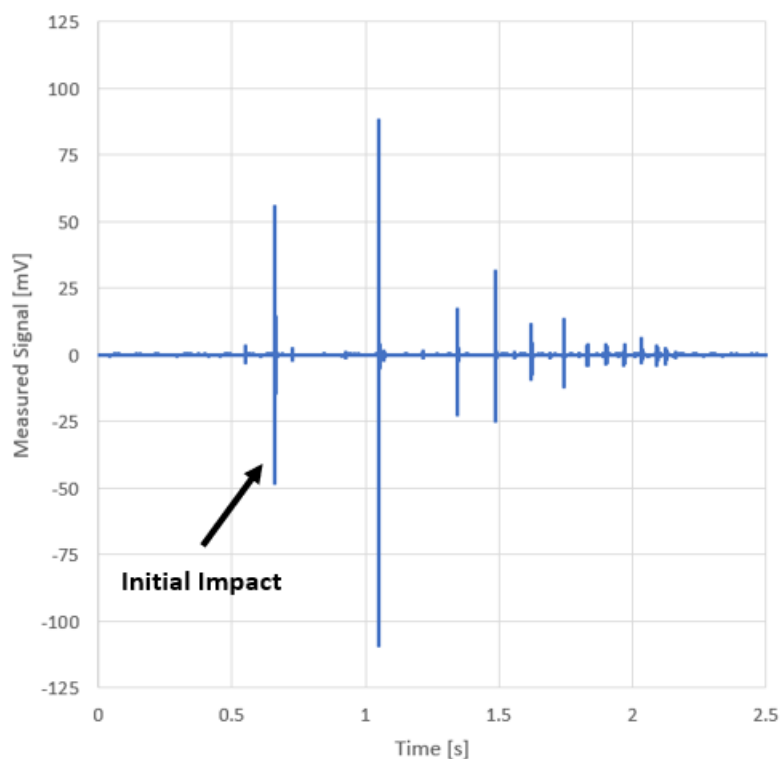


Figure 3.6: Measured vibrations of a single 2 mm glass bead dropped onto the inner wall arm of the inverted empty 16-quart acrylic V-shell

Figure 3.7 shows the results of dropping, nearly simultaneously, five 2 mm glass beads onto the lid with the attached accelerometer of an empty 16-quart acrylic inverted V-shell. The measured amplitudes for the initial impacts were in the range of approximately 50 to 110 mV with many subsequent measured vibrations due to particle bounces resulting in more particle-particle and particle-lid collisions.

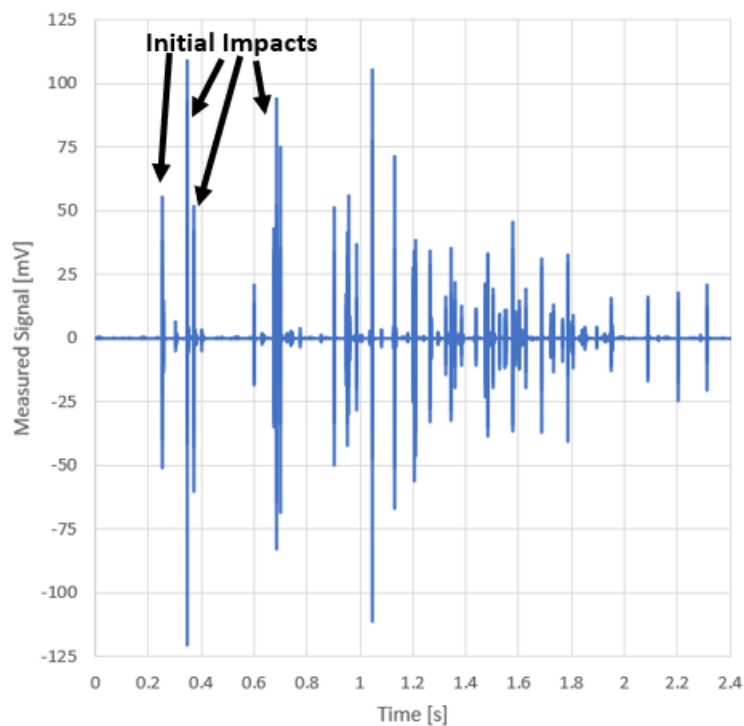


Figure 3.7: Measured vibrations of five 2 mm glass beads dropped onto the lid of the inverted empty 16-quart acrylic V-shell

Individual 2 mm glass beads were dropped onto the lid of the 16-quart steel inverted V-shell filled with increasing volumes of glass beads. Figure 3.8 shows that, as the volume of glass beads sitting on the V-shell lids increased, the measured vibration from the impact of a bead decreased in amplitude.

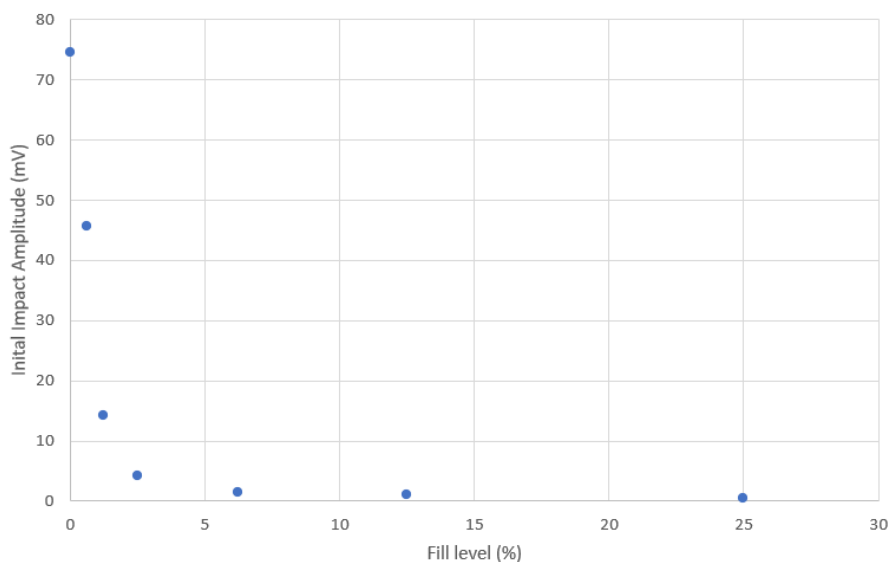


Figure 3.8: Initial measured impact amplitudes of a single 2 mm glass bead dropped into an inverted empty 16-quart acrylic V-shell with various glass bead fill levels

Trials were completed for all particles with the steel V-shells and the acrylic V-shell. For all particles and V-shells, the results were consistent. Vibration amplitudes were also higher for collisions with the acrylic V-shell than for the corresponding steel V-shell.

3.3.3 Detailed Rotation Trials

Detailed rotation trials were conducted, carefully stopping the V-shell each quarter turn, half turn, and full turn while recording vibrations. These trials complemented the visual observations and the collision tests.

Figure 3.9 shows the vibrations over a full rotation for 2 mm glass beads in a 16-quart steel V-shell. The three vibration features are indicated: Feature #1 associated with the flow of particles when the V-shell is inverted, Feature #2 associated with the flow of particles along the outer side of the V-shell arms, and Feature #3 associated with the flow of particles flowing towards the bottom V-shell as it moves back towards an upright position.

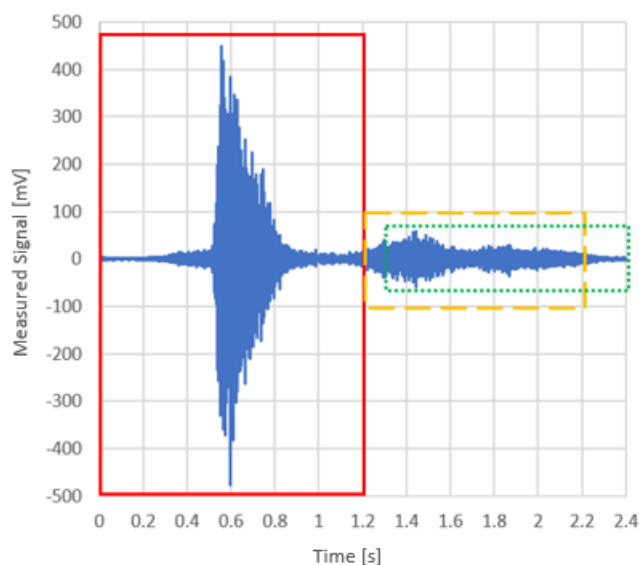


Figure 3.9: One full rotation of 2 mm glass beads in the 16-quart steel V-shell showing Feature #1 (solid line, associated with the flow of particles when the V-shell is inverted), Feature #2 (dash line, associated with the flow of particles along the outer side of the V-shell arms), and Feature #3 (dotted line, associated with the flow of particles flowing towards the bottom of the V-shell)

The partial turn trials helped identify three sub-features within Feature #1 as indicated in Figure 3.10. Feature #1a is associated with collisions and the flow of particles along the inner walls of the V-shell arms towards the lid. Feature #1b is associated with the impact of particles with the lid. Feature #1c is associated with the particles flowing outwards across the lid. Similar results were obtained for all particles in all V-shells.

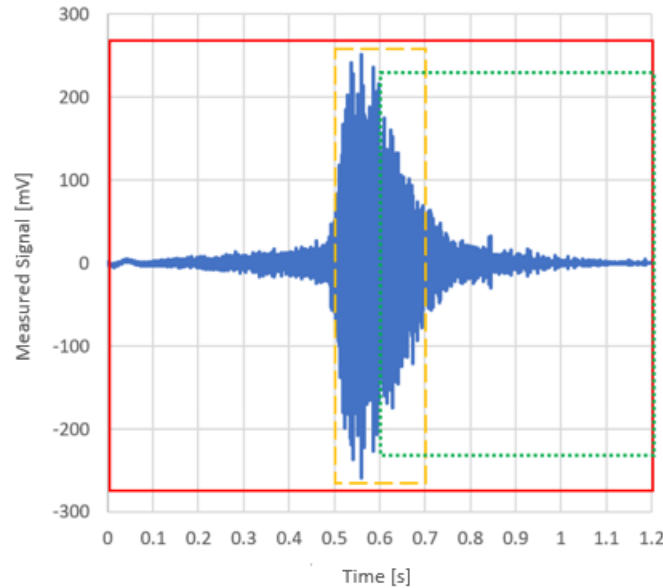


Figure 3.10: Measured vibrations of 2 mm glass beads during half-rotation of the 16-quart steel V-shell showing Feature #1a (solid line, associated with collisions and the flow of particles along the inner walls of the V-shell arms towards the lid), Feature #1b (dash line, associated with the impact of particles with the lid), and Feature #1c (dotted line, associated with the particles flowing outwards across the lid)

3.4 Discussion

A particle has kinetic energy when it collides with the V-shell. With the collision, some of the energy is retained by the particle while some can be dissipated as plastic deformation, air drag, particle rotation, and stress waves (43). For the tested particles and V-shells, most of the dissipated energy was in the form of passive acoustic emissions that were transmitted through the V-shell as stress waves and whose vibrations were measured by an accelerometer that was securely attached to the lid on the outer arm of the V-shell as illustrated in Figure 3.2.

The dissipation of energy from a particle collision into stress waves and their propagation and measurement by the accelerometer depended on many factors. The kinetic energy of a particle depends on its mass and velocity just before collision. As the kinetic energy

increases, more energy is dissipated as stress waves with less energy retained by the particles (24). The apparent density of the glass beads was almost twice the value of the starch granules (Table 1). For similar conditions of collisions on the lid, the dissipated energy measured by the accelerometer was significantly larger for a glass bead than for a starch granule. The measured dissipated energy was not directly proportional to particle density due to other factors such as particle shape. The starch granules were non-spherical with a sphericity of 0.7 compared to the spherical glass beads (Table 1). As these non-spherical granules rotated and rolled with collision, less energy was retained by these particles and less energy was dissipated as stress waves (43). The dissipation of energy with the collision further depends on the angle of collision with the V-shell relative to the particle trajectory. Collisions of a particle with an angled surface result in lower stress waves relative to collisions with a surface normal to the particle trajectory (24). Collisions with the inner arms of the V-shell associated with Feature #1a would have lower measured dissipated energy due to both the angle of collision and the distance to the accelerometer. As shown in Figure 3.6, the measured amplitude of vibrations from the collision with the inner arm was just over 50 mv while the rebound collision at an angle near perpendicular to the lid had a much larger amplitude near 100 mV. Finally, the material and the distance through which the stress waves propagate affect the attenuation and remaining energy level to be measured as vibrations by the accelerometer. Acrylic has a significantly lower acoustic impedance relative to steel (53,54) and therefore attenuation was lower in the acrylic V-shell relative to the steel V-shell. Vibration amplitudes measured by the accelerometer on the lid were higher for particle collisions close to the accelerometer compared to collisions at other locations on the lid due to the smaller distance between the impact and measurement location for any attenuation of the energy.

Controlled trials with the transparent acrylic V-shell allowed the particle motion to be observed and connected to the measured vibration profile. When the V-shell is inverted, the particles fall and most collide with the inner wall arms and flow along these walls before colliding with one of the lids. Only a few particles will fall unimpeded almost the full height of the V-shell before colliding with the lid directly. Collision tests confirmed that particle collisions directly with the lid with the attached accelerometer had the largest

measured vibration amplitudes. These particles potentially fall almost the entire height of the V-shell unimpeded and therefore have higher velocities and energies at the collision and energy from the collision is only minimally attenuated before reaching the accelerometer. For particles impacting the lid, attenuation is very low with particles impacting at the accelerometer location resulting in outliers in the measured vibrations with abnormally high amplitudes. Particles colliding with the inner arms of the V-shell would have relatively low velocities and energies and would collide at oblique angles relative to their trajectories. The low energies and oblique collisions resulted in low stress wave propagation and combined with attenuation through the V-shell to the lid, resulted in measured vibrations with lower amplitudes. However, the large number of particles that collide with the inner arm V-shell walls have an additive effect and overall make a significant contribution to the vibrations measured by the accelerometer.

As the V-shell continues to rotate into an inverted position, the particles accumulate on the lids of the arms. More particles collide with other particles rather than directly with the V-shell walls or lids. The number of collisions is large, but the energy dissipated to the V-shell walls or lids is relatively low as the particle velocities and thus energies are low, and the energies are attenuated during the transmission to the accelerometer. This was verified through the collision tests using multiple beads dropped almost simultaneously into the empty V-shell (Figure 3.7) and into the V-shell with particles resting on the lids (Figure 3.8). As particles accumulate on the lid of the V-shell, other particles continue to fall and collide with these particles. The energy from these collisions is increasingly attenuated as it must be transmitted through progressively more particles before reaching the lid with the attached accelerometer.

Figure 3.8 shows that the measured amplitude of the initial impact of a particle decreased very rapidly with particle fill level in the V-shell. As the fill level increased, the number of particles that accumulate on the lids as the V-shell rotates into an inverted position increased. A particle would fall a shorter distance before reaching the accumulated particle bed and therefore have a smaller kinetic energy; the smaller dissipated energy would then be increasingly attenuated through the growing particle bed. The location of a particle within the flow pattern will therefore affect the contribution of that particle

towards the measured acoustic emissions. This has important implications for mixing particles of different sizes and for the identification of any segregation.

The flow of particles upon inversion of the V-shell can therefore be divided into three parts: collisions with the inner arms and flow along the arms towards the lids (Feature#1a), collisions with the lids and between particles accumulating in the upper arms (Feature#1b), and flow across the lids toward the outer walls (Feature#1c). As indicated in Figures 3.3, 3.4, and 3.10, these events are not distinct but overlap in duration.

Figure 3.10 shows the vibrations measured when the V-shell is inverted with the three features highlighted. The amplitudes of the vibrations are largest when particles are first colliding with the lids (Feature #1b); the attenuation of these vibrations is small before reaching the accelerometer. The amplitude of the vibrations then decreases as the particles accumulate on the lid, as their kinetic energy decreases and attenuation increases. There are also vibrations from particles colliding with the inner wall (Feature #1a) adding to the measured amplitudes.

As the V-shell rotates from an inverted position back to upright, there are further distinct observed particle motions and measured vibration profiles. The particles flow along the outer wall arms towards the bottom of the V-shell. The particle velocities and energies are low as the particles continuously collide with each other and with the V-shell walls. The vibrations reaching the accelerometer on the lid have low amplitudes (Feature #2) due to a combination of the low energies and oblique collisions with the walls and attenuation through the walls to the lid. The particles then fall towards the bottom of the V-shell and collide with the bottom plate and adjacent lower walls. The vibrations that reach the accelerometer are very low in amplitude (Feature #3) due to significant attenuation especially considering the bottom plate is separate and attached through a rubber gasket and clamp. As the vibrations associated with Features #2 and #3 are transmitted through the walls of the V-shell before reaching the accelerometer, they are affected by the acoustic impedance of the V-shell wall material. There were differences in amplitudes for Features #2 and #3 between the acrylic and steel V-shells, but these

were not large as the amplitudes for both were already small due to the significant attenuation through the V-shell to the accelerometer.

Preliminary research indicated that the amplitude of vibrations from Feature #1 provided the most relevant and reliable information about the behavior of the particles within the V-shell blender; the average of the amplitudes of the three largest vibrations within Feature #1 varied with particle mass and could indicate differences in fill level and changes in the dispersion of magnesium stearate into another powder (25,42,43). Challenges in extracting information from the vibrations for powders with wide size distributions were identified (43). Information about particle behavior within the V-shell was difficult to extract from Features #2 and #3 due to the significant attenuation of the vibrations before measurement by the accelerometer.

The collision tests showed that the measured vibrations vary with collision location relative to the location of the accelerometer. There is, therefore, a range of vibration amplitudes for very similar particles and flow patterns within the V-shell. To extract information about the overall flow rather than the movement of an individual particle, a range of measurements should be considered. Figure 3.11 shows the effect on the coefficient of variation of measured vibration amplitude averages as the number of vibration peaks included in the calculations was varied, using glass beads as an example. With uniform glass beads, the vibration amplitudes associated with a specific particle flow should be similar. When only a few peaks were included in the average calculations, the coefficient of variation was high due to random collisions of particles at the sensor location. As more peaks were included in the calculations, the coefficient of variation decreased until an approximately constant value was reached. When 50 peaks were included in the calculations, the effect of an individual particle motion and collision was minimized and the extracted information from the measured vibrations best reflected the overall powder flow within the V-shell. For all particles and V-shells tested, it was confirmed that the top 50 peaks for this calculation were within the period identified as Feature #1b.

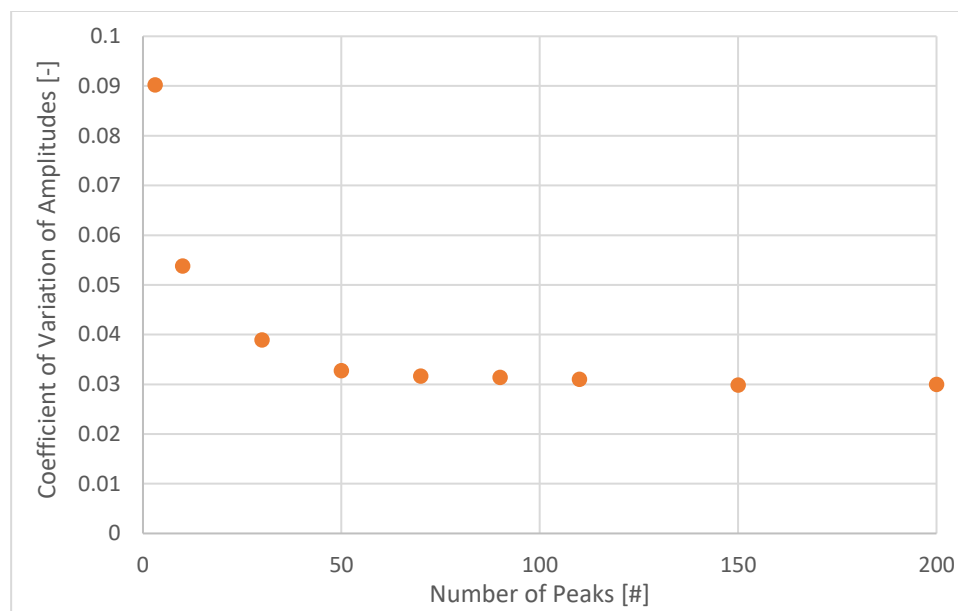


Figure 3.11: Coefficient of Variation of Amplitude values for 2mm glass bead control samples in the 16-quart steel V-shell averaged over various peaks

Figure 3.12 shows the reproducibility of amplitude average calculations for 2 mm glass beads over 50 revolutions of the V-shell using 50 peaks instead of only 3 peaks in the average amplitude calculations. The use of 50 peaks resulted in lower, but more stable amplitude values. Figures 3.13 and 3.14 show similar results for the starch granules.

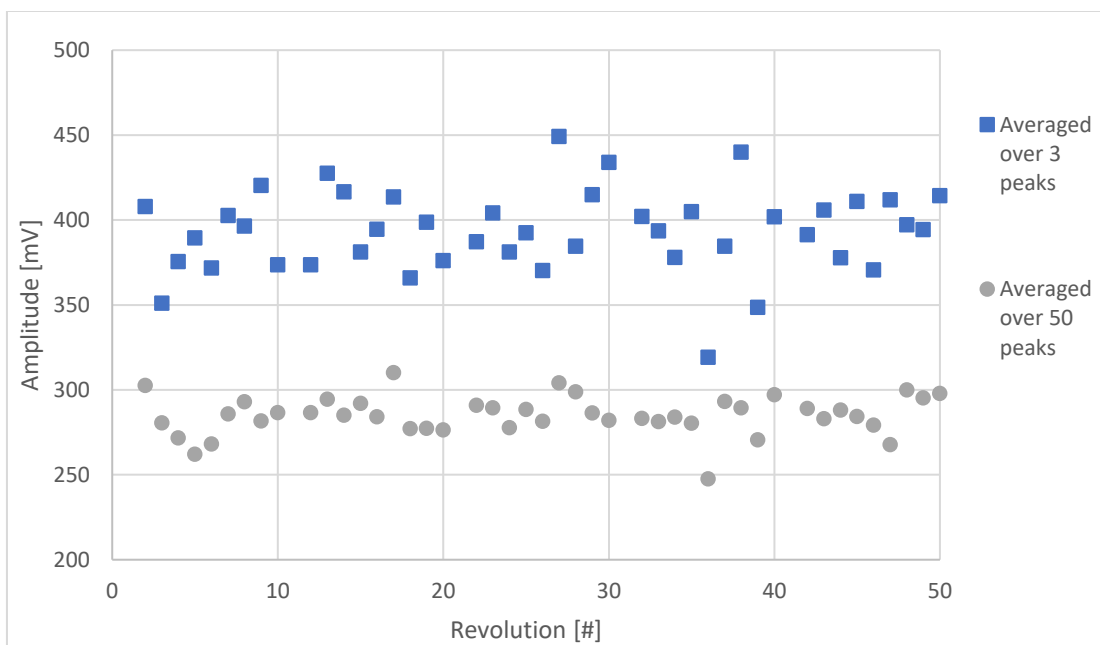


Figure 3.12: Comparison of 2 mm Glass bead control sample in the 16-quart steel V-shell averaged over 3 peaks and 50 peaks

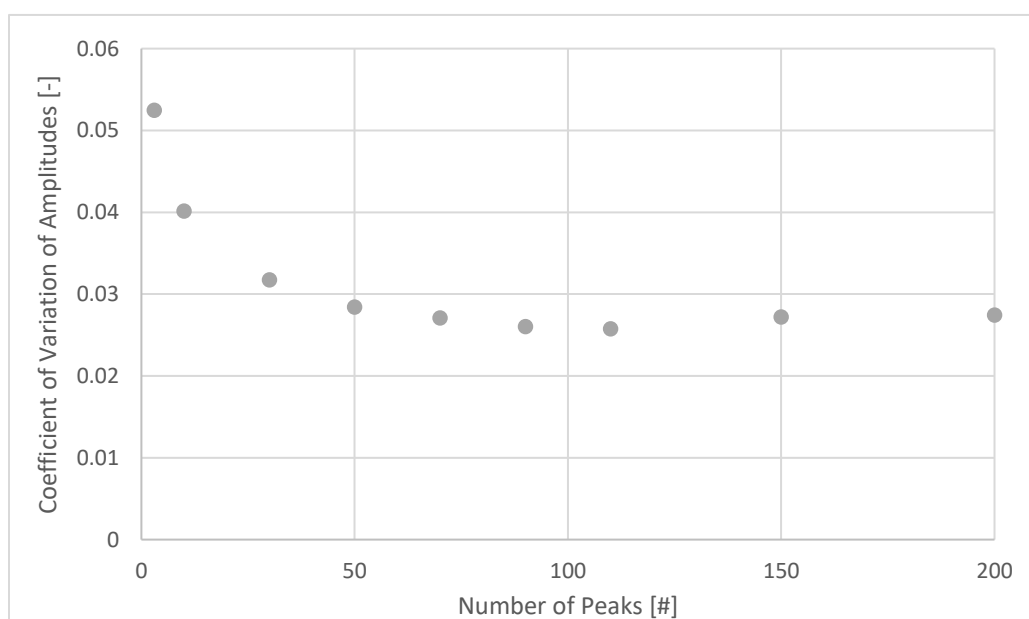


Figure 3.13(a): Coefficient of Variation of Amplitude values for Cut #3 (1.40-1.18mm) Starch Granules control samples in the 16-quart steel V-shell averaged over various peaks

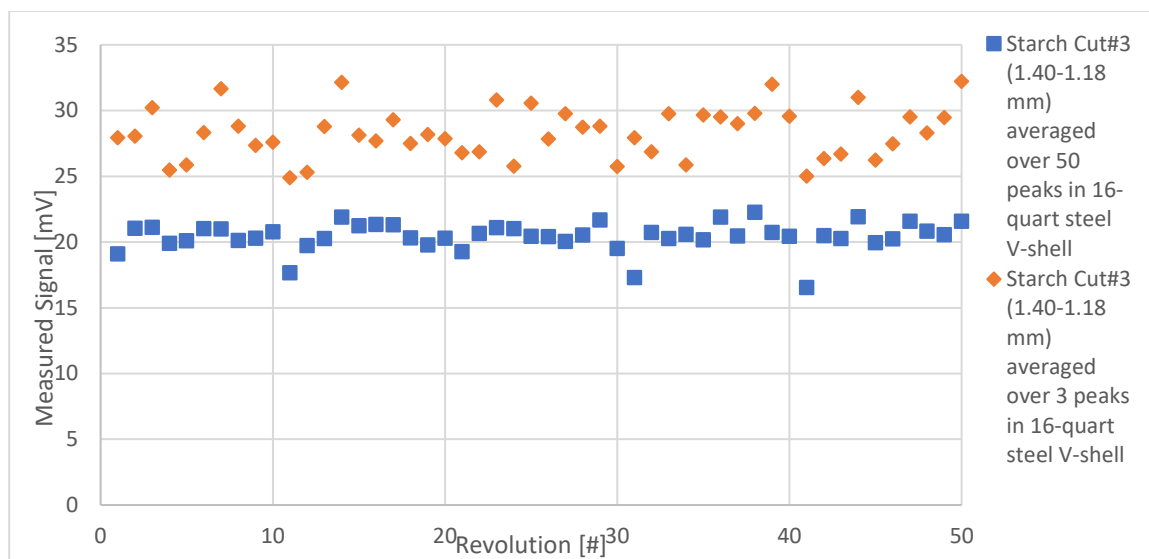


Figure 3.13(b): Comparison of Cut #3 (1.40-1.18mm) Starch Granules control sample in the 16-quart steel V-shell averaged over 3 peaks and 50 peaks

In comparison to the glass beads, the starch granules have a low density, distribution of sizes, and irregular shapes. The low density of the granules resulted in low kinetic energies at collisions and thus low energies dissipated as stress vibrations to be measured by the accelerometer. Irregular shapes also contributed to low energy dissipation as stress waves as some energy was dissipated through rolling and spinning at collision. The distribution of sizes resulted in a range of energies at collision. The properties of the granules, therefore, provided a range of measured vibration amplitudes for a given flow pattern within the V-shell. An analysis technique that reliably extracts information from the vibration measurements was critical. Figure 3.14 illustrates the use of vibration amplitudes to create a mixing profile of starch granules. The profile indicates that the two cuts of granules required almost 30 revolutions of the V-shell to become mixed.

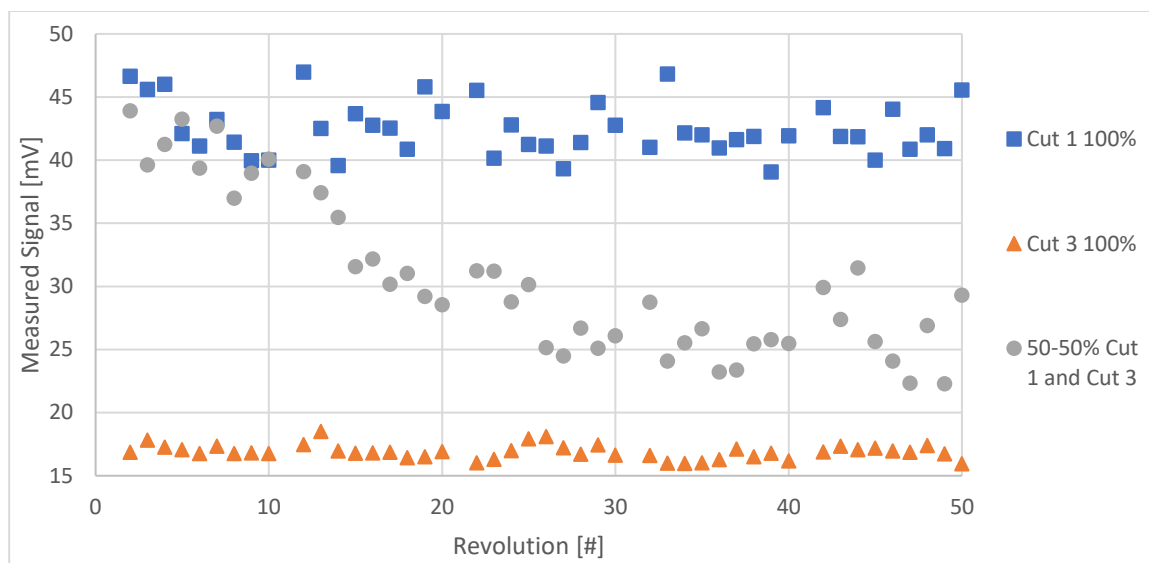


Figure 3.14: Mixture of 50% Starch Granules Cut#1 (2.36-2.00mm) and 50% Cut#3 (1.40-1.18mm) averaged over 50 peaks in a 16-quart steel V-shell with Cut#1 loaded horizontally on top

For the system shown in Figure 3.14, a binary mixture of starch granules was used with initial loading of the larger fraction horizontal on top of the smaller fraction in a 50-50 ratio by volume. The measured amplitudes of the mixture were initially high and similar to the amplitudes of the large fraction. This was the fraction that was loaded on top and therefore the granules that initially collided with the V-shell lids and were the primary contributors to the measured vibrations. As the V-shell rotated, the two fractions mixed and the granules that collided with the V-shell lids included both fractions. As the smaller size granules produced smaller emissions, the amplitude of the mixture decreased until an approximately stable amplitude just above 25 mV was reached at 30 revolutions indicating an approximate mixing endpoint.

3.5 Conclusions

The vibrations from passive acoustic emissions were measured while glass beads or starch granules were tumbled in a V-blender using an accelerometer attached to the lid of the outer V-shell arm. The measured vibrations were carefully connected to specific phases of particle behaviour within the V-shell. The average of the 50 largest measured

vibration amplitudes associated with the collisions of particles with the V-shell lid provided reliable and relevant information about particle behaviour in the V-shell.

Initially, the measured passive acoustic emissions will have amplitudes corresponding to the particles loaded horizontally last into the V-shell. As the particles mix, the emissions amplitudes will change to values representing the mixture. This research further supports the potential of passive acoustic emissions inline monitoring of pharmaceutical powder mixing.

3.6 References

1. Léonard G, Bertrand F, Chaouki J, Gosselin PM. An experimental investigation of effusivity as an indicator of powder blend uniformity. *Powder Technol* 2008; 181: 149-159.
2. Debotton N, Dahan A. Applications of polymers as pharmaceutical excipients in solid oral dosage forms. *Med Res Rev* 2016; 37: 52-97
3. Bridgewater, J. Mixing of powders and granular materials by mechanical means—a perspective. *Particuology* 2012; 10: 397-427.
4. Asachi M, Nourafkan E, Hassanpour A. A review of current techniques for the evaluation of Powder Mixing. *Adv Powder Technol* 2018; 29: 1525–1549.
5. U.S. Department of Health and Human Services, Food and Drug Administration, Center for Drug Evaluation and Research (CDER), Center for Biologics Evaluation and Research (CBER). Guidance for Industry – Q8(R2) Pharmaceutical Development; 2009. Available from: <https://www.fda.gov/regulatory-information/search-fda-guidance-documents/q8r2-pharmaceutical-development>
6. Tewari J, Strong R, Boulas P. At-line determination of pharmaceuticals small molecules' blending end point using chemometric modeling combined with Fourier transform near infrared spectroscopy. *Spectrochim Acta A Mol Biomol Spectrosc* 2017; 173: 886-891.
7. El-Hargrasy A, Drennen J. A Process Analytical Technology approach to near-infrared process control of pharmaceutical powder blending. Part III: Quantitative near-infrared calibration for prediction of blend homogeneity and characterization of powder mixing kinetics. *J Pharm Sci* 2006; 95: 422-434.
8. Sulub Y, Konigsberger M, Cheney J. Blend uniformity end-point determination using near-infrared spectroscopy and multivariate calibration. *J Pharm Biomed Anal* 2011; 55: 429-434.
9. Jaumot J, Igne B, Anderson C, Drennen C, de Jaun A. Blending process modeling and control by multivariate curve resolution. *Talanta* 2013; 117: 492-504.
10. Besseling R, Damen M, Tran T, Nguyen T, van den Dries K, Oostra W, Gerich A. An efficient, maintenance free and approved method for spectroscopic control and

- monitoring of blend uniformity: the moving F-test. *J Pharm Biomed Anal* 2015; 114: 471-481.
11. Lee WB, Widjaja E, Heng PWS, Chan LW. Near infrared spectroscopy for rapid and inline detection of particle size distribution variability in lactose during mixing. *Int J Pharm* 2019; 566: 454-462.
 12. Blanco M, Gozález Bañó R, Bertran E. Monitoring powder blending in pharmaceutical processes by use of near infrared spectroscopy. *Talanta* 2002; 56: 203-212.
 13. Koc AB, Silleli H, Koc C, Dayioglu MA. Monitoring of dry powder mixing with real-time image processing. *J Appl Sci* 2007; 7: 1218-1223.
 14. Le Coënt A, Rivoire A, Briançon S, Lieto J. An original image-processing technique for obtaining the mixing time: The box-counting with erosions method. *Powder Technol* 2005; 152: 62-71.
 15. Chen C, Yu C. Two-dimensional image characterization of powder mixing and its effects on the solid-state reactions. *Mater Chem Phys* 2004; 85: 227-237.
 16. Liu X, Zhang C, Zhan J. Quantitative comparison of image analysis methods for particle mixing in rotary drums. *Powder Technol* 2015; 282: 32-36.
 17. Nakagawa M, Altobelli Sam Caprihan A, Fukushima E, Jeong EK. Non-invasive measurements of granular flows by magnetic resonance imaging. *Exp Fluids* 1993; 16: 54-60.
 18. Kawaguchi T, Tsutsumi K, Tsuji Y. MRI Measurement of Granular Motion in a Rotating Drum. *Part Part Syst Charact* 2006; 23: 266-271.
 19. Hill KM, Caprihan A, Kakalios J. Bulk Segregation in Rotated Granular Material Measured by Magnetic Resonance Imaging. *PLR* 1997; 78: 50-53.
 20. Porion P, Sommier N, Faugère AM, Evesque P. Dynamics of size segregation and mixing of granular materials in a 3D-blender by NMR imaging investigation. *Powder Technol* 2004; 141: 55-68.
 21. Yang C, Fu X. Development and validation of a material-labeling method for powder process characterization using X-ray computed tomography. *Powder Technol* 2004; 146: 10-19.

22. Chester A, Kowalski J, Coles M, Muegge E, Muzzio F, Brone D. Mixing dynamics in catalyst impregnation in double-cone blenders. *Powder Technol* 1999; 102: 85-94.
23. Liu R, Yin X, Li H, Shao Q, York P, He Y, Xiao T, Zhang J. Visualization and quantitative profiling of mixing and segregation of granules using synchrotron radiation X-ray microtomography and three dimensional reconstruction. *Int J Pharma* 2013; 445: 125-133.
24. Cameron A, Briens L. Monitoring Magnesium Stearate Blending in a V-Blender Through Passive Vibration Measurements. *AAPS PharmSciTech* 2019; 20: 269.
25. Crouter A, Briens L. Monitoring lubricant addition using passive acoustic emissions in a V-blender. *Powder Technol* 2016; 301: 1119-1129.
26. Crouter A, Briens L. Methods to assess mixing of pharmaceutical powders. *AAPS PharmSciTech* 2019; 20: 84.
27. Bruneau M. *Fundamentals of Acoustics*. London, England: ISTE Ltd; 2006.
28. Anselmet F, Mattei PO. *Acoustics, aeroacoustics and vibrations*. Hoboken, New Jersey: John Wiley & Sons Inc; 2016.
29. Whitaker M, Baker GR, Westrup J, Goulding PA, Rudd DR, Belchamber RM. Application of acoustic emission to the monitoring and end point determination of a high shear granulation process. *Int J Pharm* 2000; 205: 79-91.
30. Briens L, Daniher D, Tallevi A. Monitoring high-shear granulation using sound and vibration measurements. *Int J Pharm* 2007; 331: 54-60.
31. Papp MK, Pujara CP, Pinal R. Monitoring of high-shear granulation using acoustic emission: Predicting granule properties. *J Pharm Innov* 2008; 3: 113-122.
32. Hansuld EM, Briens L, Sayani A, McCann JAB. The effect of process parameters on audible acoustic emissions from high-shear granulation. *Drug Dev Ind Pharm* 2012; 39: 331-341.
33. Daniher D, Briens L, Tallevi A. End-point detection in high-shear granulation using sound and vibration signal analysis. *Powder Tech* 2008; 181: 130-136.
34. Gamble J, Dennis AB, Tobyn M. Monitoring and end-point prediction of a small scale wet granulation process using acoustic emission. *Pharm Dev Technol* 2009; 14: 299-304.

35. Hansuld EM, Briens L, McCann JAB, Sayani A. Audible acoustics in high-shear wet granulation: Application of frequency filtering. *Int J Pharm* 2009; 378: 37-44.
36. Hansuld EM, Briens L, Sayani A, McCann JAB. Monitoring quality attributes for high-shear wet granulation with audible acoustic emissions. *Powder Technol* 2012; 216: 117-123.
37. Hansuld EM, Briens L, Sayani A, McCann JAB. An investigation of the relationship between acoustic emissions and particle size. *Powder Technol* 2012; 219: 111-117.
38. Briens L, Smith R, Briens C. Monitoring of a rotary dryer using acoustic emissions. *Powder Technol* 2008; 181: 115-120.
39. Tily P, Porada S, Scruby C, Lidington S. Monitoring of mixing processes using acoustic emission. In: Harnby N, Benkreira H, Carpenter K, Mann R, eds. *Fluid Mixing III*. Rugby: The Institute of Chemical Engineers 1988; 75-94.
40. Bellamy L, Nordon A, Littlejohn D. Non-invasive monitoring of powder mixing with near infrared spectrometry and acoustics. *Spectrosc Eur* 2004; 16: 30-32.
41. Allen P, Bellamy L, Nordon A, Littlejohn D. Non-invasive monitoring of the mixing of pharmaceutical powders by broadband acoustic emission. *Analyst* 2010; 135: 518-524.
42. Cameron A, Briens L. An Investigation of Magnesium Stearate Mixing Performance in a V-Blender Through Passive Vibration Measurements. *AAPS PharmSciTech* 2019; 20: 199.
43. Cameron A, Briens L. Monitoring lubricant addition in pharmaceutical tablet manufacturing through passive vibration measurements in a V-blender. *Powder Technol* 2020; 364: 708-718.
44. Alexander A, Shinbrot T, Johnson B, Muzzio F. V-blender segregation patterns for free-flowing materials: Effects of blender capacity and fill level. *Int J Pharm* 2004; 269: 19-28
45. Kuo HP, Knight PC, Parker DJ, Seville JPK. Solids circulation and axial dispersion of cohesionless particles in a V-mixer. *Powder Technol* 2005; 152: 133-140.
46. Brone D, Alexander A, Muzzio F. Quantitative characterization of mixing of dry powders in V-blenders. *AIChE J* 1998; 44: 271-278.

47. Lemieux M, Bertrand F, Chaouki J, Gosselin P. Comparative study of the mixing of free-flowing particles in a V-blender and a bin-blender. *Chem Eng Sci* 2007; 62: 1783-1802.
48. Van der Wel P. Powder Mixing. *Powder Handl Process* 1999; 11: 83-86.
49. Jarray A, Shi H, Scheper BJ, Habibi M, Luding S. Cohesion-driven mixing and segregation of dry granular media. *Sci Rep* 2019; 9.
50. Alexander A, Muzzio F, Shinbrot T. Segregation patterns in V-blenders. *Chem Eng Sci* 2003; 58: 487-496.
51. Oka S, Sahay A, Meng W, Muzzio F. Diminished segregation in continuous powder mixing. *Powder Technol* 2017; 309: 79-88.
52. Crouter A, Briens L. The effect of granule moisture on passive acoustic emissions in a V-blender. *Powder Technology* 2016; 299: 226-234.
53. Selfridge AR. Approximate material properties in isotropic materials. *IEEE Trans Sonics Ultrason* 1985; 32: 381-394.
54. Regtien PPL, Dertien E. *Sensors for mechatronics*. Amsterdam, Netherlands: Elsevier; 2018.

Chapter 4

4 Passive Acoustic Emissions Application for Segregation Prone Mixture in a V-blender

4.1 Introduction

Approximately 80% of pharmaceuticals are produced in the form of solid doses, such as tablets or capsules (1,2). Producing tablets requires the mixing of several powders with varying physical properties such as size, shape, and density. Ensuring powders have been uniformly combined is vital to producing tablets within required safety and quality guidelines (2,3). Powders that are not mixed correctly may result in tablets that do not contain the required amounts of the specific components and therefore their effectiveness and safety may be compromised (2). Methods that can identify the quality of a mixture would significantly improve the mixing step of pharmaceutical tablet manufacturing.

Most pharmaceuticals are manufactured through a series of batch processes. Process analytical technologies (PAT) are being explored as potential methods for monitoring powder mixing (4). These technologies are intended to replace the current offline method of analyzing thief probe samples at regular intervals to determine mixture quality. Most research into the application of PATs for powder mixing have focused on near-infrared (NIR) spectroscopy (5-11). While NIR spectroscopy has shown potential, it is limited as the NIR measurements require long pre and post-processing, costly equipment modification, and issues with blocked sensor ports (7,12). Other PATs under consideration and development for monitoring mixing include Magnetic Resonance Imaging (13-15), image analysis (16-23), X-ray computed tomography (24-26), and passive acoustic emissions (27-33).

Passive acoustic emissions in a V-blender are defined as the stress waves propagated from particle-particle and particle-V-shell collisions during powder mixing (27). The stress waves are measured as vibrations by an accelerometer affixed to the exterior of the V-shell. The amplitude of these vibrations is dependent on the physical properties of the particles such as particle mass; particles with a high mass have large possible kinetic

energies at collisions which result in more dissipated energy and larger transmitted and measured vibrations from the dissipated stress waves

Previous research into passive acoustic emissions identified preliminary connections between the different phases of motion within the V-shell and the emissions and provided guidelines for extracting information from the measured vibrations (27,28,32,33). The motion that causes direct collisions with the particles and the V-shell lid provided the most relevant and reliable information about the particle properties and their flow within the V-shell. Preliminary results have also shown that the endpoint of a mixture of particles and lubricant can be identified through changes in the vibration measurement amplitudes due to the formation of a lubricant boundary layer which decreases the amplitude due to its lowered energy transmission during collisions.

When combining particles of differing physical properties, one factor that must be considered is the possibility of segregation. Segregation, also known as de-mixing, occurs when particles separate due to variations in their physical properties thus impacting the uniformity of the mixture (34). Large differences in factors such as particle size and density lead to increased segregation risks (34-36). Particle properties such as cohesiveness in combination with processing choices such as mixer type also affect segregation (34). Prior research has indicated that some mixer geometries such as V-blenders and tote mixers are not ideal for segregation-prone mixtures as the motion of the particles within these mixers promotes segregation through trajectory segregation (36, 39). Trajectory segregation occurs due to differences in inertia between particles, with higher inertia particles having a higher propensity to follow a straight path of motion (36, 39). In a V-blender, trajectory segregation is further promoted due to the impacts on the flow path from collisions with the V-shell joint.

Depending on the physical properties of the particles and the parameters of the process, particles will segregate in different patterns. Pattern formation has been explored for a variety of different mixers including rotating drum mixers, V-blenders, and tote blenders (15,35,38). Alexander, Muzzio, and Shinbrot (2003) investigated different mixtures and identified that the fill volume and rotational speed have significant impact on segregation

patterns in V-blenders (36). In a further study, four distinct patterns were defined: ‘Small-out’, ‘Stripes’, ‘Inverse stripes’, and ‘Left-right’ (38). A ‘Big-out’ pattern was also observed as a transitional pattern when forming the ‘Left-right’ pattern.

The use of passive acoustic emissions for monitoring mixing provides several advantages over other methods including non-invasive testing, low costs, and no required permanent alterations (27). Previous research has focused on monitoring mixing of a limited number of components and those with uniform and regular properties including shape. However, tablets are formed from many different particles and therefore it is important to develop a method that can be applied to industrial conditions (27,28,32,33). The aim of this research was to investigate the potential of passive acoustic emissions for monitoring the mixing of multiple particles of different properties that are likely to segregate. Identifying segregation during powder mixing is critical in industries demanding high-quality standards, such as pharmaceuticals. Developing an acoustic emissions monitoring method for inline, real-time monitoring of segregation-prone mixtures would allow for improved efficiency and product quality assurance.

4.2 Materials and Methods

4.2.1 Materials

For all experimental trials, glass beads or starch granules were used. Glass beads were selected as a model system due to their uniform spherical size and composition. Glass bead sizes were selected to be in close range to pharmaceutical granule sizes. The starch granules were sieved into four size cuts: 2.00 – 2.36 mm, 1.40 – 2.00 mm, 1.18 – 1.40 mm, and 0.006 – 1.18 mm. Table 4.1 summarizes the particles and their properties.

Samples of granules from each size cut were dyed with iodine to allow visual observations of any segregation. Preliminary testing confirmed that the dye did not significantly change the other properties of the granules.

Flowability of the particles was examined using a Mercury Scientific Revolution Powder Analyzer. A sample size of 118 cm³ was placed in a drum with a diameter of 11 cm and a width of 3.5 cm and rotated at 0.3 rpm until 128 avalanches had occurred with an avalanche defined as a rearrangement of 0.65% volume of the particles in the drum. Optical measurements of the powder as it was rotated allowed the dynamic density and flowability indicator of avalanche time to be calculated. Samples were measured in triplicate with average values reported.

The apparent density of the particles was estimated by volume displacement measurements using 4°C distilled water. Samples were measured in triplicate with average values reported.

Photos of the starch granules were taken and examined with Image Pro software to estimate the circularity of the granules. Image Pro defines circularity as $\frac{Perimeter^2}{4\pi * Area}$, with a perfectly circular particle having a value of 1.00 (40).

Table 4.1: Summary of particles and their properties

Particle	Size (mm)	Apparent Density (g/cm ³)	Dynamic Density (g/cm ³)	Sphericity (-)	Avalanche Time (s)
Glass	1.00	2.5	1.00	1.00	2.2
Glass	2.00	2.5	1.08	1.00	3.4
Starch	2.00 – 2.36	12.5	0.45	0.66	3.6
Starch	1.40 – 2.00	12.5	0.43	0.70	4.8
Starch	1.18 – 1.40	12.5	0.46	0.72	4.1
Starch	0.006 – 1.18	12.5	0.50	0.70	3.1

4.2.2 Equipment

A Patterson-Kelly V-blender was used for the experimental trials with a 16-quart (15.1 L) steel V-shell and a 16-quart (15.1 L) transparent acrylic V-shell. The V-shells were filled to 25% volume with the selected particles and rotated at a fixed speed of 25 rpm.

A PCB Piezotronics Accelerometer (model 353B34) with an ICP signal conditioner (model 480E09) measured vibrations during the V-shell rotations. The accelerometer was attached to the lid of the outside arm of the V-shell at a radial position of $r/R=0.74$ (Figure 4.1). The vibrations were recorded at an acquisition frequency of 40,000 Hz using Labview with a National Instruments DAQ-6036E card and then filtered using a Daubechies wavelet filter to remove the large oscillations due to the V-shell motion, allowing the focus to be on the vibrations from the particles inside the V-shell.

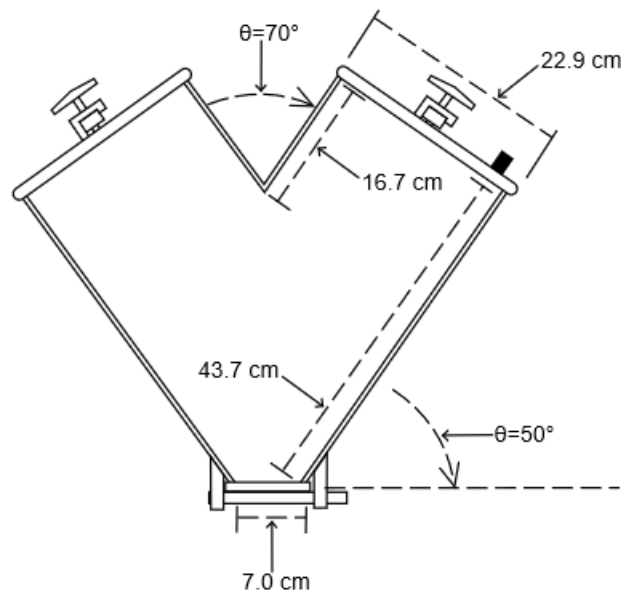


Figure 4.1: Schematic of V-shell showing accelerometer location

4.2.3 Experimental Trials

Vibration measurement trials were conducted with binary mixtures in the 16-qt steel V-shell. The binary mixtures were added in 30-70% and 50-50% ratios based upon volume. Particles were added to the shell through the outside arm in horizontal layers. The first size fraction was added and leveled. Subsequently, the second size fraction was carefully

poured on top and leveled. The goal was to create a symmetric top/bottom loading scheme with respect to the V-shell geometry. The accelerometer was attached to the lid as indicated in Figure 4.1 and vibration measurements were recorded over 50-200 revolutions of the V-shell. Following wavelet filtration, the vibration measurements were analyzed by averaging the highest 50 amplitudes within each rotation to create a vibration amplitude profile with time or revolutions (41).

Trials were also conducted in the 16-qt transparent acrylic V-shell using the same loadings and binary particle mixtures. The V-shell rotations were carefully stopped every ten rotations to take photos and samples. Photos of the dyed starch granule mixtures allowed visual observations of any segregation. Samples of the particles within the V-shell were taken using a side slot thief probe, carefully inserted 15.3 cm (~6 inches) into the bed from the outside arm as indicated in Figure 4.2. The probe removed samples of approximately 5.5 g of starch granules or 12.5 g of glass beads which were then sieved to determine the relative mass of each type of particle in the sample. The particles were carefully placed back into the V-shell at their extraction location before proceeding with subsequent rotations.

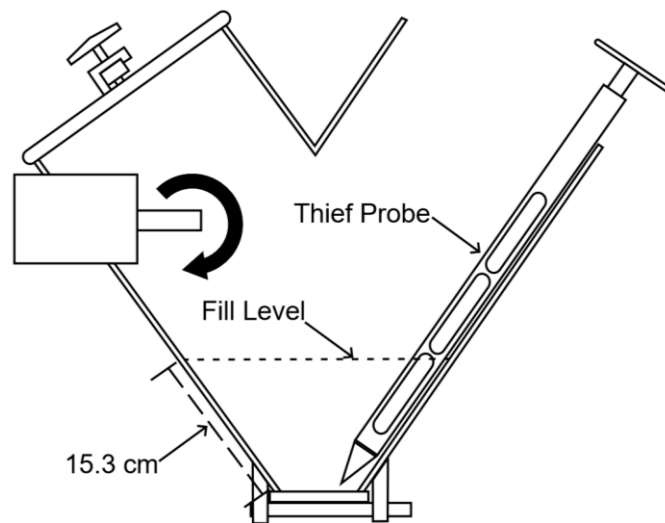


Figure 4.2: Schematic of the thief probe sampling location in the 16-qt V-shell

Further trials were completed to examine the effectiveness of the thief sampling in analyzing segregation. In these trials, the V-shell was stopped while inverted, allowing

for each arm (outer and inner) to be emptied separately. The mixtures emptied from each side were then sieved to determine the percentage composition by weight of each component. Samples were emptied after trials of 10 rotations and 50 rotations. The results of these trials were then compared to the sampling results.

Trials to identify segregation potential were independently conducted using the Revolution Powder Analyzer. A binary mixture of starch granules of a total mass of about 70.8 g was added to the drum with a diameter of 11 cm and a width of 3.5 cm and rotated at 5 rpm for 1200 avalanches. Alexander, Muzzio, and Shinbrot (2003) found both the fill level and the rotation rate had an impact on the patterns produced during segregation (36). The fill level used was restricted by the fill level requirements of the Revolution Powder Analyzer. The rpm value was selected to align closely with the fixed 25 rpm rotation rate of the V-shell while remaining within the operating constraints of the Revolution Powder Analyzer. Photos of the drum were then taken to visualize any segregation.

4.3 Results

The starch granules were sieved into four size fractions as indicated in Table 1 and some of these fractions were dyed to allow visual observations of any segregation. The potential for segregation was estimated using the Revolution Analyzer. All size fraction 50-50 mixture combinations were tumbled, and segregation patterns photographed. Segregation was observed for all combinations. However, as shown in Figure 4.3, the extent of segregation was larger for mixtures with larger differences in their size fractions.



Figure 4.3: Comparison of 50-50 mixtures after 1200 avalanches in the Revolution Analyzer: Cut 1 and 4 (left), Cut 3 and 4 (right)

Figure 4.4 shows an example of the visual observations of mixing starch granules in the acrylic V-shell. The larger dyed granules were loaded horizontally on top of the smaller undyed granules. After approximately 20 rotations, segregation in a “left-right” pattern emerged. The smaller undyed granules segregated towards the outer arm and the larger dyed granules towards the inner arm. The segregation was very visible at the bed surface. Trials continued for 200 revolutions and showed that this segregation pattern remained stable with no further changes.

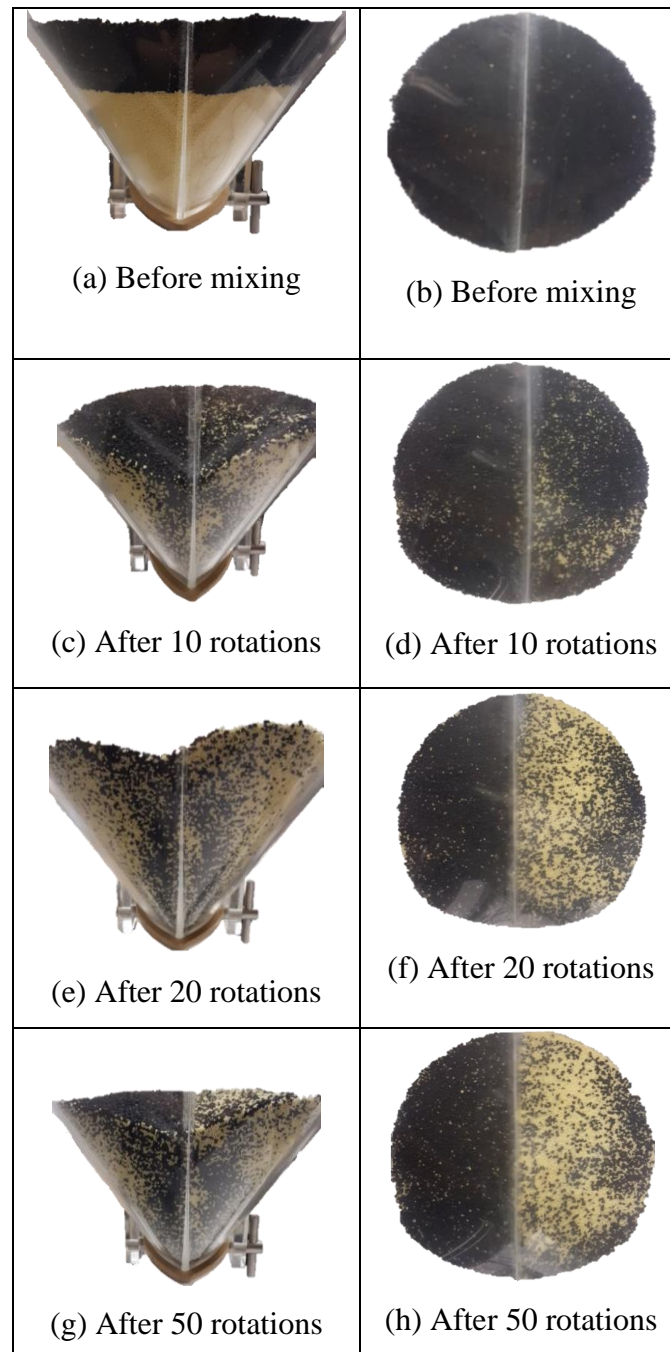


Figure 4.4: Visual observations of mixing of starch granules in the 16-qt acrylic V-shell. Dark dyed granules of Cut#1 were mixed with undyed light granules of Cut#4 in a 50-50% by volume ratio

Figure 4.5 shows the composition of samples taken after various revolutions for a 50-50 binary mixture of the largest and the smallest starch granule size fractions with the largest

starch granule loaded on top. From the thief probe samples, the composition of the mixture was near 50-50% at 10 revolutions, but then stabilized around 65-35% with further revolutions. The outer arm was emptied and analyzed for composition after 10, 20, and 50 rotations. The outer arm's smaller granule composition at 10 revolutions was approximately 62%. With further revolutions, the composition of the smaller granules in the outer arm stabilized at about 65%.

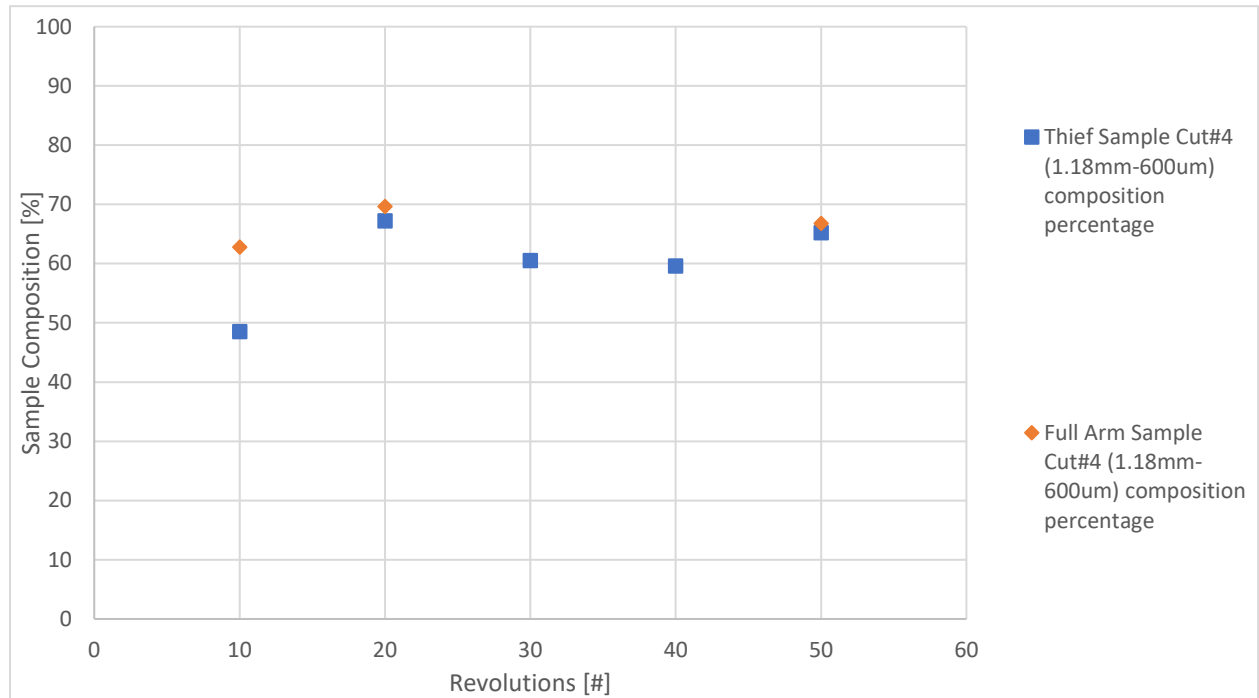


Figure 4.5: Comparison of Thief Sample and Outer Arm composition of Starch Granules 50% Cut 1 (2.36-2.00mm), 50% Cut 4 (1.18mm-600µm) mixture in 16-qt Acrylic V-shell

Figure 4.6 shows the effect of particle size on segregation. The three largest size cuts were combined with the smallest size cut in a 50-50 ratio with the larger size particles loaded horizontally on top. The composition of particles in the outer arm was determined after 50 revolutions of the V-shell. Figure 4.6 shows that segregation increased with the size range of particles. For a large size range, 65% of the smallest particles had migrated to the outer arm by 50 revolutions of the V-blender. As the size variation between

particles decreases, the percentage of the smaller particles in the outer arm approaches 50%.

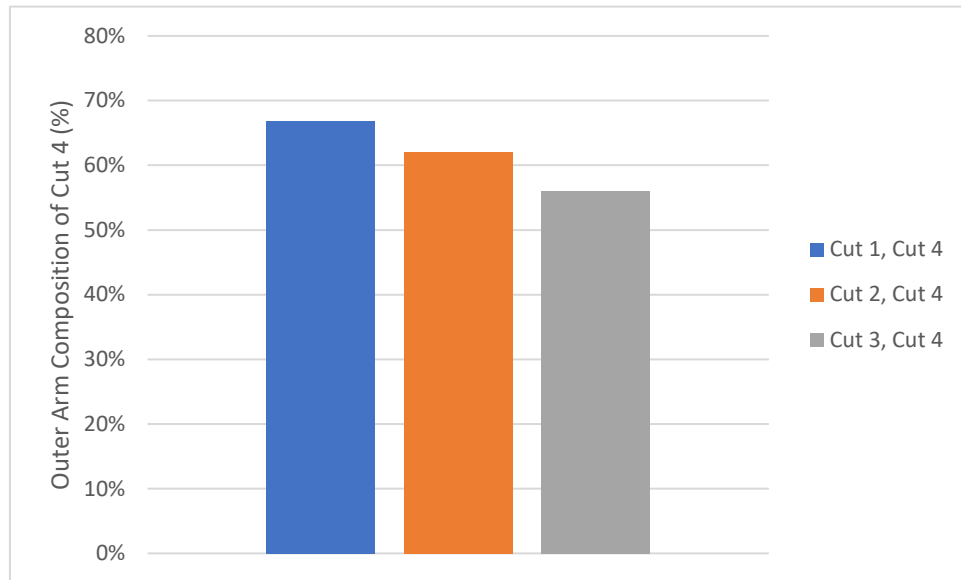


Figure 4.6: Comparison of Outer Arm Cut 4 composition for various mixtures

Figure 4.7 shows that the vibration amplitude varied approximately linearly with starch granule size. The amplitude is shown to increase with size with a trendline providing an R^2 value of 0.9992 suggesting a well-fitting linear trend. These results complement the trends previously observed with glass beads and sugar spheres (33).

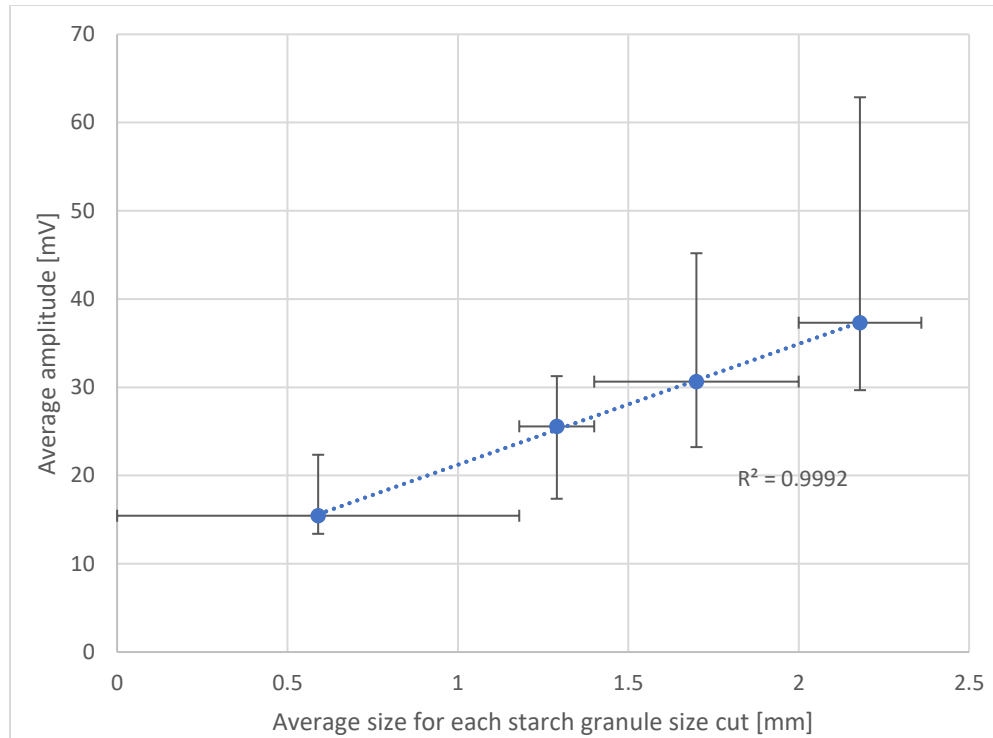


Figure 4.7: Average vibration amplitude of starch granule control samples in 16-qt Steel V-shell; with horizontal error bars representing the size range of the cut and vertical error bars representing the maximum and minimum amplitude values recorded respectively

Figure 4.8 shows the vibration amplitude profiles of the glass beads along with a 50-50 binary mixture of the glass beads with the 2 mm beads loaded horizontally on top of the 1 mm beads in the 16-qt acrylic V-shell. The vibration amplitudes of the mixture were initially similar to the average amplitude of about 400 mV for the 2 mm beads. The mixture amplitudes then decreased over almost 20 revolutions before reaching a plateau at about 200 mV. This plateau is above the average amplitude of about 90 mV for the 1 mm beads. Sampling with the thief probe indicated that 40 revolutions were required for mixing.

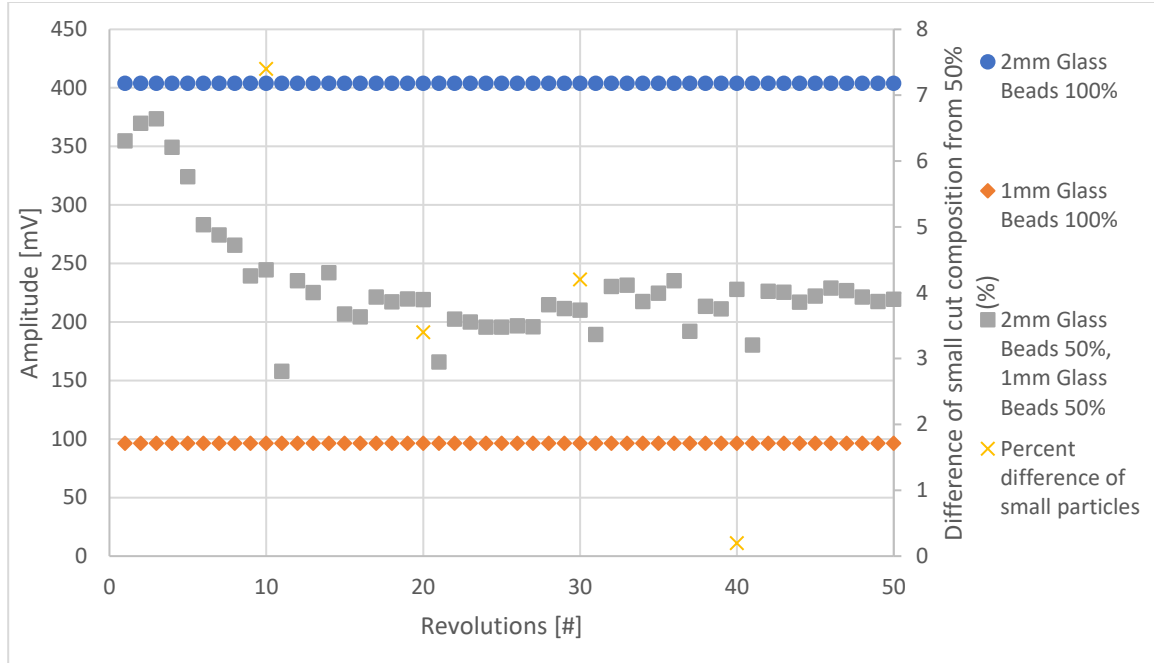


Figure 4.8: Glass beads 50% 1mm, 50% 2mm mixture in 16-qt Acrylic V-shell; with the percent difference from 50% composition of the 1mm glass beads of thief probe samples shown

Figure 4.9 shows the vibration amplitude profiles of the largest and the smallest starch granule size fractions. The vibration profiles of 50-50 binary mixtures of these size fractions are also shown. For the large size fraction loaded horizontally on top of the small size fraction, the amplitude of the mixture was initially similar to the 65 mV amplitude of the large size fraction and then decreased to about 40 mV after about 25 revolutions. For the small size fraction loaded horizontally on top of the large size fraction, the amplitude of the mixture was initially about 25 mV which was similar to the amplitude of the small size fraction. The amplitude then increased to about 55 mV after about 20 revolutions before decreasing to 40 mV at about 50 revolutions. The weighted average was determined based upon the concentration of small and large particles in the outer V-shell arm after 50 revolutions. This was determined by sieving and weighing the particles in the outer V-shell arm after 50 revolutions. These concentrations along with the average amplitude of each size fraction were then used to determine an approximate weighted average. If there is segregation it is expected that the measured signal will plateau at this value.

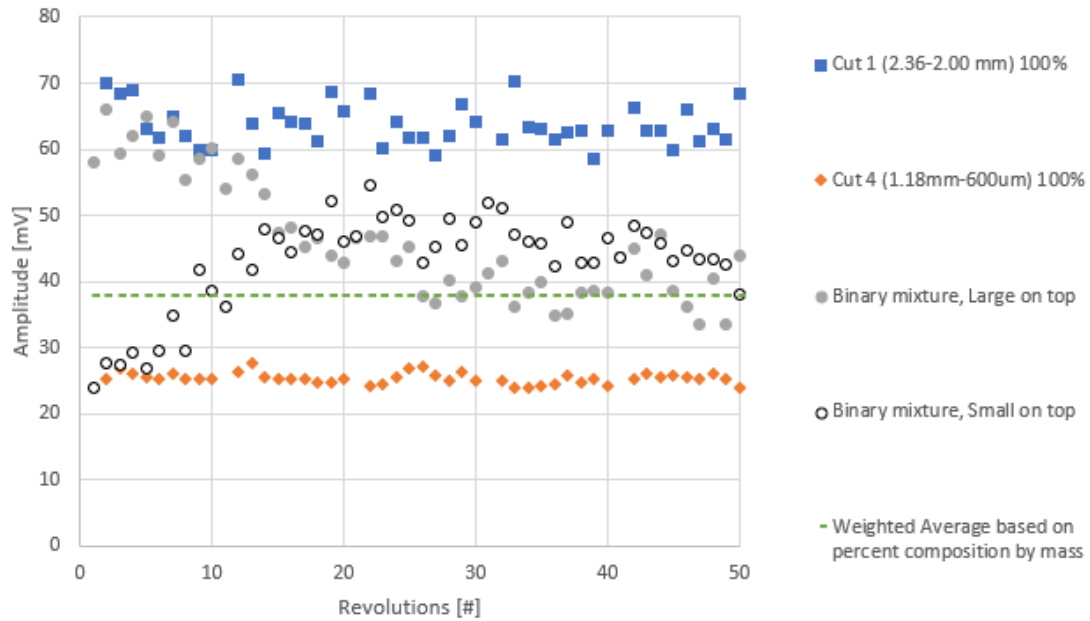


Figure 4.9: Combined Loading Order Trials of Starch Granules 50% Cut 1 (2.36-2.00mm), 50% Cut 4 (1.18mm-600 μ m) mixture in 16-qt Acrylic V-shell

Figure 4.10 shows the vibration amplitude profiles of two closely sized starch granule size fractions and their binary mixtures. For the larger size fraction loaded horizontally on top of the smaller size fraction, the amplitude of the mixture was initially similar to the 50 mV amplitude of the larger size fraction and then decreased to about 32 mV after about 25 revolutions. For the small size fraction loaded horizontally on top of the large size fraction, the amplitude of the mixture was initially about 30 mV which was similar to the amplitude of the small size fraction. The amplitude then increased to about 40 mV after about 20 revolutions before decreasing to 35 mV at about 50 revolutions.

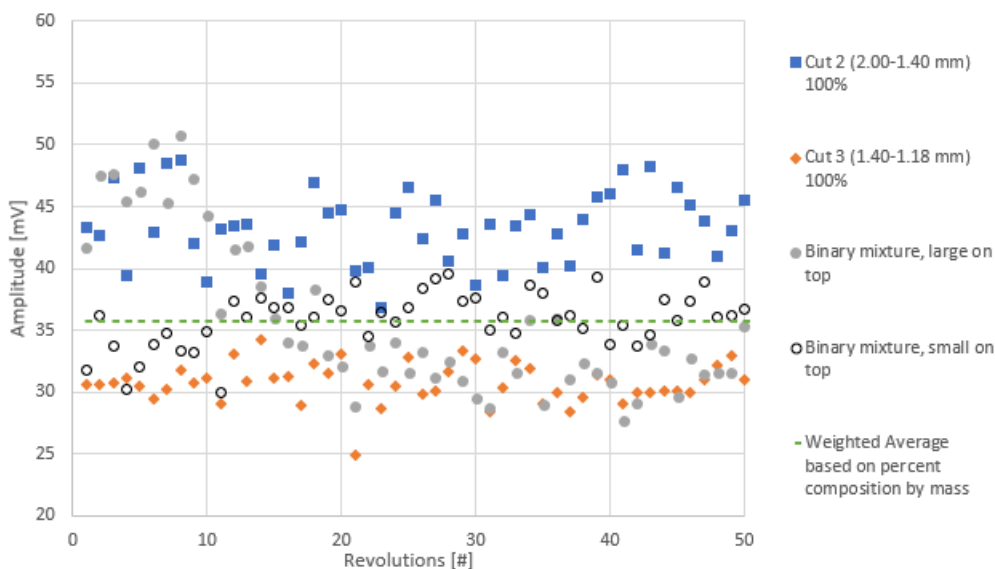


Figure 4.10: Combined Loading Order Trials of Starch Granules 50% Cut 2 (2.00-1.40mm), 50% Cut 3 (1.40-1.18mm) mixture in 16-qt Acrylic V-shell

4.4 Discussion

Stress waves are propagated from particle-particle and particle-wall collisions. During a collision, some of the kinetic energy is retained by the particle with the rest dissipated through stress waves, deformations, rotational motion, and drag forces (28). Dissipation through deformations of the equipment or particles were negligible and low, as were rotational motion and drag forces. Most of the energy was either retained by the particle or dissipated as stress waves. The stress waves propagated were measured using an accelerometer affixed to the V-shell.

Segregation refers to areas of particles within a mixture where there is a high concentration of particles with similar properties. During mixing in a V-blender, segregation can occur and is primarily due to trajectory and percolation segregation mechanisms. These mechanisms occur with powders that flow well, have a range of sizes, and are subjected to a curving flow field. Although the granules were not spherical with sphericities ranging from 0.66 to 0.72, their flowability potential was very good as indicated by the low avalanche times below 4.8 s (Table 4.1). The granules were sieved into the four size fractions that are indicated in Table 1 and therefore had a range of sizes.

The curving flow field during the operation of the V-blender was easily observed using the transparent V-shell (41). The potential for segregation was further estimated with rotating tests using the Revolution Analyzer; for all size fraction mixture combinations, segregation patterns were observed with more distinct patterns visible for mixtures with larger differences in their size fractions (Figure 4.3). The results of the Revolution Analyzer tests show the importance of particle size and mass when determining if a mixture is likely to segregate.

As shown in Figure 4.4, although the granules were loaded in horizontal layers symmetrically, segregation occurred, with each arm of the V-blender having a disproportionate fraction of one of the size fractions: the smaller undyed granules segregated towards the outer arm and the larger dyed granules towards the inner arm. This “left-right” segregation pattern was observed for all test mixtures with the pattern more distinct at the top of the particle bed. When viewed from the side of the V-shell (Figure 4 (c), (e), (g)) it is noted that there was secondary segregation of a higher concentration of the larger dyed particles towards the interior of the V-shell with the smaller undyed particles lining the far sides of the V-shell. These patterns were observable after 20 rotations. Alexander et al. (2003) observed a “left-right” segregation pattern for 50-50 mixtures by volume of spherical glass beads in size fractions of 700 – 850 microns and 150 – 250 microns for fill levels from 30 to 80% by volume and rotation rates from 6 to 30 rpm and indicated that the potential for this segregation pattern increased with fill level and rotation rate (36). This finding was supported and expanded upon in a further study (39).

The degree of “left-right” segregation between the V-shell arms was measured by sampling and also by stopping the V-shell while in its inverted orientation, emptying each arm separately and then sieving to determine the relative amount of each size fraction. Figure 5 shows an example of these sampling results for a 50-50 mixture of dyed cut #1 loaded horizontally on top of undyed cut #4. At 10 revolutions, there were differences between the results from the sampling thief and the entire arm measurements. This shows the limitations and errors of sampling thief probes. The thief probe only examines a small

amount of material (5.5 g of granules or 12.5 g of glass beads) and from a very localized location and therefore can miss detecting segregation (43).

The sampling results also indicated the transience of the emerging segregation pattern. Visual observations indicated that, at 10 revolutions, the segregation pattern was not fully established. The sampling thief only indicated a local measurement near the outer wall of the outer arm which was not representative of the particle composition in the entire arm. For the example shown in Figure 4.5, the segregation pattern was established by 20 revolutions of the V-shell with the outer arm containing approximately 69% of the larger, dyed particles. At this point, the sampling thief and whole arm measurements became similar within the intrinsic limitations and errors associated with the thief.

V-shell arm composition analysis was completed for all test mixtures. Figure 4.6 shows an example comparison of the cut #4 composition for 50-50 mixtures of each size cut combination. As the size cuts became closer in size, the percentage of cut #4 present in the sample decreased towards a value of 50%. This result is supported by the results of initial segregation trials in the Revolution Analyzer which indicated that more similarly sized cuts showed less signs of segregation when combined. Lower differences in particle sizes and masses minimize the risk for particles to segregate.

Flow patterns were observed during rotation with the transparent V-shell. When the V-shell is inverted, the particles fall downwards towards the joint between the two arms and then flow along the inner arm walls towards the lids. Due to trajectory segregation, the larger particles will accumulate near the joint and the inner arms, while the smaller particles will travel with the curved flow towards the lids (Figure 4.11). Trajectory segregation occurs again when the V-shell rotates back to its upright position with the larger particles following a more rectilinearly path than the smaller particles. Due to the differences in particle sizes, there will be percolation segregation, but it is harder to observe, and trajectory segregation is hypothesized to be the driving force to creating the left-right segregation pattern.

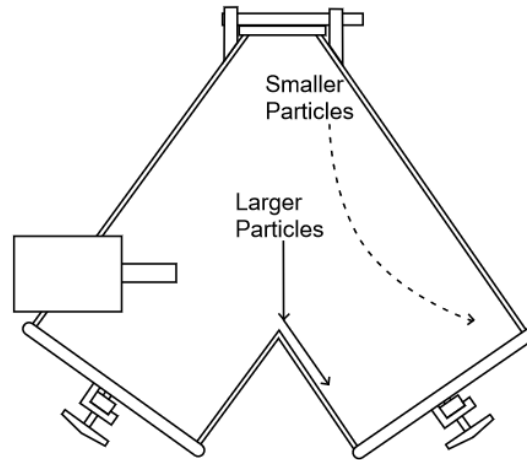


Figure 4.11: Trajectory segregation flow path schematic showing the path of motion for larger and smaller particles

For all combinations of size fractions and horizontal loading order, a left-right segregation pattern was observed by 50 rotations and with the smaller particles segregated into the outer arm and the larger particles into the inner arm. It is hypothesized that the V-blender support that protrudes slightly into the V-shell influences the segregation of the larger particles into the inner arm. As the particles tumble, those in the inner arm space may collide with the support. Due to their larger inertia and thus tendency to follow a rectilinear flow path, larger particles would potentially collide more frequently with the support than smaller particles. The collisions reduce the kinetic energy of the particles and therefore the particles are even more likely to travel rectilinearly than to follow the curved flow pattern (Figure 4.12). After many revolutions of the V-shell, the larger particles will begin to segregate to the inner arm.

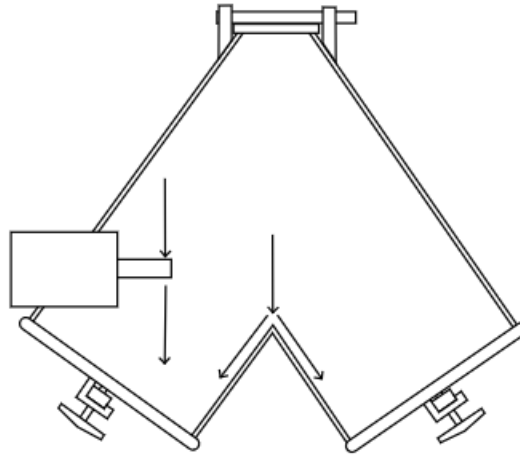


Figure 4.122: Trajectory segregation flow path schematic showing the path of motion for larger particles impacting with the V-shell joint and support

In industry, pharmaceutical powder mixing predominantly occurs in opaque metal V-shells. Equipment used in industrial settings would require expensive modification to install windows to allow for visual observation which also compromise the integrity of the V-shell. In addition, pharmaceutical mixtures are often made up of various powders of similar colours, mainly white, resulting in limited ability to visually identify segregation in the mixture. Changing the colour of these powders poses several challenges, such as the risk of inadvertently altering the properties of the powders. It is therefore challenging and not practical to visually identify segregation. As demonstrated, sampling and analysis with thief probes is limited and not always effective in reliably and accurately identifying segregation. A potential inline method such as passive acoustic emissions measurements would be valuable for monitoring mixing and identifying any problems.

As shown in Figure 4.7, the amplitude of the vibrations from passive acoustic emissions measured from Feature 1b, which correspond primarily to collisions of the particles with the lid with attached accelerometer, are proportional to the particle size or mass (41) and additionally depend on flow patterns in the V-shell. Therefore, it was hypothesized that passive acoustic emissions should be able to identify segregation within a V-shell.

Figure 4.9 shows the extracted vibration amplitudes for granules from size cut#1 and from size cut #4 along with a 50-50 mixture of these two size fractions in different horizontal loading orders. The amplitude for the larger size cut#1 was about 65 mV and about 25 mV for the smaller size cut#4. The particles with the larger size and mass have higher kinetic energies upon collision and thus the potential for more energy dissipation as vibrations that are measured by the accelerometer. When the larger particles were loaded horizontally on top of the smaller particles, initially the measured vibrations from the mixture were about the same as the vibrations for the larger size particles. When the V-shell is inverted, the particles that initially collide with the lids are almost all larger particles. As the particles become mixed, the relative amount of larger particles colliding with the lids decreases, and the dissipated energy from the collisions decreases. After about 20 revolutions, the measured vibrations of the mixture reach a plateau at about 38 mV. This amplitude of about 38 mV corresponds to the interpolated weighted amplitude of approximately 34% larger particles in the outer arm as measured through the entire arm sample.

When the smaller particles were loaded horizontally on top of the larger particles, initially the measured vibrations were low and close to the vibrations of the smaller particles. The measured vibration amplitudes increased as the particles became mixed and more of the larger particles collided with the lids. An initial peak in the measured amplitude was observed around 20 revolutions. This peak is attributed to the greater potential for percolation with the loading order of smaller particles on top horizontally. Percolation occurs when smaller particles fall through the void spaces between larger particles (44). At the beginning of the mixing process, the percolation is high for a loading order of small on top. The small particles percolate through the larger particles when the V-shell rotates into its upright position and the particles flow towards the bottom plate of the V-shell. In comparison, for a loading order of large on top, percolation would only occur when the V-shell is inverted. When the V-shell is inverted, the mixture is separated into each arm and the smaller volumes over larger cross-sectional areas would minimize percolation. The different flow of particles with loading order impacts the time required to reach a stable mixture.

Figure 4.10 shows the mixing profiles from the acoustic emissions for two size cuts of particles that are similar. The emission amplitudes of the larger particles are only about 15 mV larger than the amplitudes of the smaller particles. The transition of the mixing profile to a plateau indicating a relatively stable mixture is not as distinct as for mixtures with a larger size difference (Figure 9) especially for a loading order of small on top.

Mixing is very important in pharmaceutical tablet manufacturing to ensure that each tablet contains the correct specified amounts of each component, particularly the API. Many of the new APIs are very potent and therefore the required amount in a dosage is very small. Ensuring that this small amount of API is appropriately distributed within the formulation mixture is challenging but very critical. Most pharmaceutical powders are white, similar in density, and almost spherical. The major difference is size and therefore there is potential for segregation. Selecting excipients that minimize the size range can reduce segregation. However, this might not be possible. Some components have documented differences in dissolution and absorption due to particle size and therefore affect the bioavailability and pharmacologic activity of the tablet (45,46). Dissolution and absorption in general increase as particle size is reduced as the specific surface area of the component increases. Therefore, a formulation should be developed, tested, and certified not just with specified components, but also with sizes of components. The tolerance to adjust the particles sizes to mitigate segregation challenges in mixing is therefore limited. A non-intrusive method to monitor mixing inline and in real time is needed to ensure mixing is reached at a required level of homogeneity at a specified scale of scrutiny especially for mixtures prone to segregation and with potent components.

4.5 Conclusion

Segregation is a challenge in mixing pharmaceutical formulations for tablets. Although V-blenders are commonly used, they are prone to segregation including a “left-right” segregation pattern with larger particles migrating towards the outer arm and smaller particles towards the inner arm. Sampling with thief probes only provides composition information and does not always capture extent of segregation. Vibrations from passive acoustic emissions created by particles within a V-blender provided large scale information about particle movement in the V-shell. The information identified “left-

right” segregation due to particle size and trajectory particle differences. The profile created from passive acoustic emissions also identified the point at which the mixture becomes stable which is important in optimizing mixing.

4.6 References

1. Debotton N, Dahan A. Applications of polymers as pharmaceutical excipients in solid oral dosage forms. *Med Res Rev* 2016; 37: 52-97
2. Léonard G, Bertrand F, Chaouki J, Gosselin PM. An experimental investigation of effusivity as an indicator of powder blend uniformity. *Powder Technol* 2008; 181: 149-159.
3. Muzzio F, Goodridge C, Alexander A, Arratia P, Yang H, Sudah O, Mergen G. Sampling and characterization of pharmaceutical powders and granular blends. *Int. J Pharm* 2003; 250: 51-64.
4. U.S. Department of Health and Human Services, Food and Drug Administration, Center for Drug Evaluation and Research (CDER), Center for Biologics Evaluation and Research (CBER). Guidance for Industry – Q8(R2) Pharmaceutical Development; 2009. Available from: <https://www.fda.gov/regulatory-information/search-fda-guidance-documents/q8r2-pharmaceutical-development>
5. Tewari J, Strong R, Boulas P. At-line determination of pharmaceuticals small molecules' blending end point using chemometric modeling combined with Fourier transform near infrared spectroscopy. *Spectrochim Acta A Mol Biomol Spectrosc* 2017; 173: 886-891.
6. El-Hargasy A, Drennen J. A Process Analytical Technology approach to near-infrared process control of pharmaceutical powder blending. Part III: Quantitative near-infrared calibration for prediction of blend homogeneity and characterization of powder mixing kinetics. *J Pharm Sci* 2006; 95: 422-434.
7. Sulub Y, Konigsberger M, Cheney J. Blend uniformity end-point determination using near-infrared spectroscopy and multivariate calibration. *J Pharm Biomed Anal* 2011; 55: 429-434.
8. Jaumot J, Igne B, Anderson C, Drennen C, de Jaun A. Blending process modeling and control by multivariate curve resolution. *Talanta* 2013; 117: 492-504.
9. Besseling R, Damen M, Tran T, Nguyen T, van den Dries K, Oostra W, Gerich A. An efficient, maintenance free and approved method for spectroscopic control and monitoring of blend uniformity: the moving F-test. *J Pharm Biomed Anal* 2015; 114: 471-481.

10. Lee WB, Widjaja E, Heng PWS, Chan LW. Near infrared spectroscopy for rapid and inline detection of particle size distribution variability in lactose during mixing. *Int J Pharm* 2019; 566: 454-462.
11. Blanco M, Gozález Bañó R, Bertran E. Monitoring powder blending in pharmaceutical processes by use of near infrared spectroscopy. *Talanta* 2002; 56: 203-212.
12. Rinnan A, van den Berg F, Engelsens SB. Review of the most common preprocessing techniques for near infrared spectra. *TrAC* 2009; 28: 1201-1222.
13. Nakagawa M, Altobelli Sam Caprihan A, Fukushima E, Jeong EK. Non-invasive measurements of granular flows by magnetic resonance imaging. *Exp Fluids* 1993; 16: 54-60.
14. Kawaguchi T, Tsutsumi K, Tsuji Y. MRI Measurement of Granular Motion in a Rotating Drum. *Part Part Syst Charact* 2006; 23: 266-271.
15. Hill KM, Caprihan A, Kakalios J. Bulk Segregation in Rotated Granular Material Measured by Magnetic Resonance Imaging. *PLR* 1997; 78: 50-53.
16. Koc AB, Silleli H, Koc C, Dayioglu MA. Monitoring of dry powder mixing with real-time image processing. *J Appl Sci* 2007; 7: 1218-1223.
17. Le Coënt A, Rivoire A, Briançon S, Lieto J. An original image-processing technique for obtaining the mixing time: The box-counting with erosions method. *Powder Technol* 2005; 152: 62-71.
18. Chen C, Yu C. Two-dimensional image characterization of powder mixing and its effects on the solid-state reactions. *Mater Chem Phys* 2004; 85: 227-237.
19. Liu X, Zhang C, Zhan J. Quantitative comparison of image analysis methods for particle mixing in rotary drums. *Powder Technol* 2015; 282: 32-36
20. Realpe A, Velázquez C. Image processing and analysis for determination of concentrations of powder mixtures. *Powder Technol* 2003; 134: 193-200.
21. Ammarcha C, Gatumel C, Dirion J, Cabassud M, Berthiaux H. Continuous powder mixing of segregating mixtures under steady and unsteady state regimes: Homogeneity assessment by real-time on-line image analysis. *Powder Technol* 2017; 315: 39-52.

22. Daumann B, Fath A, Anlauf H, Nirschl H. Determination of the mixing time in a discontinuous powder mixer by using image analysis. *Chem Eng Sci* 2009; 64: 2320-2331.
23. Berthiaux H, Mosorov V, Tomczak L, Gatumel C, Demeyre JF. Principal component analysis for characterising homogeneity in powder mixing using image processing techniques. *Chem Eng Process* 2006; 45: 397-403.
24. Yang C, Fu X. Development and validation of a material-labeling method for powder process characterization using X-ray computed tomography. *Powder Technol* 2004; 146: 10-19.
25. Chester A, Kowalski J, Coles M, Muegge E, Muzzio F, Brone D. Mixing dynamics in catalyst impregnation in double-cone blenders. *Powder Technol* 1999; 102: 85-94.
26. Liu R, Yin X, Li H, Shao Q, York P, He Y, Xiao T, Zhang J. Visualization and quantitative profiling of mixing and segregation of granules using synchrotron radiation X-ray microtomography and three dimensional reconstruction. *Int J Pharma* 2013; 445: 125-133.
27. Crouter A, Briens L. The effect of granule moisture on passive acoustic emissions in a V-blender. *Powder Technology* 2016; 299: 226-234.
28. Cameron A, Briens L. Monitoring lubricant addition in pharmaceutical tablet manufacturing through passive vibration measurements in a V-blender. *Powder Technol* 2020; 364: 708-718.
29. Tily P, Porada S, Scruby C, Lidington S. Monitoring of mixing processes using acoustic emission. In: Harnby N, Benkreira H, Carpenter K, Mann R, eds. *Fluid Mixing III*. Rugby: The Institute of Chemical Engineers 1988; 75-94.
30. Bellamy L, Nordon A, Littlejohn D. Non-invasive monitoring of powder mixing with near infrared spectrometry and acoustics. *Spectrosc Eur* 2004; 16: 30-32.
31. Allen P, Bellamy L, Nordon A, Littlejohn D. Non-invasive monitoring of the mixing of pharmaceutical powders by broadband acoustic emission. *Analyst* 2010; 135: 518-524.
32. Cameron A, Briens L. An Investigation of Magnesium Stearate Mixing Performance in a V-Blender Through Passive Vibration Measurements. *AAPS PharmSciTech* 2019; 20: 199.

33. Cameron A, Briens L. Monitoring Magnesium Stearate Blending in a V-Blender Through Passive Vibration Measurements. *AAPS PharmSciTech* 2019; 20: 269.
34. Oka S, Sahay A, Meng W, Muzzio F. Diminished segregation in continuous powder mixing. *Powder Technol* 2017; 309: 79-88.
35. Bridgewater, J. Mixing of powders and granular materials by mechanical means—a perspective. *Particuology* 2012; 10: 397-427.
36. Alexander A, Muzzio F, Shinbrot T. Segregation patterns in V-blenders. *Chem Eng Sci* 2003; 58: 487-496.
37. Poux M, Fayolle P, Bertrand J, Bridoux D, Bousquet J. Powder mixing: Some practical rules applied to agitated systems. *Powder Technol* 1991; 68: 213-234.
38. Van der Wel P. Powder Mixing. *Powder Handl Process* 1999; 11: 83-86.
39. Alexander A, Shinbrot T, Johnson B, Muzzio F. V-blender segregation patterns for free-flowing materials: Effects of blender capacity and fill level. *Int J Pharm* 2003; 269: 19-28.
40. Media Cybernetics. FAQ. Available from:
<https://www.mediacy.com/component/fsf/?view=faq&catid=4&start=10>
41. Wilson K, Briens L. Investigation of passive acoustic emissions during powder mixing in a V-blender. *Powder Technol* 2022; 408.
42. Alexander et al. (2003b) observed a “left-right” segregation pattern for 50-50 mixtures by volume of spherical glass beads in size fractions of 700 – 850 microns and 150 – 250 microns for fill levels from 30 to 75% by volume and rotation rates from 5 to 30 rpm and indicated that the potential for this segregation pattern increased with fill level and rotation rate
43. Berman J, Schoeneman A, Shelton JT. Unit Dose Sampling: A Tale of two Thieves. *Drug Dev Ind Pharm* 1996; 11: 1121-1132.
44. Alchikh-Sulaiman B, Alian M, Ein-Mozaffari F, Lohi A, Upreti SR. Using the discrete element method to assess the mixing of polydisperse solid particles in a rotary drum. *Particuology* 2016; 25: 133-142.
45. am Ende DJ, Rose PR. Strategies to Achieve Particle Size of Active Pharmaceutical Ingredients. In: Abdel-Magid AF, Caron S, eds. *Fundamentals of Early Clinical Drug*

Development: From Synthesis Design to Formulation. New Jersey, USA: John Wiley & Sons, Inc 2006; 247-267.

46. Mcinnes GT, Asbury MJ, Ramsay LE, Shelton JR, Harrison IR. Effect of micronization on the bioavailability and pharmacologic activity of spironolactone. J Clin Pharmacol 1982; 22: 410-417.

Chapter 5

5 Conclusion

5.1 General Discussion and Conclusions

Powder mixing is a vital step in the production of pharmaceutical tablets and capsules. Tablet production is a multi-stage batch process requiring powder mixing at several points. If incorrectly mixed, produced tablets may have incorrect physical properties and amounts of APIs (1,2). To minimize the risk of poorly mixed powders, effective inline monitoring is required. Effective monitoring is especially important for mixtures involving components with large variances in physical properties as this may lead to segregation, thus impacting the quality of the final mixture (3-5). Current monitoring methods are offline requiring samples to be taken from several areas throughout the mixture (6). These samples are then subjected to destructive testing methods. This method of monitoring is inefficient, invasive, and expensive. Process analytical technologies (PATs) provide mechanisms to maintain high quality standards and improve processes (7). There are several PATs currently in development. However, most of these methods require costly permanent alterations to existing equipment or have specific limitations or requirements for the components involved in the process. Passive acoustic emissions provide a potential effective low-cost inline monitoring method for powder mixing.

Preliminary studies identified the best location for the sensor and extraction of information from the emissions using the amplitude of the measured vibrations (8-11). These studies focused on determining the sensitivity of passive acoustic emissions to changes in different process conditions and the ability of passive acoustic emissions to identify the dispersion of a lubricant into another powder. The objective of the current research was to extensively investigate the connections between particle motion and passive acoustic emissions from a V-blender and to identify methods to best extract relevant process information. An additional objective was to apply passive acoustic emissions to segregation prone formulations to determine if the emissions could detect segregation and allow its further study. An accelerometer was affixed to the lid of a V-

shell to allow for the measurement of passive acoustic emissions. Trials were conducted using glass beads and starch granules to understand the connection between particle motion and measured vibrations. From these tests, Feature #1b was identified and determined to provide the measurements with the most relevant process information. Feature #1b is associated with the collisions of the particles with the V-shell lid and using an average of the 50 largest amplitudes from this feature provided the most reliable information about the particle flow while minimizing the impact of individual particle behavior. The information gained from this research allowed the optimization of extraction of relevant process information from passive acoustic emissions from a V-blender.

Starch granules with a similar density to commonly used pharmaceutical granules were identified and separated into four size cuts. The particles were loaded into the V-shell horizontally. The rotation rate of the V-shell and the fill level was kept consistent and a “left-right” segregation pattern always emerged. The amplitudes of the passive acoustic emissions would initially be similar to that of the particle loaded on top before starting to trend towards the bottom particle’s amplitude and reaching a plateau. The plateau amplitude was representative of the weighted average amplitude based on the particle composition in the outer V-shell arm. This plateau indicated that the mixture had reached a stable state. This research demonstrated the ability of passive acoustic emissions for identification of segregation during mixing. In addition, secondary percolation segregation was identified through the emissions and contributed to the mixing time. The limitations of thief probe sampling were highlighted through examination of larger scale contents of the mixer and comparisons to visual observations and the measured passive acoustic emissions.

The results of this research support the potential of passive acoustic emissions as a PAT for inline monitoring of multi-component powder mixtures. Passive acoustic emissions provide reliable particle flow process information that will allow for improved inline control and monitoring of mixing. Current research should be expanded upon to further develop and refine the application of passive acoustic emissions for monitoring powder mixing. Currently research has been completed using offline analysis of the signals,

further studies should determine methods to apply passive acoustic emissions for real-time monitoring. This along with other research is required to help commercially implement passive acoustic emissions for monitoring powder mixing. The pharmaceutical industry is hesitant to adopt new technologies even when endorsed by governing groups such as the FDA, by providing large amounts of supporting studies showing the benefits of passive acoustic emissions there is a greater possibility of this technology being embraced by industry.

The application of passive acoustic emissions monitoring of mixing for segregation prone compositions requires further future development. In this research, process conditions selected resulted in a 'Left-Right' segregation pattern; subsequent work should be completed to evaluate the effectiveness of passive acoustic emissions for identifying other segregation patterns. As well, other particle loadings should be examined. By further exploring these applications, a greater number of potential future industrial applications can be identified. Overall, passive acoustic emissions provide an effective inline method for monitoring powder mixing. Use of this method can help to improve process quality, safety, and control while helping to identify and take actions to mitigate segregation.

5.2 References

1. Léonard G, Bertrand F, Chaouki J, Gosselin PM. An experimental investigation of effusivity as an indicator of powder blend uniformity. *Powder Technol* 2008; 181: 149-159.
2. Muzzio F, Goodridge C, Alexander A, Arratia P, Yang H, Sudah O, Mergen G. Sampling and characterization of pharmaceutical powders and granular blends. *Int. J Pharm* 2003; 250: 51-64.
3. Bridgewater, J. Mixing of powders and granular materials by mechanical means—a perspective. *Particuology* 2012; 10: 397-427.
4. Alexander A, Muzzio F, Shinbrot T. Segregation patterns in V-blenders. *Chem Eng Sci* 2003; 58: 487-496.
5. Oka S, Sahay A, Meng W, Muzzio F. Diminished segregation in continuous powder mixing. *Powder Technol* 2017; 309: 79-88.
6. Asachi M, Nourafkan E, Hassanpour A. A review of current techniques for the evaluation of Powder Mixing. *Adv Powder Technol* 2018; 29: 1525–1549.
7. U.S. Department of Health and Human Services, Food and Drug Administration, Center for Drug Evaluation and Research (CDER), Center for Biologics Evaluation and Research (CBER). Guidance for Industry – Q8(R2) Pharmaceutical Development; 2009. Available from: <https://www.fda.gov/regulatory-information/search-fda-guidance-documents/q8r2-pharmaceutical-development>
8. Cameron A, Briens L. Monitoring lubricant addition in pharmaceutical tablet manufacturing through passive vibration measurements in a V-blender. *Powder Technol* 2020; 364: 708-718.
9. Crouter A, Briens L. The effect of granule moisture on passive acoustic emissions in a V-blender. *Powder Technology* 2016; 299: 226-234.
10. Cameron A, Briens L. An Investigation of Magnesium Stearate Mixing Performance in a V-Blender Through Passive Vibration Measurements. *AAPS PharmSciTech* 2019; 20: 199.
11. Cameron A, Briens L. Monitoring Magnesium Stearate Blending in a V-Blender Through Passive Vibration Measurements. *AAPS PharmSciTech* 2019; 20: 269.

Curriculum Vitae

Katherine Wilson

Post-secondary Education and Degrees

Master of Engineering Science	2020-2022
Chemical Engineering	
Western University, London, Ontario, Canada	
<i>Thesis title: Application of passive acoustic emissions for inline monitoring of segregation prone mixtures in a V-blender</i>	

Bachelor of Engineering Science	
Chemical Engineering	2015-2020
Western University, London, Ontario, Canada	

Honors and Awards:

Ontario Graduate Scholarship	2021-2022
Western University, London, Ontario, Canada	

Mitacs Research Training Award	2020
Western University, London, Ontario, Canada	

Related work Experience

Graduate Teaching Assistant	2021-2022
Western University, London, Ontario, Canada	

Undergraduate Research Assistant	2020
Western University, London, Ontario, Canada	

Publications and Conference Proceedings

Refereed Contributions

Wilson, K. Investigation of passive acoustic emissions during powder mixing in a V-blender. Status: Published.

Non-Refereed Contributions

Wilson, K. Monitoring Segregation in a V-blender using Passive Acoustic Emissions. Poster presentation at: CBE Graduate Research Day, Western University; July 8, 2022; London, ON
